| Title | Studies on Molecular Recognition and Structural Change of Porous Isotactic Poly (methyl methacrylate) Thin Films |
|---|---|
| Author(s) | Kamei, Daisuke |
| Citation | 大阪大学, 2013, 博士論文 |
| Version Type | VoR |
| URL | https://doi.org/10.18910/26259 |
| rights | |
| Note | |

Doctoral Dissertation

# Studies on Molecular Recognition and Structural Change of Porous Isotactic Poly(methyl methacrylate) Thin Films

Daisuke Kamei

June 2013

Graduate School of Engineering,

Osaka University

# CONTENTS

**Part 1 Analyses of Structure and Molecular Recognition Ability of Porous Isotactic Poly(methyl methacrylate) Thin Films at Nanolevel Scale**

**Chapter 1**

**Dynamics of Polymer Chains in Porous Isotactic Poly(methyl methacrylate) Thin Films**

**Chapter 2**

**Solvent Effects on Isotactic Poly(methyl methacrylate) Crystallization and Syndiotactic Poly(methacrylic acid) Incorporation in Porous Thin Films**

**Chapter 3**

**Specific Recognition of Syndiotactic Poly(methacrylic acid) in Porous Isotactic Poly(methyl methacrylate) Thin Films Based on the Effects of Complexing Solvent, Temperature, and Stereoregularity**

**Part 2 Morphological Observations of Porous Isotactic Poly(methyl methacrylate) Thin Films at Micrometer Scale**

**Chapter 4**

**Morphological Change of Isotactic Poly(methyl methacrylate) Thin Films by Self-organization and Stereocomplex Formation**

**Chapter 5**

**Stability and Fusion of Porous Isotactic Poly(methyl methacrylate) Thin Films Fabricated on Silica Nanoparticles**

# Part 3 Mechanistic Studies on Template Polymerization in Porous Isotactic Poly(methyl methacrylate) Thin Films

**Chapter 6**

**Methacrylic Acid and Methyl Methacrylate Oligomers Adsorbed to Porous Isotactic Poly(methyl methacrylate) Ultrathin Filims**

# General Introduction

Naturally occurring macromolecules have uniform molecular weights, and their stereoregularites, sequences, and even higher-order conformations are completely controlled, thus providing functionality, uniqueness, and forms to all living matter. In the 1950s, it was discovered that protein and deoxyribonucleic acid (DNA) form an $\alpha$-helix[1] and a double-stranded helix[2] with each other, as a secondary structure fundamental to the higher-order structure. In the case of DNA, complementary base pairs, such as adenine and thymine or cytosine and guanine, are formed by hydrogen bond interactions inside the double-stranded helix. Each base pair of DNA piles up 0.34 nm apart along the strands, and about 10.5 base units ride the entire loop; the pitch length of the strand is 3.6 nm. This structure is the so called 'B form' that DNA inside the cell ordinarily adopts (Figure 1a).[3] Two types of helical grooves, a 'major groove' and a 'minor groove', are formed between each nucleotide chain outside the B form DNA, where the terminal atom of each base can be accessed by DNA binding proteins to inform the base sequence. Therefore, this structure, which is formed by complementary polymer-polymer interactions, is important for signal transduction in biological systems and could be applied to controlling higher-order structures in macromolecule syntheses.
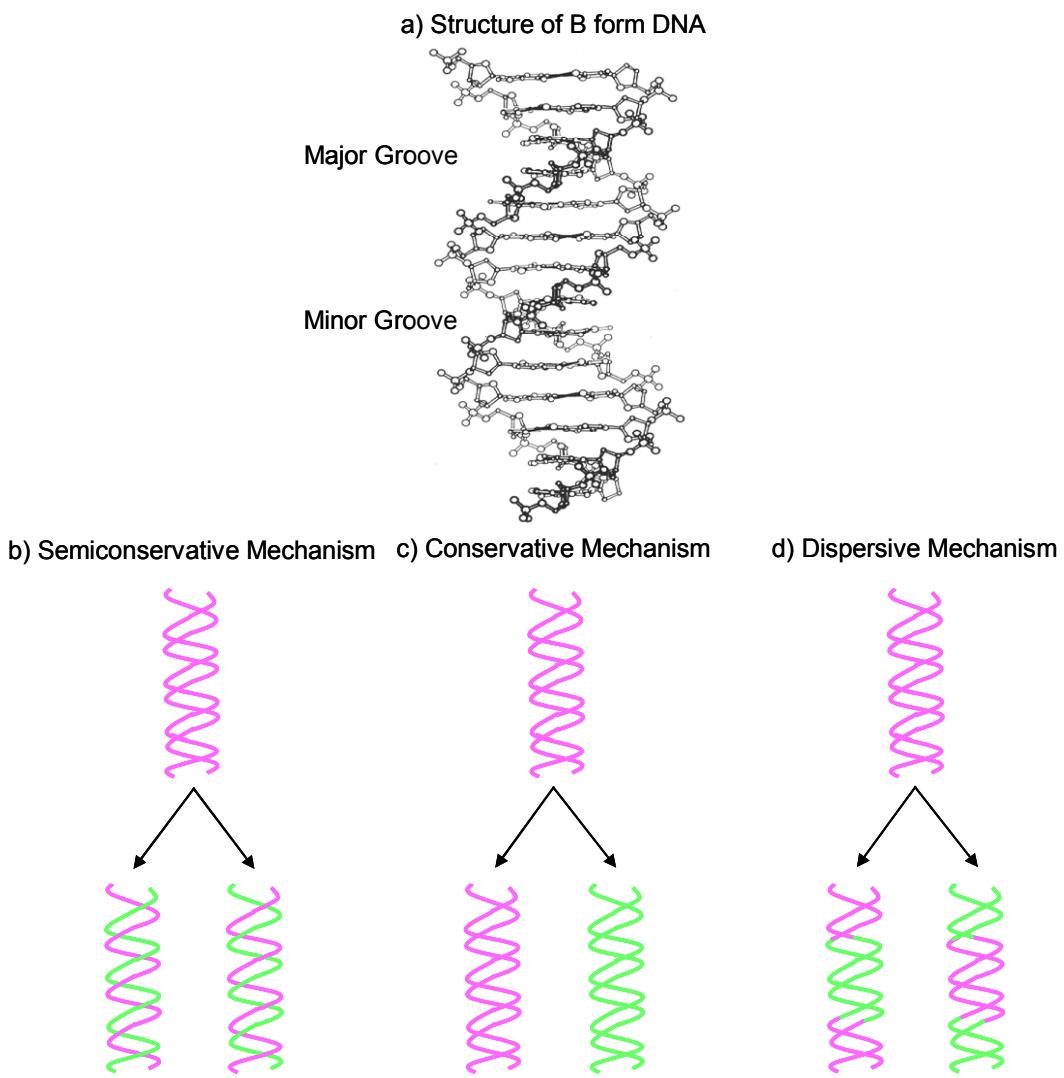
**Figure 1.** (a) Structure of the B form DNA and a schematic representation of DNA replication: (b) the semiconservative mechanism, (c) the conservative mechanism, and (d) the dispersive mechanism.

Replication of the DNA strands was achieved by the formation of complementary daughter strands from the parent strands as a template. DNA template replication can proceed according to one of three different mechanisms (Figure 1b—d). In the semiconservative mechanism, the parent double-stranded helix separates and each chain forms a new double-stranded helix with the daughter chain, which was proposed by J. D.

Watson and F. C. Crick.[4] In the conservative mechanism, two daughter chains form a new double-stranded helix, while the parent double-stranded helix remains preserved.[5] In the dispersive mechanism, two double-stranded helices, both containing distinct regions composed of either both parent chains or both daughter chains, would be produced.[6] M. Meselson and F. W. Stahl proved that DNA synthesis was achieved by the semiconservative mechanism[7] employing Escherichia coli culture in medium containing the nitrogen isotope $^{15}N$ and subsequent incubation in medium with $^{14}N$. The fully-transcribed double-stranded helix cannot be synthesized without the template chain in the semiconservative mechanism. Therefore, a precise template structure is considered to be essential for complete structural control of synthetic polymers, which has not been achieved yet.

In the field of synthetic polymers, some stereoregular polymers have been known as their regularly-structured crystals. In the 1950s, it was demonstrated that isotactic (*it-*) polypropylene (PP) forms a 3/1 single helix, whereas syndiotactic (*st-*) PP and *it*-polystrene form a 2/1 single helix and a 3/1 single helix, respectively.[8] These structural discoveries of the poly-*α*-olefins were important, because even vinyl monomers could form artificial helices and have functions similar to natural polymers by controlling their tacticities precisely. In addition to these findings, it has also been observed that various stereoregular synthetic polymers formed helices[9] such as polyisocyanate,[10,11] polyisocyanide,[12] polychloral,[13] polysilane,[14] polyacetylene,[15-18] and polythiophene.[19]

Numerous studies have been performed on structural control of vinyl polymers not only by carefully designing monomers,[20,21] metal catalysts,[22-26] and additives[27] but also by the fabrication of reaction fields.[28] However, they still have some intractable

problems as follows. In monomer design, the steric repulsion of monomer units has been generally employed, but this strategy requires a bulky monomer structure and lacks versatility. In addition, complete control of the nanospaces around the reaction point by catalysts or additives has been unattainable probably because of the lack of a structure fitting between the monomer and the agent, which could be improved by efficiently employing van der Waals interactions with the precise control of atomic distances and bond angles. Furthermore, trapping the monomer into the nanospaces was only modestly beneficial in controlling the tacticity due to a lack of interactions between the monomer and the cage. Therefore, a novel approach completely different from the aforementioned studies was considered to be essential to synthesize stereoregular polymers. Template polymerization inspired by the mechanism of DNA replication has great potential to precisely control the polymer structure by complementary polymer-polymer interactions.

Template polymerization, defined as the process in which monomer units are organized by a preformed template matrix, has also been intensely researched[29] since the first report by M. Szwarc.[30] The organization of a monomer unit can be modified by variable interactions, hydrogen bonds,[31-33] electrostatic forces,[34,35] and covalent bonds.[36-38] Template polymerization can proceed via two different mechanisms described as follows. In the Zip mechanism, monomer units interact with a template by strong interactions. In contrast, in the Pick-up mechanism, the monomer is free at the beginning of the reaction, and then complex formation between the growing species and the template occurs, and the polymerization proceeds along the template by monomer supply (Figure 2). In most of the following examples, a template effect on the change in the kinetics or molecular weight was discussed, and the polymerization proceeded via the

Zip mechanism due to strong interactions between the monomer unit and the template, although the aforementioned DNA replication is also classified as a Zip mechanism.
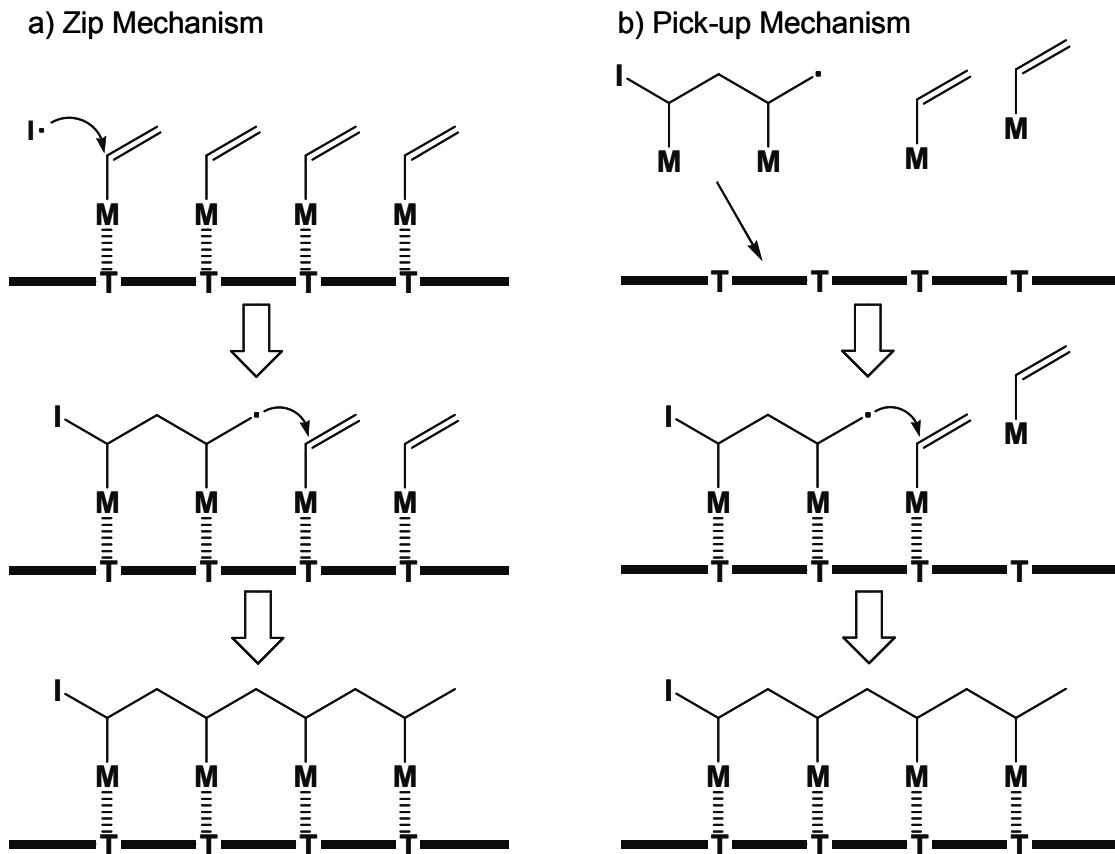


**Figure 2.** Schematic representation of chain template polymerization: (a) Zip mechanism and (b) Pick-up mechanism. I, initiator; M, monomer; T, template.

In the first example, strong hydrogen bonds were employed for the polymerization of acrylic acid (AA)[31,32] or methacrylic acid (MAA)[33] in the presence of different templates, which was reported by J. Ferguson *et al.* for the first time. The Zip-mechanism was proposed for the polymerization of AA or MAA on a poly(vinyl pyrrolidone) (PVP) template, and the maximum polymerization rate was closed to the equivalence of the acid and PVP unit concentration. The higher the molecular weight of

the template, the higher that of the daughter polymer. For example, the degree of polymerization (DP) of AA increased almost directly proportional to that of the template PVP.[32] These results suggest that strong interactions between the monomer and the template will be effective in increasing the polymerization rate and controlling the molecular weight. In contrast, controlling the tacticity by template polymerization has been very difficult.

Second, electrostatic interactions were used early on by E. Tsuchida and Y. Osada for the polymerization of AA or MAA in the presence of poly(*N,N,N',N'*-tetramethyl-*N*-*p*-xylylene-ethylenediammonium dichloride) as a positively charged template matrix.[34] In the presence of the matrix, the rates of polymerization increased remarkably in high pH values, while the blank reaction was prevented by electrostatic repulsion between the oligomers and the monomers. Later, P. Cerrai *et al.* examined the template polymerization of sodium acrylate on poly(allylamine hydrochloride) using $K_2S_2O_8$ as an initiator.[35] Kinetic experiments revealed that the maximum rate was also closed to the equivalence of the monomer unit and the template concentration, and that the template polymerization proceeded by a typical Zip-mechanism. These studies showed that electrostatic interactions are useful to improve the template polymerization of acrylates but still not sufficient to control conformational structures.

Third, the template polymerization of monomer units connected with a template matrix by covalent bonds was reported by H. Kämmerer *et al.*[36] for the first time, and by S. Połowiński *et al.* in a subsequent set of papers.[37,38] The specific characteristic of this system is the fact that the daughter polymer has the same DP as the template polymer. For example, the polymerization of acrylates connected with polynuclear phenolic

compounds and their subsequent decomposition generated acrylate oligomers with the imprinted molecular weight and the original polynuclear phenolic compounds, which could be treated again with acrylate derivatives.[36] In addition, the polymerization of methacrylate connected with poly(vinyl alcohol) was performed resulting in the formation of a ladder-type complex.[38] Template polymerizations achieved by covalent bonding are superior for the complete control of molecular weight. However, most of these studies focused mainly on the polymerization rate and the dependence of the molecular weight of the daughter polymer on that of the template, and the polymerization proceeded by Zip mechanism.

Stereocontrol of the main chains is more important in terms of the expression of function. Thus, it is necessary for the precise control of conformational structure to utilize not the strong polymer-monomer interactions between the monomer and the template in the Zip mechanism, but also a suitable polymer-polymer interaction. Indeed, two innovative approaches on template polymerization to control the tacticity of the daughter polymer have been developed; one was a biomimetic approach to the design of monomers containing nucleic acid bases,[39] and the other was the utilization of existing synthetic polymer complexes.[40]

The strategy of the former template polymerization method was inspired by DNA duplication, employing the specific interactions of complementary nucleic acid bases such as adenine, uracil, thymine, and theophylline connected with methacryloyl group by ethylene linker (Figure 3).[39] These complementary base-base interactions are crucial for the template polymerization. For instance, the rate of polymerization of $N$-$\beta$-methacryloyloxyethyladenine (MAOA) was accelerated in the present of the complementary template polymer, poly-($N$-$\beta$-methacryloyloxyethylthymine)

11

(poly-MAOT), as compared with that of the blank polymerization, whereas the polymerization of MAOT was not accelerated. The polymerization proceeded via the Pick-up mechanism because the interaction between the dimer model compound of MAOA and poly-($N$-$\beta$-methacryloyloxyethyluracil) (poly-MAOU) could be seen only at high concentrations,[41] whereas the interaction between a monomeric model compound and poly-MAOU was never observed.
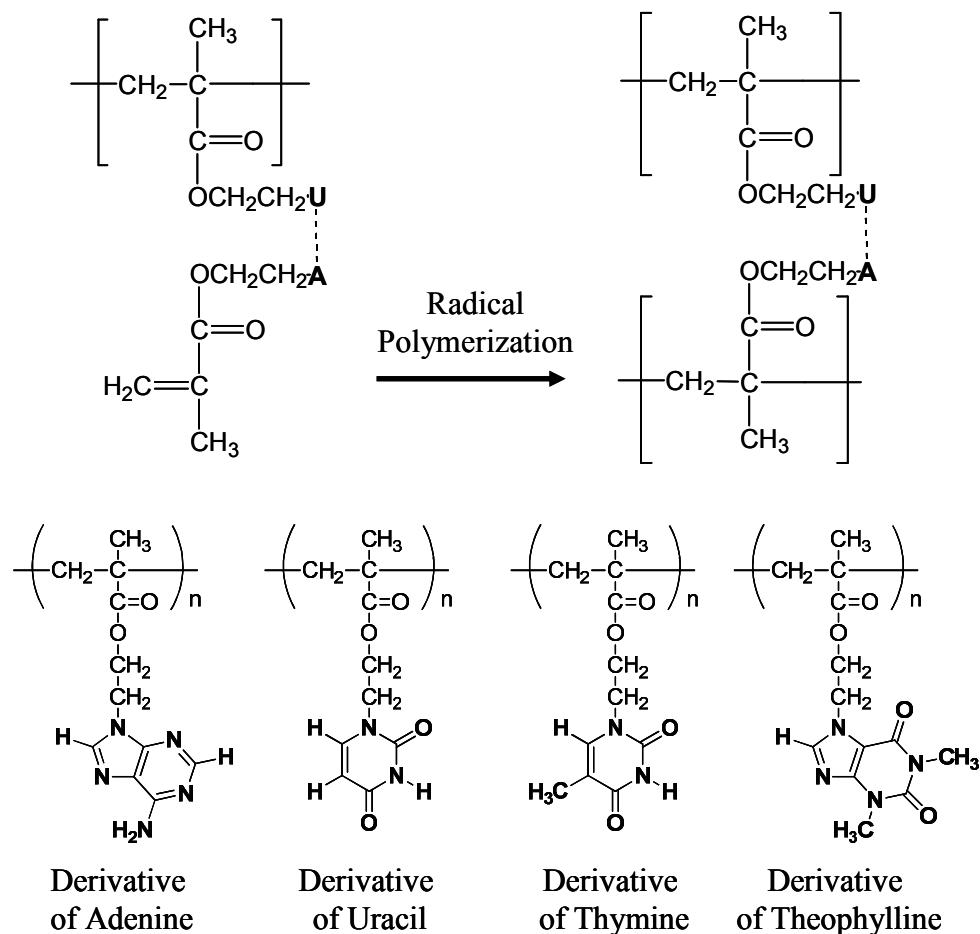


**Figure 3.** Template polymerization of methacrylate derivatives using specific interactions between complementary nucleic acid bases such as adenine, uracil, thymine, and theophylline.

The hydrogen bonds were affected by the temperature and solvent. Competition

between the intramolecular self-association of the bases along the template and the intermolecular complementary base-base interaction would occur. Indeed, the higher the temperature, the more unstable the intramolecular self-association becomes but the more stable the complex formation of the complementary bases, which increases the conversion. In addition, a strong interaction between the solvent and bases would also prevent the specific base-base interactions between the polymers. Therefore, the rate of the template polymerization of MAOA in the presence of MAOU was significantly accelerated in pyridine, a poorer solvent for both poly-MAOU and the synthesized poly-MAOA, as compared with dimethylformamide (DMF) and dimethyl sulfoxide (DMSO).

This approach suggests that the formation of the complementary polymer complex is important for template polymerization. However, stereocontrol of the obtained polymethacryloxyethyl derivatives was not achieved. This is because the base-base interactions would be too strong to control the conformation precisely, or the C—C bond of the ethylene group between the main chain and the interacting site could spin freely (Figure 3). Thus, an accurate design of the bond angles and distances between the atoms in polymer backbones is extremely important, while fixing the bond rotation of the linker by an ethylene bridge between the main chain and nucleic acid base[42] would improve the stereocontrol of the synthesized polymers.

In the other strategy for template polymerization, an existing synthetic polymer complex was utilized to resolve the aforementioned issue. It would be a reasonable approach to employ one of the polymers as a template, which is known to interact wish the other polymer. The complementary polymer complex (stereocomplex) formation of *it*-poly(methyl methacrylate) (PMMA) and *st*-PMMA was reported by J. D. Stroup *et al.*

13

for the first time in the 1950s.[40] The crystal structure was initially proposed to be nonhelical; *st*-PMMA chains in a conformation with a glide plane lay in grooves formed by the 5/1 helices of the *it*-PMMA chains.[43]

Structural analysis of the PMMA stereocomplex has been important because this unique structure could be applied to template polymerization inspired by the DNA replication. G. Challa *et al.* suggested that the stereocomplex formed a complementary double-stranded helix, in which a 9/1 *it*-PMMA helix was surrounded by an 18/1 *st*-PMMA helix with a helical pitch of 1.84 nm, on the basis of X-ray analysis of the stretched fibers (Figure 4).[44] There is a groove between each outside helix of the *st*-PMMA chain, which closely resembles the structure of B form DNA. Recently, E. Yashima *et al.* proposed a triple-stranded helix model, in which the 9/1 *it*-PMMA double-stranded helix was surrounded by the 18/1 *st*-PMMA single helix with a helical pitch of 0.92 nm, on the basis of high-resolution atomic force microscopy (AFM) images of stereocomplex monolayers obtained using the Langmuir-Blodgett (LB) technique (Figure 4).[45,46] The 10/1 *it*-PMMA double-stranded helical structure was proposed by Y. Chatani *et al.* based on X-ray analysis.[47] The *it*-PMMA films were prepared by casting from toluene solution, followed by stretching and heating.[48] The 18.5/1 *st*-PMMA single helical structure was also postulated when *st*-PMMA co-crystallized in cyclohexane and benzene.[49,50] It has been claimed that each component of the aforementioned stereocomplex model is almost identical to the original helical structure.
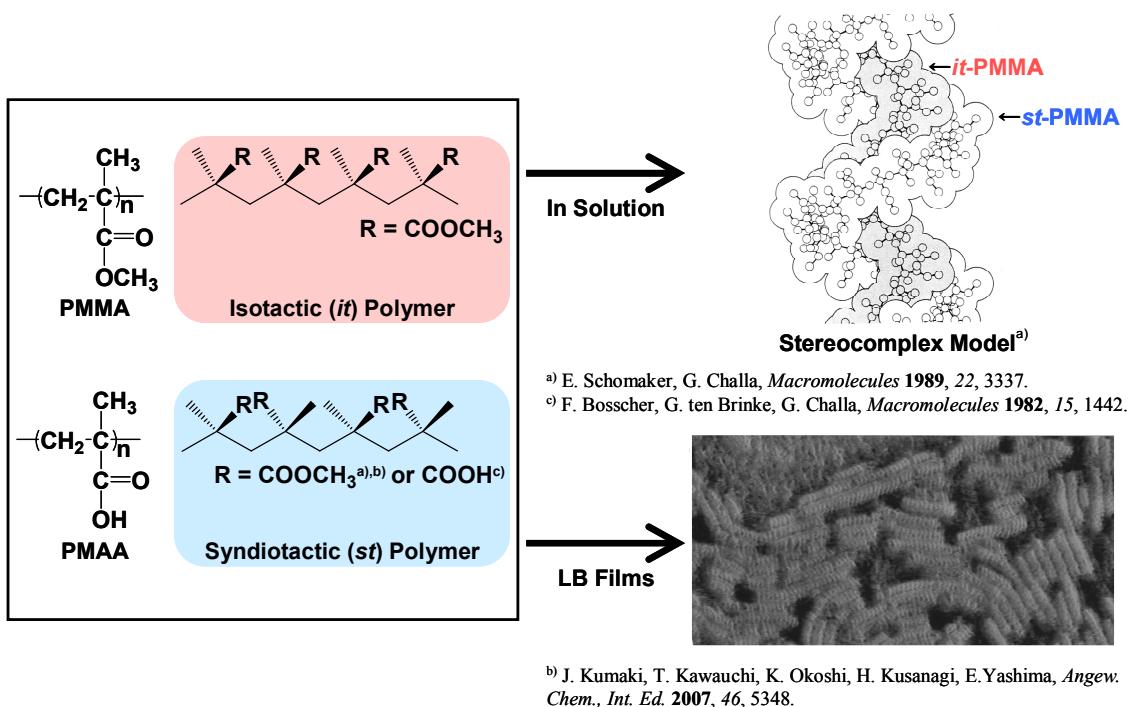
**Figure 4.** Basic stereocomplex models of (a, b) *it*-PMMA/*st*-PMMA and (c) *it*-PMMA/*st*-PMAA.

Herein, the structures of the PMMA stereocomplexes were compared with that of B form DNA. In both cases, the PMMA stereocomplex is composed of two kinds of helices (*it*-PMMA and *st*-PMAA), whereas DNA forms a double-stranded helix from the same helices. In addition, both the distance of each unit and the helical pitch of the PMMA stereocomplex models are shorter than those of the B form DNA, probably according to the different driving forces, van der Waals interaction in the stereocomplex and hydrogen bonding in DNA. These differences would make it difficult to apply the nucleic base pairs of DNA directly to the stereospecific template polymerization of a vinyl polymer as described above. In spite of the differences in bond distances and binding modes, it would be most useful to employ one component of the existing multiple-stranded helical polymer complex as a template. Therefore, this structural

15

discovery of a complementary helix of the PMMA stereocomplex was very important for applying the replication mechanism of DNA to synthetic polymers.

The formation of stereocomplexes has also been well analyzed by infrared (IR) spectroscopy,[51] differential scanning calorimetry, viscometry,[52] and nuclear magnetic resonance analysis.[53] Thus, the PMMA stereocomplex should be a good research subject due to the large amounts of information available to confirm the complexation. The stereocomplex formation is driven by a good steric fit between the two chains in specific solvents or in solids.[54-56] The solvent type affects complexing formation, and the solvents can be divided into three groups: strongly complexing solvents such as DMF, DMSO, acetone and acetonitrile; weakly complexing solvents like toluene and benzene; and non-complexing solvents like chloroform and dichloromethane.[52] Since stereocomplex formation occurred between *it*-PMMA and *st*-polyalkylmethacrylate[53] or *st*-poly(methacrylic acid) (PMAA)[57,58] with different stoichiometries depending on the solvent, it would proceed through an interaction of the methyl ester groups of *it*-PMMA and the $\alpha$-methyl groups of *st*-polyalkylmethacrylate or *st*-PMAA.[44,53]

G. Challa *et al.* investigated the template polymerization of methacrylates in complexing solvents based on the idea that stereocomplex formation could be applied to the stereospecific polymerization of a complementary monomer in the presence of a template polymer.[59-67] *st*-PMMA propagated in the presence of *it*-PMMA, while the presence of *st*-PMMA afforded *it*-PMMA using a suitable solvent.[59,61] The stereospecificity decreased with conversion and was higher in the presence of a higher average molecular weight of template polymer.[59-61] For PMMA, the solvents could be devided in three types: polar solvents such as DMF, DMSO and acetone; nonpolar aromatic solvents like benzene and toluene; and good solvents such as chloroform and

dichloromethane.[63] For instance, the template effect was strong in DMF, very weak in benzene, and disappeared in chloroform, which corresponded with the strength of the stereocomplex formation in the solvents as described above.[52] The effect was also more pronounced at lower temperatures, whereas the polymerization proceeded at the same rate as the blank polymerization at higher temperature.[64] The rate effects increased not only with decreasing initiator concentration,[65] but also with increasing the template concentration until the template chains overlapped each other.[66]

However, the tacticities of the obtained polymers were not controlled effectively (*mm*<60%, *rr*<80%).[61,63,67] This was probably because the thermal motion and conformation of the template polymer chains could not be precisely controlled in solution, which could also result in poor interactions of the growing species with the template polymer. In addition, van der Waals interactions and structural fitting of the complementary polymers in this system would be much weaker than the multiple hydrogen bonds in DNA duplication *in vivo*. Therefore, a novel approach to effectively utilize the weak polymer-polymer interactions is essential to transcribe the stereoregular structure of the template polymer.

Surprisingly, the tacticities of polymethacrylates synthesized by free radical polymerization in artificially-designed macromolecularly porous thin films were almost perfectly controllable (*mm*>90%, *rr*>90%) with a layer-by-layer (LbL) assembly technique.[68,69] These results suggests that fabrication of a reaction field with stereoregular nanospaces, in which the template polymer matrix appropriately interacts with the growing species by polymer-polymer interactions, is essential for stereospecific template polymerization. In this way, the transcription of stereoregularity of a synthetic polymer has been achieved at last, based on the mechanism of DNA replication.

The LbL assembly technique has been known to be as a versatile technique to prepare polymer thin films on a substrate by simple alternate immersion into interactive polymer solutions.[70] Electrostatic interactions between oppositely charged polymers have been widely utilized as the driving force for LbL assembly. The principles of LbL assembly can be applied to other interactions, not only to charge transfer interactions[71,72] and hydrogen bonding,[73] but also to weak polymer-polymer interactions such as the stereocomplex formation of poly(lactide),[74] inclusion complex formation,[75] and biological recognition.[76,77] In particular, these weak interactions would make it possible to arrange polymers into the most stable conformation in films, whereas strong interactions can increase the amounts of the polymer adsorbed but not control the structure of the polymer complex in the films. Therefore, such LbL films can be applied to the stereospecific template polymerization by employing this characteristic feature of weak interactions.

Indeed, stepwise stereocomplex assemblies between *it*-PMMA and *st*-PMMA,[78] *st*-PMAA[79] or *st*-polyalkylmethacrylate[80] were achieved by the LbL technique. IR spectroscopy demonstrated the formation of stereocomplex assemblies, and static contact angle measurements confirmed that *it*-PMMA adsorbed onto the substrate physically, and a molecular rearrangement occurred by the penetration of *st*-polymethacrylate into the *it*-PMMA layer. In other words, the formation of the aforementioned multiple-stranded helices of the stereocomplexes in the LbL films was revealed by surface analyses.

It is noteworthy that macromolecularly porous thin films could be prepared by the selective extraction of *it*-PMMA or *st*-PMAA from *it*-PMMA/*st*-PMAA stereocomplex films with chloroform or an alkaline aqueous solution.[68,69] These porous films could be

used for the selective recognition of stereoregular polymers,[81] which strongly suggests that the porous films possessed stereoregular nanospaces. Stereocomplex films of *it*-PMMA/*st*-PMAA with a 1:1 (length/length) stoichiometry were fabricated from a mixed solvent of DMF/water.[68] In contrast, stereocomplex films of *it*-PMMA/*st*-PMAA (1:2, length/length), which would be the same structure as the PMMA stereocomplex as described above, were prepared from a mixed solvent of acetonitrile/water.[69]

The present approach was superior to template polymerization in solution due to the following three points: 1) focusing on the stereocomplex assembly of *it*-PMMA/*st*-PMAA[79] with different solvent solubilities enabled the selective extraction of one component from the original films[81]; 2) employing multilayered thin films with LbL assembly[78] would make it possible to regulate the conformation of the preformed stereocomplex assemblies and strongly suppress the molecular motion of the growing species in the films as compared with in solution; and 3) utilizing macromolecularly porous films[68,69] with stereoregular nanospaces can precisely control the structure of the synthesized polymers in the films by complementary polymer-polymer interactions. By this means, stereoregular template polymerization has been achieved and the tacticity and molecular weight can be effectively transcribed from the template polymers.

For the aforementioned stereocomplex of *it*-PMMA/*st*-PMAA (1:2, length/length), it would be important to investigate the two kinds of stereocomplex models, double-stranded helix[44] and triple-stranded helix,[45,46] since the *it*-PMMA/*st*-PMMA stereocomplex and the *it*-PMMA/*st*-PMAA stereocomplex are considered to be basically the same structure.[82,83] In contrast, it is easier to understand that the stereocomplex of *it*-PMMA/*st*-PMAA can be treated as a double-stranded helix composed of single helices of *it*-PMMA and *st*-PMAA. The reason is that the number-average molecular weight of

*st*-PMAA synthesized in the porous films by template polymerization was about twice that of *it*-PMMA,[69] and that the stereocomplex was considered to be most stable when the ratio of the molecular weights was about 1:2 (*it*-PMMA/*st*-PMAA).[78,81] In the case of a double-stranded helix of *it*-PMMA in the porous films, the average molecular weight of the *st*-PMAA thus obtained must be quadruple of that of *it*-PMMA, which was in disagreement with the experimental results. In this thesis, the structure of the *it*-PMMA/*st*-PMAA stereocomplex can be discussed on the basis of the double-stranded helix model.[44,83]

Since isospecific template polymerization occurs in porous *st*-PMAA thin films, investigations into porous *st*-PMAA films are important. However, fabrication of the porous *st*-PMAA films was difficult because the *it*-PMMA inside the stereocomplex of *it*-PMMA/*st*-PMAA (1:2, length/length) could not be extracted with conventional organic solvents, except a particular one (tetrafluoroacetylacetone), resulting in a disarrayed *st*-PMAA conformation. In contrast, it is interesting that *it*-PMMA can form two kinds of double-stranded helices with both *st*-PMAA[83] (or *st*-PMMA)[44] and *it*-PMMA itself,[47,48] which is different from the molecular recognition system of DNA and the unique identity for *it*-PMMA. Furthermore, the crystal structure of *it*-PMMA, the helical shape or packing-mode, has been intensely investigated.[47,48,84-88] Thus, in this thesis, porous *it*-PMMA thin films prepared from stereocomplex films of *it*-PMMA/*st*-PMAA (1:2, length/length) were employed.

Stereospecific template polymerization in porous thin films is also useful in terms of the quantity synthesis of stereoregular polymethacrylates. This is not only because the porous films are reusable at least three times,[68,69] but because the stereoregular polymethacrylates are easily synthesized by free radical polymerization, whereas the

stereoregular polymers are ordinarily synthesized by anionic polymerization. Anionic polymerization needs strict conditions and is unsuitable for industrial applications. In addition, stereoregular PMMAs can also be applied to biocompatible thin films,[89,90] fibers,[91] membranes,[92,93] and hollow capsules.[94] Furthermore, their stereocomplex formation or inclusion ability are also utilized in electrical switches[95] as well as the construction of specific architectures like nanoparticles, nanonetworks,[96] and nano-to-microscale assemblies.[97]

As described above, understanding stereospecific template polymerization in macromolecularly porous thin films using LbL assembly[68,69] is a very important research area in terms of industrial applications, and can be thought of as the first step to achieve the complete structural control of natural polymers. This approach is completely different from conventional precise polymerization, but makes it possible to control the structure of the synthesized polymers by utilizing a complementary polymer-polymer interaction and structural regulated nanospaces as the reaction field. On the other hand, there still remain several issues to be solved regarding stereospecific template polymerization.

One issue is the resolution of the mechanism of template polymerization. It remains unclear whether template polymerization in porous *it*-PMMA thin films would proceed via the Zip or Pick-up mechanism, and how the growing species could interact with the template during polymerization. A comparison with studies on ordinary precise polymerizations would be helpful for understanding these mechanisms. For example, 1,1-diphenylethylene does not produce a homopolymer through any kind of catalysis due to steric reasons, whereas dibenzofulvene, whose structure is closely related to that of 1,1-diphenylethylene, can polymerize easily.[98] In another example, the bulkiness of aluminum substituent groups of an auxiliary agent significantly affected the tacticities of

the obtained polymers in the living anionic polymerization of methacrylate derivatives.[99] These facts imply that polymerization reactivity is affected by a subtle environmental difference in the reaction site. Therefore, nanostructural analyses are considered to be important for template polymerization in macromolecularly porous thin films.

Another issue with stereospecific template polymerization[68,69] is the poorly-reproducible results, probably due to the heterogeneous reaction field, where monomers polymerize both in solution and in porous thin films. For instance, the yields and tacticities of the obtained polymers were greatly reduced in a concentrated monomer solution or a mixed solvent of acetonitrile/water (4/6, v/v) instead of water,[100] which suggests that the porous films could not remain stable under these conditions. Therefore, the fabrication of a stable reaction field is essential to synthesize stereoregular polymers from porous thin films with high reproducibility. The author considers solvent effects toward the films and the morphological changes of the films as two major aspects regarding the stability of the porous it-PMMA thin films.

First, solvent effects on the porous it-PMMA films are referred to in this thesis. Among the aforementioned strong complexing solvents, acetonitrile is a specific one because it is the poorest solvent of PMMA[101] as compared to acetone and DMF. In general, poor solubility promotes polymer adsorption on a substrate,[102] which would accelerate stereocomplex assembly on the substrate. Indeed, the amount of it-PMMA/st-PMMA stereocomplexes fabricated by LbL assembly was the largest in acetonitrile under certain conditions,[78] in contrast to in solution.[54] Therefore, the poor solubility of PMMA might also promote the stereocomplex assembly of it-PMMA/st-PMAA during the template polymerization of MAA in porous it-PMMA thin films. In contrast, a counterproductive result was observed, which indicated that

porous thin films could not function effectively as templates in the presence of acetonitrile. Thus, the stability of the porous *it*-PMMA thin films in a mixed solvent of acetonitrile/water (4/6, v/v) was investigated.

Second, morphological observations of the porous thin films at the micrometer scale are also necessary because this system is heterogeneous, and the surface morphology of the porous films will significantly affect the DP when the monomers are soused from a solution. Indeed, in a typical case of emulsion polymerization, the rate of growth depends on the surface area of the nuclei or particles in solution.[103] In addition, the propylene polymerization activity is also proportional to the surface area of heterogeneous Ziegler-Natta catalysts such as core-shell $MgO/MgCl_2/TiCl_4$, which has been recently reported by M. Terano *et al*.[104] Since silica particles are employed as substrates for template polymerization due to their large surface area,[68,69] thedispersibility of the silica particles is also important for degree of template polymerization.

In this thesis, the author conceived the idea to simplify this phenomenon. The phenomenon of template polymerization is too complicated to observe directly, because there are several kinds of growing radicals with different molecular weights in solution and in porous films during polymerization. Thus, the growing radicals interacting with the porous films were clarified to be monomeric, oligomeric, and polymeric. Next, studies on the recognition of a complementary polymer or oligomer in the porous films were taken as a model for understanding template polymerization. In addition, interactions between monomers and the template were investigated changing the monomer structure. If this approach is taken, then the findings from this thesis could be used as a mechanism of template polymerization.

The purpose of this thesis is to understand stereospecific template polymerization in the porous *it*-PMMA thin films. First, solvent effects on the molecular motion of the polymer chains in the porous films were mainly investigated to obtain knowledge on the nanospaces as a reaction field for the template polymerization. Second, morphological observations were performed to confirm the stability (structural change) of the porous films. Third, the effects of the molecular structure on the porous films were analyzed by investigating the interactions (molecular recognition) between the template polymer *it*-PMMA and MAA, the oligomer, or *st*-PMAA in the porous thin films under hypothetical conditions as a model of template polymerization (Figure 5).
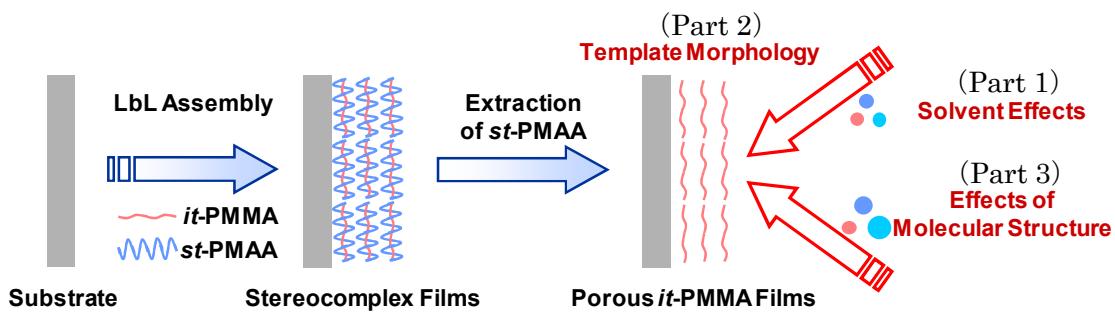


**Figure 5.** Schematic illustration of the effects of template morphology, solvent, and molecular structure on porous *it*-PMMA films prepared by the LbL assembly of *it*-PMMA/*st*-PMAA in incorporating variable molecules.

This thesis is divided into Part 1 (analyses of the structure and molecular recognition ability of porous films at the nanolevel scale), Part 2 (morphological observations of porous films at the micrometer scale), and Part 3 (mechanistic studies on template polymerization in porous films).

In Part 1, the effects of acetonitrile solvation on porous *it*-PMMA thin films were investigated at the nanolevel scale, in order to obtain knowledge on the nanospaces of the

porous films as a reaction field for template polymerization.

In Chapter 1, X-ray diffraction (XRD) analysis was employed as a powerful tool to confirm the packing structure of the polymer chains in order to observe the porous structure of the *it*-PMMA thin films. The XRD patterns of crystalline *it*-PMMA on a substrate changed when the surrounding *st*-PMAA eluted out and was incorporated.

In Chapter 2, the solvent effects on the crystallization of porous *it*-PMMA thin films as well as the incorporation of *st*-PMAA into porous films were investigated. The packing structure, conformation, and surface structural changes of the *it*-PMMA thin films were observed using XRD, IR spectroscopy, and AFM, respectively.

In Chapter 3, the effects of the stereoregularity, temperature, and solvent on the specific recognition of *st*-PMAA in the porous *it*-PMMA thin films were investigated to give important insights into the regularity and stability of the nanospaces in the porous *it*-PMMA films as well as template polymerization. Quartz crystal microbalance (QCM) analysis and IR spectroscopy revealed the first case of stereocomplex formation using *st*-PMAA with lower stereoregularity ($rr = 73\%$) in the LbL films.

In Part 2, macroscopic observations of the surface of the porous *it*-PMMA thin films were made in order to investigate the effects of the structural changes, as described in Part 1, toward the morphology of the porous films as a reaction field for the template polymerization.

Chapter 4 describes the morphological changes of the porous thin films during *it*-PMMA crystallization and the subsequent *st*-PMAA incorporation. Surface analyses of the films were performed by scanning electron microscopy (SEM), AFM, X-ray photoelectron spectroscopy, and static contact angles.

In Chapter 5, the dispersibilities of the silica nanoparticles coated with stereocomplex

thin films composed of *it*-PMMA/*st*-PMAA and with porous *it*-PMMA thin films under gentle stirring or static conditions were analyzed by dynamic light scattering and SEM, respectively.

In Part 3, the mechanisms responsible for the template polymerization and nanospaces in the porous *it*-PMMA thin films were studied. I focused on the adsorption of the oligomers, as well as monomers with different bulkiness with or without the *α*-methyl groups described above, and their polymerization behavior in porous *it*-PMMA thin films.

In Chapter 6, MAA, methyl methacrylate (MMA), methacrylamide (MAm), and oligomers of MAA and MMA were selected as models of active radical species during template polymerization using stereocomplex formation. The adsorption behaviors of the aforementioned model compounds were examined with regard to the porous *it*-PMMA thin films by QCM analyses.

In Chapter 7, a macroporous silicagel (diameter: 7 μm, pore: 100 nm) was employed as a suitable substrate for template polymerization in order to use it repeatedly as an available polymerization container. The template polymerization of MAA on porous *it*-PMMA thin films formed on these macroporous silicagels was described, and the curvature effect and reproducibility were discussed.

In Chapter 8, the postpolymerization of various vinyl monomers was investigated for mechanistic studies of the template polymerization of MAA in porous *it*-PMMA thin films on QCM substrates, and on silica gels. QCM analyses, IR, $^1$H NMR, and size exclusion chromatography were employed to investigate the polymerization mechanism.

# REFERENCES

1) L. Pauling, R.B. Corey, H. R. Branson, *Proc. Natl. Acad. Sci. USA* **1951**, *37*, 205.

2) J. D. Watson, F. C. Click, *Nature* **1953**, *171*, 737.

3) R. Wing , H. Drew, T. Takano, C. Broka, S. Tanaka, K. Itakura, R. E. Dickerson, *Nature* **1980**, *287*, 755.

4) J. D. Watson, F. C. Click, *Cold Spring Harb. Symp. Quant. Biol.* **1953**, *18*, 123.

5) D. P. Bloch, *Proc. Natl. Acad. Sci. USA* **1955**, *41*, 1058.

6) M. Delbrück, *Proc. Natl. Acad. Sci. USA* **1954**, *40*, 783.

7) M. Meselson, F. W. Stahl, *Proc. Natl. Acad. Sci. USA* **1958**, *44*, 671.

8) G. Natta, P. Pino, P. Corradini, F. Danusso, E. Mantina, G. Mazzanti, G. Moraglio, *J. Am. Chem. Soc.* **1955**, *77*, 1708.

9) T. Nakano, Y. Okamoto, *Chem. Rev.* **2001**, *101*, 4013.

10) M. Green, C. Andrea, M. Reidy, *J. Am. Chem. Soc.* **1988**, *110*, 4063.

11) Y. Okamoto, M. Matsuda, E. Yashima, *J. Polym. Sci., Part A: Polym. Chem.* **1994**, *32*, 309.

12) P. Kamer, R. Nolte, W. Drenth, *J. Am. Chem. Soc.* **1988**, *110*, 6818.

13) K. Ute, K. Hirose, K. Hatada, *J. Am. Chem. Soc.* **1991**, *113*, 6305.

14) M. Fujiki, *J. Am. Chem. Soc.* **1994**, *116*, 11976.

15) E. Yashima, S. Huang, Y. Okamoto, *Macromolecules* **1995**, *28*, 4184.

16) E. Yashima, T. Matsushima, Y. Okamoto, *J. Am. Chem. Soc.* **1997**, *119*, 6345.

17) H. Nakako, R. Nomura, T. Masuda, *Macromolecules* **1999**, *32*, 2861.

18) H. Nakako, Y. Mayahara, T. Masuda, *Macromolecules* **2000**, *33*, 3978.

19) B. Langeveld-Voss, E. Meijier, *J. Am. Chem. Soc.* **1996**, *118*, 4908.

20) T. Nakano, M. Mori, Y. Okamoto, *Macromolecules* **1993**, *26*, 867.

21) K. Yamada, T. Nakano, Y. Okamoto, *Macromolecules* **1998**, *31*, 7598.

22) S. D. Ittel, L. K. Johnson, M. Brookhart, *Chem. Rev.* **2000**, *100*, 1169.

23) G. W. Coates, *Chem. Rev.* **2000**, *100*, 1223.

24) M. Kamigaito, T. Ando, M. Sawamoto, *Chem. Rev.* **2001**, *101*, 3689.

25) S. Habaue, Y. Okamoto, *Chem. Rev.* **2001**, *101*, 46.

26) Y. Isobe, D. Fujioka, S. Habaue, Y. Okamoto, *J. Am. Chem. Soc.* **2001**, *123*, 7180.

27) T. Hirano, Y. Okumura, M. Seno, T. Sato, *Eur. Polym. J.* **2006**, *42*, 2114.

28) T. Uemura, S. Horike, S. Kitagawa, *Chem. Asian. J.* **2006**, *1*, 36.

29) S. Połowiński, *Prog. Polym. Sci.* **2002**, *27*, 537.

30) M. Szwarc, *J. Polym. Sci.* **1954**, *13*, 317.

31) J. Ferguson, S. A. O. Shah, *Eur. Polym. J.* **1968**, *4*, 343.

32) J. Ferguson, S. A. Alawi, R. Granmayeh, *Eur. Polym. J.* **1983**, *19*, 475.

33) R. Muramatsu, T. Shimidzu, *Bull. Chem. Soc. Jpn.* **1972**, *45*, 2538.

34) E. Tsuchida, Y. Osada, *J. Polym. Sci., Polym. Chem. Ed.* **1975**, *13*, 559.

35) P. Cerrai, G. D. Guerra, S. Maltini, M. Tricoli, *Macromol. Rapid. Commun.* **1994**, *15*, 983.

36) H. Kämmerer, S. Ozaki, *Makromol. Chem.* **1966**, *91*, 1.

37) S. Połowiński, G. Janowska, *Eur. Polym. J.* **1975**, *11*, 183.

38) R. Jantas, S. Połowiński, *J. Polym. Sci., Part A: Polym. Chem.* **1986**, *24*, 1819.

39) M. Akashi, H. Takada, Y. Inaki, K. Takemoto, *J. Polym. Sci., Polym. Chem. Ed.* **1979**, *17,* 747.

40) T. G. Fox, B. S. Garret, W. E. Goode, S. Gratch, J. F. Rincaid, A. Spell, J. D. Stroupe, *J. Am. Chem. Soc.* **1958**, *80*, 1768.

41) M. Akashi, T. Okimoto, Y. Inaki, K. Takemoto, *J. Polym. Sci., Polym Chem. Ed.*

**1979**, *17,* 905.

42)  P. Lang, A. Mayer, P. Jung, D. Tritsch, J.-F. Biellmann, A. Burger, *Tetrahedron Lett.* **2004**, *45*, 4013.

43)  A. M. Liquori, G. Anzuino, V. M. Coiro, M. D'Alagni, P. De Santis, M. Savino, *Nature* **1965**, *206*, 358.

44)  E. Schomaker, G. Challa, *Macromolecules* **1989**, *22*, 3337.

45)  J. Kumaki, T. Kawauchi, K. Okoshi, H. Kusanagi, E. Yashima, *Angew. Chem., Int. Ed.* **2007**, *46*, 5384.

46)  J. Kumaki, T. Kawauchi, K. Ute, T. Kitayama, E. Yashima, *J. Am. Chem. Soc.* **2008**, *130*, 6373.

47)  H. Kusanagi, H. Tadokoro, Y. Chatani, *Macromolecules* **1976**, *9*, 531.

48)  H. Tadokoro, Y. Chatani, H. Kusanagi, M. Yokoyama, *Macromolecules* **1970**, *3*, 441.

49)  H. Kusuyama, M. Takase, Y. Higashiyama, H.-T. Tseng, Y. Chatani, H. Tadokoro, *Polymer* **1982**, *23*, 1256.

50)  H. Kusuyama, N. Miyamoto, Y. Chatani, H. Tadokoro, *Polymer* **1983**, *24*, 119.

51)  M. Mihailov, S. Dirlikov, N. Peeva, Z. Georgieva, *Macromolecules* **1973**, *6*, 511.

52)  E. J. Vorekamp, F. Bosscher, G. Challa, *Polymer* **1979**, *20*, 59.

53)  F. Bosscher, D. Keekstra, G. Challa, *Polymer* **1981**, *22*, 124.

54)  J. Spevacek, B. Schneider, *Adv. Colloid Interface Sci.* **1987**, *27*, 81.

55)  K. te Nijenhuis, *Adv. Polym. Sci.* **1997**, *130*, 67.

56)  K. Hatada, T. Kitayama, *Polym. Int.* **2000**, *49*, 11.

57)  J. H. G. M. Lohmeyer, G. Kransen, Y. Y. Tan, G. Challa, *Polym. Lett. Ed.* **1975**, *13*, 725.

58) J. H. G. M. Lohmeyer, Y. Y. Tan, P. Lako, G. Challa, *Polymer* **1978**, *19*, 1171.

59) R. Buter, Y. Y. Tan, G. Challa, *J. Polym. Sci., Part A-1: Polym. Chem.* **1972**, *10*, 1031.

60) R. Buter, Y. Y. Tan, G. Challa, *J. Polym. Sci., Polym. Chem.* **1973**, *11*, 989.

61) R. Buter, Y. Y. Tan, G. Challa, *J. Polym. Sci., Polym. Chem.* **1973**, *11*, 1003.

62) R. Buter, Y. Y. Tan, G. Challa, *J. Polym. Sci., Polym. Chem.* **1973**, *11*, 1013.

63) R. Buter, Y. Y. Tan, G. Challa, *J. Polym. Sci., Polym. Chem.* **1973**, *11*, 2975.

64) J. Gons, E. J. Vorenkamp, G. Challa, *J. Polym. Sci., Polym. Chem.* **1975**, *13*, 1699.

65) J. Gons, E. J. Vorenkamp, G. Challa, *J. Polym. Sci., Polym. Chem.* **1977**, *15*, 3031.

66) J. Gons, L. J. P. Straatman, G. Challa, *J. Polym. Sci., Polym. Chem.* **1978**, *16*, 427.

67) J. H. G. M. Lohmeyer, Y. Y. Tan, G. Challa, *J. Macromol. Sci., Chem.* **1980**, *A14*, 945.

68) T. Serizawa, K.-i. Hamada, M. Akashi, *Nature* **2004**, *429*, 52.

69) K.-i. Hamada, T. Serizawa, M. Akashi, *Macromolecules* **2005**, *38*, 6759.

70) G. Decher, *Science* **1997**, *277*, 1232.

71) Y. Shimazaki, M. Mitsuishi, S. Ito, M. Yamamoto, *Langmuir* **1997**, *13*, 1385.

72) Y. Shimazaki, M. Mitsuishi, S. Ito, M. Yamamoto, *Langmuir* **1998**, *14*, 2768.

73) W. B. Stockton, M. F. Rubner, *Macromolecules* **1997**, *30*, 2717.

74) T. Serizawa, H. Yamashita, T. Fujiwara, Y. Kimura, M. Akashi, *Macromolecules* **2001**, *34*, 1996.

75) T. Kida, T. Minabe, S. Nakano, M. Akashi, *Langmuir* **2008**, *24*, 9227.

76) M. Matsusaki, K. Kadowaki, Y. Nakahara, M. Akashi, *Angew. Chem., Int. Ed.* **2007**, *46*, 4689.

77) M. Matsusaki, H. Ajiro, T. Kida, T. Serizawa, M. Akashi, *Adv. Mater.* **2012**, *24*, 454.

78) T. Serizawa, K.-i. Hamada, T. Kitayama, N. Fujimoto, K. Hatada, M. Akashi, *J. Am. Chem. Soc.* **2000**, *122*, 1891.

79) T. Serizawa, K.-i. Hamada, T. Kitayama, K.-i. Katsukawa, K. Hatada, M. Akashi, *Langmuir* **2000**, *16*, 7112.

80) K.-i. Hamada, T. Serizawa, T. Kitayama, N. Fujimoto, K. Hatada, M. Akashi, *Langmuir* **2001**, *17*, 5513.

81) T. Serizawa, K.-i. Hamada, T. Kitayama, M. Akashi, *Angew. Chem., Int. Ed.* **2003**, *42*, 1118.

82) F. Bosscher, D. Keekstra, G. Challa, *Polymer* **1981**, *22*, 124.

83) F. Bosscher, G. ten Brinke, G. Challa, *Polymer* **1982**, *15*, 1442.

84) J. D. Stroupe, R. E. Hughes, *J. Am. Chem. Soc.* **1958**, *80*, 2341.

85) V. M. Coiro, P. De Santis, A. M. Liquori, L. Mazzarella, *J. Polym. Sci. (C)* **1969**, *16*, 4591.

86) H. Tadokoro, Y. Chatani, H. Kusanagi, M. Yokoyama, *Macromolecules* **1970**, *3*, 441.

87) F. Bosscher, G. ten Brinke, A. Eshuis, G. Challa, *Macromolecules* **1982**, *15*, 1364.

88) H. Kusanagi, Y. Chatani, H. Tadokoro, *Macromolecules* **1994**, *35*, 2028.

89) T. Serizawa, K. Yamashita, M. Akashi, *Polym. J.* **2006**, *38*, 503.

90) T. Serizawa, Y. Nagasaka, H. Matsuno, M. Shimoyama, K. Kurita, *Bioconjugate Chem.* **2007**, *18*, 355.

91) M. Crne, J. O. Park, M. Srinivasarao, *Macromolecules* **2009**, *42*, 4353.

92) H. Sugaya, Y. Sakai, *Contrib. Nephrol.* **1998**, *125*, 1.

93) T. Takeyama, Y. Sakai, *Contrib. Nephrol.* **1998**, *125*, 9.

94) T. Kida, M. Mouri, M. Akashi, *Angew. Chem., Int. Ed.* **2006**, *45*, 7534.

95) S. Qi, H. Iida, L. Liu, S. Irie, W. Hu, E. Yashima, *Angew. Chem., Int. Ed.* **2013**, *52*, 1049.

96) T. Kawauchi, J. Kumaki, E. Yashima, *J. Am. Chem. Soc.* **2006**, *128*, 10560.

97) T. K. Goh, J. F. Tan, S. N. Guntari, K. Satoh, A. Blencowe, M. Kamigaito, G. G. Qiao, *Angew. Chem., Int. Ed.* **2009**, *48*, 8707.

98) T. Nakano, K. Takewaki, T. Yade, Y. Okamoto, *J. Am. Chem. Soc.* **2001**, *123*, 9182.

99) T. Kitayama, S. He, Y. Hironaka, T. Iijima, K. Hatada, *Polym. J.* **1995**, *27*, 314.

100) K.-i. Hamada, T. Serizawa, M. Akashi, unpublished data.

101) *Polymer Handbook, 3rd ed.*, ed. by J. Brandrup, E. H. Immergut, John Wiley & Sons, New York, Chichester, Brisbane, Toronto, Singapore, **1989**.

102) *Polymers at Interfaces*, ed. by G. D. Fleer, M. A. C. Stuart, J. M. H. M. Scheutjens, T. Cosgrove, B. Vincent, Chapman & Hall: London, Glasgow, New York, Tokyo, Melbourne, Madras, **1993**.

103) *Emulsion Polymerization and Emulsion Polymers*, ed. by P. A. Lovell, M. S. EI-Aasser, John Wiley & Sons: New York, Chichester, Brisbane, Toronto, Singapore, **1997**.

104) T. Taniike, P. Chammingkwan, M. Terano, *Catal. Commun.* **2012**, *27*, 13.

# Part 1 Analyses of Structure and Molecular Recognition Ability of Porous Isotactic Poly(methyl methacrylate) Thin Films at Nanolevel Scale

# Chapter 1

# Dynamics of Polymer Chains in Porous Isotactic Poly(methyl methacrylate) Thin Films

## 1. 1 INTRODUCTION

Porous nanospaces composed of a regular structure in solids and membranes have been of great interest for decades, because such structures provide precise reaction fields and enable specific molecular recognition. For example, S. Kitagawa *et al.* recently reported the polymerization of styrene in self-assembled porous coordination polymer materials.[1] Y. Tsujita *et al.* prepared a smart membrane with syndiotactic polystyrene and molecular cavities after the removal of small molecules from the polymer–solvent complex.[2] However, little data is available on porous nanospaces based on polymer–polymer interactions.

Recently, E. Yashima *et al.* observed atomic force microscopy (AFM) image of a monolayer of isotactic (*it*) poly(methyl methacrylate) (PMMA) and syndiotactic (*st*) PMMA stereocomplex formed by van der Waals interactions.[3] In contrast, layer-by-layer (LbL) assembly is a convenient procedure to prepare multilayered thin

polymer films with polymer–polymer interactions by the simple alternating immersions of a substrate into each polymer solution.[4] In our laboratory, thin films of *it*-PMMA/*st*-PMMA stereocomplexes were fabricated on a substrate with the LbL assembly.[5] Similarly, *it*-PMMA/*st*-poly(methacrylic acid) (PMAA) stereocomplex thin films were also formed, in which the component polymers possess different solvent solubilities.[6]

It is noteworthy that porous *it*-PMMA films could be prepared by the selective extraction of *st*-PMAA from *it*-PMMA/*st*-PMAA stereocomplex films with an alkaline solution. The porous *it*-PMMA films were used for the recognition of stereoregular polymers[7] and template polymerization,[8] which strongly suggests that these porous films possess stereoregular (*st*-PMAA) nanospaces. However, the detailed structure remains unclear at present, although the surface roughness and conformation were analyzed by AFM and infrared (IR) spectroscopy. On the other hand, X-ray diffraction (XRD) analysis is a powerful tool to confirm the packing structure of polymer chains. For example, *it*-PMMA/*st*-PMMA stereocomplex thin films on silica particles were analyzed by XRD.[9] In this study, we used XRD analysis for porous *it*-PMMA films obtained from *it*-PMMA/*st*-PMAA stereocomplex films. The evidences of dynamics of *it*-PMMA chains in the thin films, as well as its porous structure, were confirmed by XRD analyses (Figure 1-1).
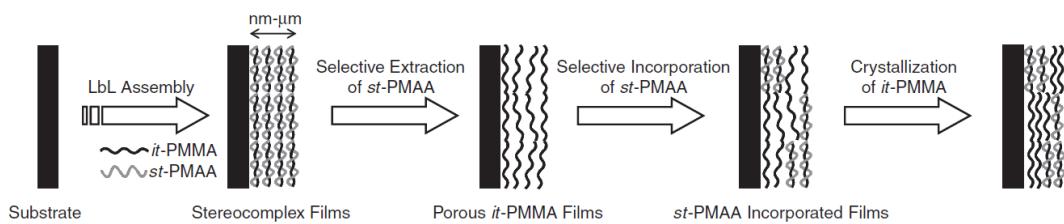
**Figure 1-1.** Schematic illustration of the dynamics of *it*-PMMA chains in porous thin films: fabrication of *it*-PMMA/*st*-PMAA stereocomplex films with LbL assembly, selective extraction of *st*-PMAA, and subsequent *st*-PMAA incorporation and *it*-PMMA crystallization.

## 1. 2 EXPERIMENTAL

*it*-PMMA ($M_n$ = 22900, $M_w/M_n$ = 1:21, *mm:mr:rr* = 96:2:2) and *st*-PMAA ($M_n$ = 33700, $M_w/M_n$ = 1:45, *mm:mr:rr* = 1:5:94) were synthesized by conventional anionic polymerization.[10,11] Porous *it*-PMMA thin films were prepared as follows. A 100-step alternative immersion process into an *it*-PMMA acetonitrile solution and a *st*-PMAA acetonitrile/water (4/6, v/v) mixed solution of 0.017 unitM was performed to generate stereocomplexes of *it*-PMMA/*st*-PMAA on a glass substrate at 25 ºC. Next, 10mM NaOH aq. was used to extract the *st*-PMAA from the stereocomplex by simple immersion for 30 min, which resulted in porous *it*-PMMA thin films. Subsequently, *st*-PMAA was incorporated into the porous films by immersing the films in the same *st*-PMAA solution at 25 ºC. The XRD patterns were taken by Rigaku RINT2000. Ni-filtered CuK$\alpha$ ($\lambda$ = 0.154 nm) was used as X-ray source and operated with Rigaku ultraX18 (40 kV, 200 mA). Films were examined in the scanning angle range from 5 to 35º at a scan rate of 0.5º/min.

## 1. 3 RESULTS AND DISCUSSION

The observed reflections of the multilayered polymer films are ascribed to the packing of the polymer chains. The XRD patterns from the LbL assembly of *it*-PMMA and *st*-PMAA for a 100-step assembly (Figure 1-2a) showed two characteristic peaks of *it*-PMMA/*st*-PMAA stereocomplex ($2\theta$ = 12 and 15°, *d* = 0.74 and 0.59 nm, respectively),[12] none of which are present in *it*-PMMA or *st*-PMAA. This result clearly indicates that *it*-PMMA/*st*-PMAA stereocomplex films were formed on the glass surface.
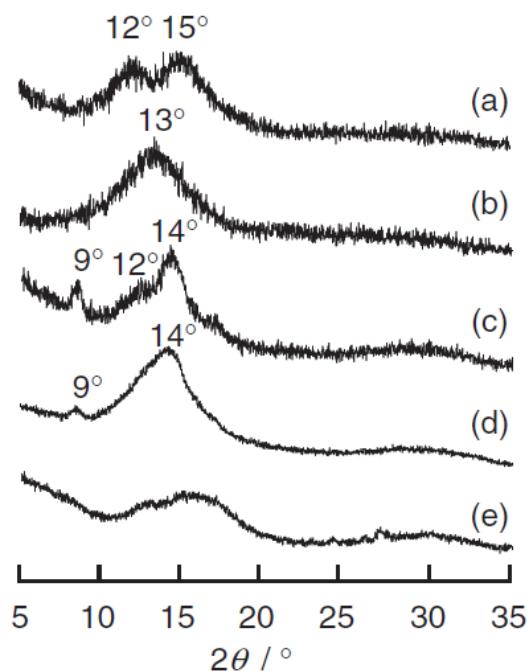


**Figure 1-2.** XRD patterns of (a) *it*-PMMA/*st*-PMAA stereocomplex films, (b) porous *it*-PMMA films, (c) *st*-PMAA incorporated films (after 600 min of immersion), (d) *it*-PMMA powder, and (e) *st*-PMAA powder.

*st*-PMAA was then selectively extracted from the stereocomplex thin films to form porous *it*-PMMA thin films, supported by IR spectra.[7] Surprisingly, the peak from the

porous films (Figure 1-2b) shifted from that of the stereocomplex films. The broad reflection at $2\theta = 13^{\circ}$ ($d = 0.67$ nm) suggests that the crystallinity in the films had decreased. The distance between the polymer chains in the films also expanded as compared to *it*-PMMA powder (Figure 1-2d),[13] suggesting that the evidence of porous structure was obtained and that stereoregular (*st*-PMAA) nanospaces could be fabricated in the thin films. In a previous report using AFM,[7] the surface roughness of the porous films increased after the extraction of *st*-PMAA, supporting the molecular-level extraction in this result.

Next, *st*-PMAA was incorporated into porous *it*-PMMA films. In Figure 1-2c, the XRD pattern of *st*-PMAA incorporated films (after 600-min immersion) showed a shoulder peak characteristic of the stereocomplex ($2\theta = 12^{\circ}$) with two peaks of crystalline *it*-PMMA ($2\theta = 9$ and $14^{\circ}$, $d = 0.96$ and $0.62$ nm, respectively).[13] It is known that *st*-PMAA was incorporated into about 80% of the *it*-PMMA in the porous films analyzed by a quartz crystal microbalance (12-step assembly).[7] The present result indicates that the stereocomplexes were partially formed, and the residual semicrystalline *it*-PMMA crystallized. Thus, we propose that the molecular motion to assemble caused by polymer—polymer interactions could be a driving force to crystallize even at the solid—liquid interface, regardless of whether it is *it*-PMMA itself or the *it*-PMMA/*st*-PMAA stereocomplex.

The temporal changes of the aforementioned porous *it*-PMMA structure were monitored by immersing the films into a *st*-PMAA solution (Figure 1-3). The intensities at $2\theta = 9$ and $14^{\circ}$, which were assigned to crystalline *it*-PMMA, gradually increased. Probably, the movement of the *it*-PMMA chains in the crystalline thin films depends on appropriate solubilities, such as acetonitrile. In contrast, as the intensities around $2\theta =$

12º were constant, the stereocomplex formation occurred more rapidly than *it*-PMMA crystallization.
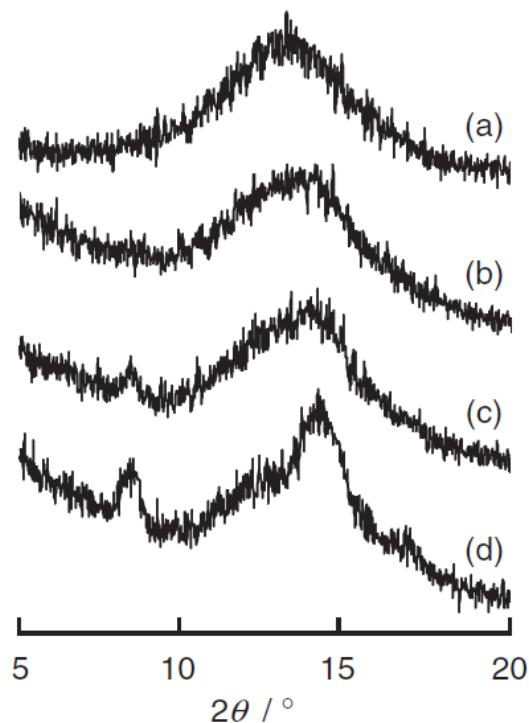


**Figure 1-3.** XRD patterns of (a) porous *it*-PMMA films, *st*-PMAA incorporated films after (b) 40 min of immersion, (c) 115 min of immersion, and (d) 600 min of immersion, respectively.

## 1.4 CONCLUSIONS

The porous structure of *it*-PMMA films with stereoregular (*st*-PMAA) nanospaces was confirmed by XRD analysis for the first time. Furthermore, the polymer chains moved slightly at the interface, changing the packing distances. The porous *it*-PMMA films not only incorporated *st*-PMAA, but also slowly crystallized. Thus, competition

between the stereocomplex formation and *it*-PMMA crystallization occurred when the porous films immersed into a *st*-PMAA solution. Further research is currently underway testing various conditions in order to apply this useful nanospace for specific recognition of stereoregular polymers and template polymerization efficiently.

## REFERENCES

1) T. Uemura, S. Horike, S. Kitagawa, *Chem. Asian. J.* **2006**, *1*, 36.

2) Y. Tsujita, H. Yoshimizu, S. Okamoto, *J. Mol. Struct.* **2005**, *739*, 3.

3) J. Kumaki, T. Kawauchi, K. Okoshi, H. Kusanagi, E. Yashima, *Angew. Chem., Int. Ed.* **2007**, *46*, 5348.

4) G. Decher, *Science* **1997**, *277*, 1232.

5) T. Serizawa, K.-i. Hamada, T. Kitayama, N. Fujimoto, K. Hatada, M. Akashi, *J. Am. Chem. Soc.* **2000**, *122*, 1891.

6) T. Serizawa, K.-i. Hamada, T. Kitayama, K.-i. Katsukawa, K. Hatada, M. Akashi, *Langmuir* **2000**, *16*, 7112.

7) T. Serizawa, K.-i. Hamada, T. Kitayama, M. Akashi, *Angew. Chem., Int. Ed.* **2003**, *42*, 1118.

8) T. Serizawa, K.-i. Hamada, M. Akashi, *Nature* **2004**, *429*, 52.

9) T. Kida, M. Mouri, M. Akashi, *Angew. Chem., Int. Ed.* **2006**, *45*, 7534.

10) K. Hatada, K. Ute, K. Tanaka, T. Kitayama, Y. Okamoto, *Polym. J.* **1985**, *17*, 977.

11) T. Kitayama, S. He, Y. Hironaka, T. Iijima, K. Hatada, *Polym. J.* **1995**, *27*, 314.

12) J. H. G. M. Lohmeyer, Y. Y. Tan, P. Lako, G. Challa, *Polymer* **1978**, *19*, 1171.

13) R. P. Kusy, *J. Polym. Sci., Polym. Chem. Ed.* **1976**, *14*, 1527.

# Chapter 2

# Solvent Effects on Isotactic Poly(methyl methacrylate) Crystallization and Syndiotactic Poly(methacrylic acid) Incorporation in Porous Thin Films

## 2. 1 INTRODUCTION

Biomacromolecules have a higher order nanostructure, and assemble by themselves in certain environments. For example, DNA forms a double helix via complementary base-pair hydrogen bond interactions in water, which precisely recognizes the sequence to control the replication process.[1] In synthetic polymers, isotactic (*it*) poly(methyl methacrylate) (PMMA) and syndiotactic (*st*) PMMA form a stereocomplex driven by a good steric fit between the two chains in specific solvents or in solids.[2-4] G. Challa *et al.* suggested that the stereocomplex formed a complementary double-stranded helix, in which *it*-PMMA was surrounded by *st*-PMMA based on an X-ray analysis of the stretched fibers.[5] Recently, E. Yashima *et al.* proposed a triple-stranded helix model, in which a double-stranded of *it*-PMMA was surrounded by a single helix of *st*-PMMA, based on high-resolution atomic force microscopy (AFM) images of the stereocomplex monolayers obtained with the Langmuir-Blodgett technique.[6,7] On the other hand, layer-by-layer (LbL) assembly has been known as a versatile technique to prepare polymer thin films on a substrate by simple alternate immersion into interactive polymer solutions.[8] Electrostatic interactions between oppositely charged polymers have been widely utilized as a driving force for LbL assembly. In our laboratory, van der

Waals interactions have been applied to stereoregular polymer thin films such as polymethacrylate[9-12] or poly(lactic acid)[13] stereocomplexes.

Stereocomplexes were also formed when the methyl ester groups of *st*-PMMA were replaced by carboxyl or other alkyl ester groups, whereas the methyl ester of *it*-PMMA was essential.[2-4,14,15] Therefore, stereocomplex formations between *it*-PMMA and various *st*-polymethacrylates have been well-researched. In particular, a stereocomplex thin film composed of *it*-PMMA and *st*-poly(methacrylic acid)[11] (PMAA) is very attractive due to the fact that a porous *it*-PMMA thin film can be prepared by the selective extraction of *st*-PMAA from the stereocomplex film, taking advantage of the different solubilities of each component polymer. In this manner, macromolecular porous thin films were utilized as a host film for stereoregular polymers[16] or oligomers[17] and for the template polymerization of methacrylates,[18,19] although the mechanisms responsible for these phenomena are still under study.

For the aforementioned *it*-PMMA/*st*-PMAA stereocomplex, it would also be important to examine two kinds of stereocomplex models (double-stranded helix[5] versus triple-stranded helix[6,7]), since the stereocomplex composed of *it*-PMMA/*st*-PMMA and that composed of *it*-PMMA/*st*-PMAA are considered to be basically the same structure on X-ray analysis.[15,20] *it*-PMMA would form a single helix in the double-stranded stereocomplex model, and a double-stranded helix in the triple-stranded stereocomplex model, respectively. We anticipated that it could be a significant approach to elucidate whether the *it*-PMMA helix inside the stereocomplexes would adopt a single-strand or a double-strand shape by extracting only the *st*-PMAA component from the stereocomplex films to observe the *it*-PMMA chains directly. It is also believed that the helical shape of *it*-PMMA is maintained after *st*-PMAA extraction

from the stereocomplex films with an aqueous alkaline solution, because the residual *it*-PMMA is insoluble in water. More recently, we observed porous *it*-PMMA thin films, *st*-PMAA incorporation into these films, and partial *it*-PMMA crystallization in the films using X-ray diffraction (XRD) analysis.[21]

*it*-PMMA has been famous not only for its unique crystalline double-stranded helix,[22] but also for its extremely slow crystallization rate. It takes several days to develop a semicrystalline morphology in melt or cast *it*-PMMA film by annealing at high temperature.[23-26] The *it*-PMMA chains, however, are more flexible than *st*-PMMA and atactic (*at*) PMMA chains, because the glass transition temperature of *it*-PMMA (around 40 ºC) is much lower than *st*-PMMA and *at*-PMMA (both above 100 ºC).[27] Recently, the snake-like motion of a single *it*-PMMA chain deposited on a substrate under humid air was observed by in-situ AFM.[28,29] Various solvents have been studied to investigate the nature of PMMA, because some solvents can affect *it*-PMMA dynamics. Among them, acetonitrile is a theta solvent[30] and water is a nonsolvent for PMMA, respectively. Mixed solvents of acetonitrile and water have been utilized for the LbL assembly of *it*-PMMA/*st*-PMAA stereocomplexes due to the controllable solubilities of *it*-PMMA and *st*-PMAA.[11,16,17,19,21] *it*-PMMA crystallization and *st*-PMAA incorporation in the porous *it*-PMMA thin films were also occurred in a mixed solvent of acetonitrile/water (4/6, v/v).[16,21]

In this study, we further investigated the molecular motion of *it*-PMMA chains in porous thin films after various solvent treatments by XRD, infrared (IR), and AFM, as well as the solvent effects and incorporation rates of *st*-PMAA into the porous films using a quartz crystal microbalance (QCM). According to the present results, the mechanisms of *st*-PMAA incorporation and template polymerization in the porous

*it*-PMMA films are also discussed.


## 2. 2 EXPERIMENTAL

**Materials** *it*-PMMA ($M_n$ = 22900, $M_w/M_n$ = 1.21) and *st*-PMAA ($M_n$ = 33700, $M_w/M_n$ = 1.45) were synthesized by anionic polymerization in toluene at −78 ºC with *t*-C$_4$H$_9$MgBr[31] and *t*-C$_4$H$_9$Li/bis(2,6-di-*t*-butylphenoxy)methyl-aluminium[32] as initiators, respectively. The number average molecular weights and their distribution were measured by gel permeation chromatography (Tosoh System HLC-8120GPC) with PMMA standards at 40 ºC. Two commercial columns (TSKgel SuperH4000 and TSKgel GMH$_{XL}$) were connected in series, and tetrahydrofuran was used as an eluent. Their tacticities (*mm*:*mr*:*rr*), which were analyzed from their $\alpha$-methyl proton signals using 400-MHz NMR (nitrobenzene-$d_5$, 110 ºC), were 96:2:2 and 1:5:94, respectively. The characterization of *st*-PMAA was achieved after methylation of the carboxyl group to *st*-PMMA by diazomethane solutions. Acetonitrile was purchased from Wako Pure Chemical Industries (Japan). Ultrapure distilled water was provided by the MILLI-Q laboratory (MILLIPORE).

**Stepwise Assembly** A substrate (a slide glass or QCM electrode) was cleaned 3 times with a piranha solution (H$_2$SO$_4$:40% H$_2$O$_2$ aqueous solution = 3:1 by volume) for 1 min each, followed by rinsing with ultrapure water and drying with N$_2$ gas. The cleaned substrate was immersed into an *it*-PMMA acetonitrile solution at a concentration of 0.017 unitM for 5 min at 25 ºC. The substrate was then taken out, and rinsed thoroughly with acetonitrile. The substrate was again immersed into a *st*-PMAA acetonitrile/water (4/6, v/v) solution at a concentration of 0.017 unitM for 5 min at 25 ºC. The aforementioned procedure was repeated to fabricate stereocomplexes of

*it*-PMMA/*st*-PMAA on the substrate. This alternative deposition cycle was repeated until the desired multilayers were obtained. Next, porous *it*-PMMA thin films were prepared by the extraction of *st*-PMAA by immersion into a 10 mM NaOH aqueous solution, and were characterized by IR, AFM,[16] and XRD.[21]

**X-ray Diffraction** A 100-step alternative immersion process into an *it*-PMMA solution and a *st*-PMAA solution was performed with a slide glass. The XRD patterns were taken by a Rigaku RINT2000. CuK$\alpha$ ($\lambda = 0.154$ nm) was used as the X-ray source and operated at 40 kV, 200 mA with a Ni filter (Rigaku ultraX18). The films were examined at $2\theta = 5$ to 35º at a scan rate of 0.5º/min.

**Infrared Spectroscopy** Multilayered thin films of a 16-step assembly of *it*-PMMA and *st*-PMAA were prepared on QCM substrates. Attenuated total reflection (ATR) IR spectra of the thin films were then obtained with a Spectrum 100 FT-IR spectrometer (Perkin-Elmer, USA). The interferograms were co-added 64 times, and Fourier-transformed at a resolution of 4 cm$^{-1}$.

**Atomic Force Microscopy** A 16-step alternative immersion was performed using a QCM substrate. Porous *it*-PMMA thin films were prepared by the same procedure as per the stepwise assembly. AFM images were obtained with a JSPM-5400 (JEOL, Japan) that was operated in the tapping mode in air at ambient temperature. Scanning was performed using silicon cantilevers (NSC35, $\mu$-masch; resonance frequency: around 150 kHz; spring constant: 4.5 N/m) within an area of $1 \times 1$ μm$^2$ with a 512 scan line and a scan speed of 2.0 μm/s. We did not perform any image processing other than the flat leveling. The mean square roughness ($R$a) in the observed areas was estimated from the following equation where $F(x,y)$ is the surface relative to the center plane, and $Lx$ and $Ly$ are the dimensions of the surface.

$$Ra = 1/(LxLy)\int_0^{Lx} \int_0^{Ly} \mid F(x,y) \mid \,\mathrm{d}x\,\mathrm{d}y$$

**Quartz Crystal Microbalance** An AT-cut QCM with a parent frequency of 9 MHz was obtained from USI (Japan). The frequency was monitored by an Iwatsu frequency counter (Model 53131A). The quartz crystal (9 mm diameter) was coated on both sides with mirror-like polished gold electrodes (4.5 mm in diameter). The alternative immersion process was performed with QCM substrates.

## 2. 3 RESULTS AND DISCUSSION

Using an acetonitrile/water (4/6, v/v) solvent, *st*-PMAA incorporation and *it*-PMMA crystallization in the porous *it*-PMMA thin films occurred at the same time, though their rates were very different.[21] We paid attention to the solvent effects on *it*-PMMA crystallization in the porous films without *st*-PMAA at the beginning of this study. Acetonitrile might promote *it*-PMMA crystallization, but the *it*-PMMA multilayered thin films dissolve in it. Therefore, we selected acetonitrile/water with a 4/6 (v/v) composition as the solvent with proper solubility. To analyze the structural changes of the porous *it*-PMMA thin films, three measurement methods, XRD, Fourier transform (FT) IR, and AFM were employed as described below.
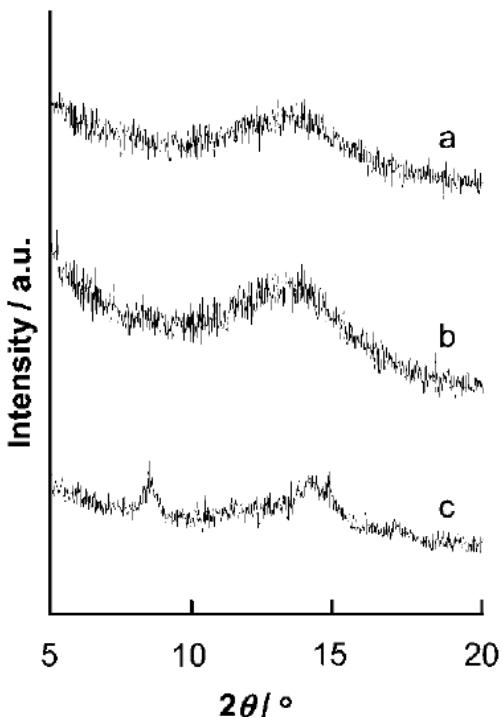
**Figure 2-1.** XRD patterns of (a) porous *it*-PMMA films and (b, c) *it*-PMMA films after 10 h of immersion (b) in water and (c) in a mixed  acetonitrile/water (4/6, v/v) solvent.

Figure 2-1 shows the XRD patterns of the *it*-PMMA thin films. After the prepared films were immersed into water for 10 h, the peak pattern of the films did not change as compared to that of the initial porous films ($2\theta = 13°$, $d = 0.67$ nm) (Figure 2-1a, b). This observation seems to be reasonable, because *it*-PMMA chains do not aggregate in water, although a peculiar repetitive movement of single *it*-PMMA chains deposited on mica under humid air was reported.[28,29] In contrast, two peaks of crystalline *it*-PMMA[33] appeared ($2\theta = 9$ and $14°$, $d =0.96$ and 0.62 nm, respectively) after immersion into acetonitrile/water (4/6, v/v) for 10 h (Figure 2-1c). This result indicates that acetonitrile plays an important role in *it*-PMMA crystallization in porous multilayered films, whereas water keeps the film structure porous. Thus, water enables template polymerization in porous *it*-PMMA films when used as a solvent.[18,19] However, the

structure of the porous *it*-PMMA thin films after *st*-PMAA extraction from the stereocomplex assembly could not be determined in detail, because the crystallinity decreased as compared to that of the stereocomplex based on the broad spectral pattern.[21] It was also demonstrated that the crystallized *it*-PMMA in the thin films formed a double-stranded helix consisting of two chains.[22,33]

The FT-IR/ATR spectra of the carbonyl vibration region were used to detect the polymer chain conformation. Two peaks assigned to *it*-PMMA (1737 cm$^{-1}$) and *st*-PMAA (1726 cm$^{-1}$) were observed for the LbL assembly, which supported stereocomplex formation (Figure 2-2a).[11] Even after removal of the *st*-PMAA from the stereocomplex by immersion into an aqueous alkaline solution, the conformation of the *it*-PMMA main chain was still maintained according to only one peak of *it*-PMMA observed at 1739 cm$^{-1}$ (Figure 2-2b),[16] although a random conformation of *it*-PMMA was observed at 1725 cm$^{-1}$ prepared by cast film.[11,16] In the present study, we observed IR spectra focused on the conformational changes of the crystallized *it*-PMMA films when immersing the films into acetonitrile/water (4/6, v/v). The peaks of the *it*-PMMA films after immersion in the mixed solvent for 10 and 40 h were observed at 1736 and 1737 cm$^{-1}$, respectively (Figure 2-2c, d). These observations indicate that *it*-PMMA chains maintain their conformation after crystallization.
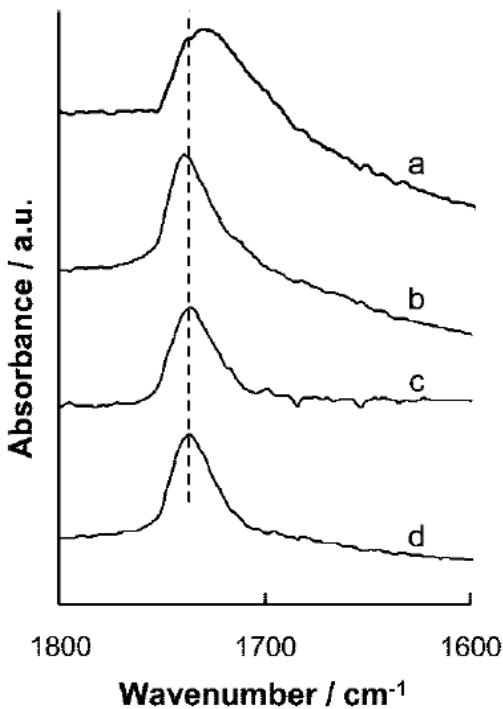
**Figure 2-2.** FT-IR/ATR spectra of (a) the LbL assembly of *it*-PMMA and *st*-PMAA for a 16-step assembly, (b) porous *it*-PMMA films, and (c, d) crystallized *it*-PMMA films after (c) 10 and (d) 40 h of immersion in a mixed acetonitrile/water (4/6, v/v) solvent.

In Figure 2-3, AFM images of the *it*-PMMA films are shown. The mean square roughness (*Ra*) of the QCM substrate and porous *it*-PMMA films after 10 h of immersion in water was 3.9 and 7.2 nm, respectively. A relatively smooth surface[16] was maintained even after the water treatment (Figure 2-3a). On the other hand, several hemispherical outshoots were observed on the surface of crystallized *it*-PMMA films after 10 h of immersion in acetonitrile/water (4/6, v/v), and the height reached several hundreds of nanometers (Figure 2-3b). The outshoots are likely aggregates of crystalline *it*-PMMA because they appeared only when immersed in acetonitrile/water (4/6, v/v) and the structure was confirmed by XRD measurement (Figure 2-1c). The *Ra* was 39 nm, which was much larger than the porous films. As reported previously, it is therefore

conceivable that the solvent affected the surface roughness of the films[9] and the dynamics of the *it*-PMMA chains[21] in the thin films.
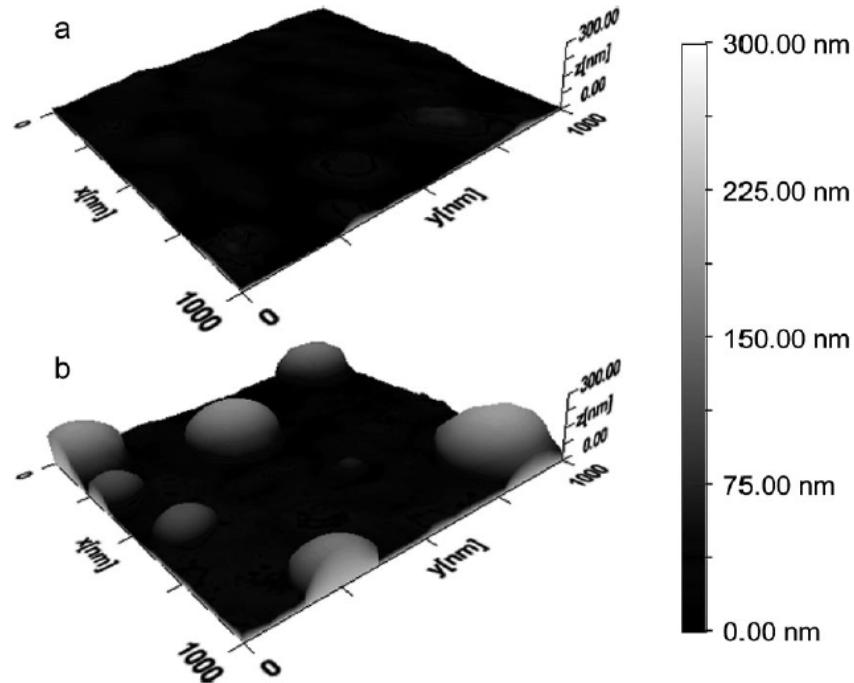


**Figure 2-3.** AFM images of (a) porous *it*-PMMA films after 10 h of immersion in water and (b) crystallized *it*-PMMA films after 10 h of immersion in acetonitrile/water (4/6, v/v).

Next, we moved to QCM analyses to investigate what percentages of stereocomplexes would be formed in the multilayered thin films. QCM analysis is a powerful tool to calculate the amount of absorbed polymer at the nano gram order, $\Delta m$, by measuring the frequency decrease, $\Delta F$, using Sauerbrey's equation.[34]

$$-\Delta F \ (\text{Hz}) = 1.15 \Delta m \ (\text{ng})$$
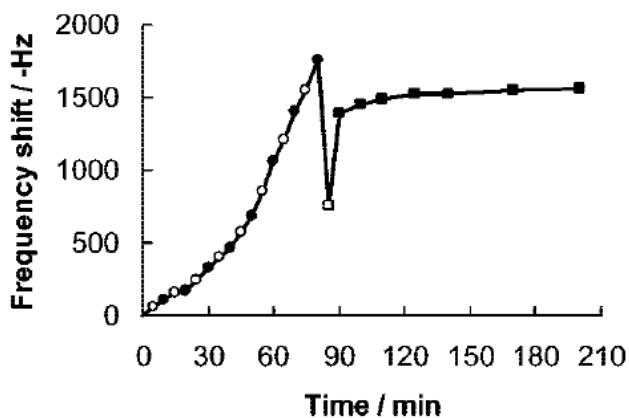
**Figure 2-4.** Typical QCM analysis of the LbL assembly and selective extraction and subsequent incorporation of *st*-PMAA. *it*-PMMA in acetonitrile (white circles) and *st*-PMAA (black circles) were alternately assembled on a QCM substrate at 0.017 unitM at 25 °C. The porous *it*-PMMA films were prepared by *st*-PMAA extraction using 10 mM NaOH(aq) (white square). The following *st*-PMAA incorporation was observed at a concentration of 0.017 unitM at 25 °C (black squares).

A typical QCM analysis is shown in Figure 2-4. The stepwise, alternative assembly of *it*-PMMA and *st*-PMAA, the selective extraction of *st*-PMAA, and the subsequent *st*-PMAA incorporation were observed as described in previous studies.[11,16] The drastic frequency shift at the extraction stage showed the total amount of adsorbed *st*-PMAA in the stepwise assembly. The ratio of extraction amount towards total amount of assembled *st*-PMAA was 102 ± 7.02 % ($n$ = 30). The molar ratios of the units assembled from *st*-PMAA and *it*-PMMA calculated from the QCM analyses were between 1 and 1.5, and were not equal to 2 (*st*-PMAA/*it*-PMMA).[14] It is suggested that a mixture of the stereocomplexes with 1/1 and 2/1 unit molar ratios (*st*-PMAA/*it*-PMMA) was formed,[11] though QCM analyses mean all amount of stepwise assembled *it*-PMMA and *st*-PMAA should interact each other because there would be almost no weight change when one component is treated.[9] Therefore, the complex efficiency defined in previous studies[16,17] was not applied to the *st*-PMAA incorporation stages in this study. We defined the

incorporation, which was calculated as a percentage of the incorporated *st*-PMAA weight against the extracted *st*-PMAA weight, under the assumption that the stereocomplex formed again with the identical ratios as the original LbL assembly.

$$\text{Incorporation (\%)} = W_{incorporation}/W_{extraction} \times 100$$
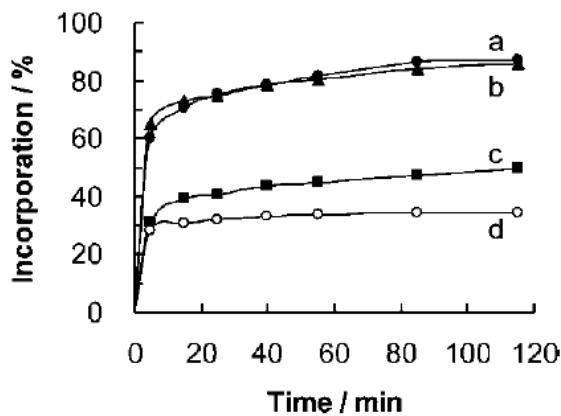


**Figure 2-5.** Time dependence of *st*-PMAA incorporation into porous *it*-PMMA films at a concentration of 0.017 unitM at 25 °C. The porous films were immersed into a *st*-PMAA mixed acetonitrile/water (4/6, v/v) solution after (a) *st*-PMAA extraction, (b) 10 h of immersion in water, and (c) 10 and (d) 40 h of immersion in a mixed acetonitrile/water (4/6, v/v) solvent.

We were interested in whether *it*-PMMA would recognize *st*-PMAA even after crystallization. The *st*-PMAA incorporation was around 80 % towards the porous *it*-PMMA thin films after immersion in water for 10 h, which was similar to the value of the porous films just after *st*-PMAA extraction (Figure 2-5a, b). This is likely because the terminal of *it*-PMMA might support the porous film structure when *st*-PMAA was extracted from the stereocomplex films, but could not incorporate *st*-PMAA.[16] It is implied that the stereocomplex formation was similarly generated without any structural

51

change of *it*-PMMA in water (Scheme 2-1A). In contrast, after immersion in acetonitrile/water (4/6, v/v) for 10 and 40 h, the incorporations was reduced to around 50 and 35 %, respectively (Figure 2-5c, d). The decreased values suggest that crystallized *it*-PMMA in the thin films lost their stereocomplex formation capability as it may have shortened the packing distance (Scheme 2-1B) and formed hemispherical outshoots under immersion in acetonitrile/water (4/6, v/v) (Figure 2-3b). However, the macroscopic deformation such as destroy of pores in the porous *it*-PMMA films could not significantly influence incorporation of *st*-PMAA because reversible incorporation and extraction of *st*-PMAA were occurred using spin-coated *it*-PMMA films with no pores.[16] It is believed that the films are slightly swollen by acetonitrile, and interfacial rearrangement is occurred in the spin-coated films. FT-IR/ATR spectra also confirmed that incorporation of *st*-PMAA into the crystallized *it*-PMMA films was occurred not through physical adsorption but thorough stereocomplex formation. The carbonyl vibration peak of *st*-PMAA in the stereocomplex assembly was observed around 1726 cm$^{-1}$, although a random conformation of *st*-PMAA was observed at 1695 cm$^{-1}$ prepared by cast film.[11,16]

**Scheme 2-1. Schematic Illustration of the Molecular Motion of *it*-PMMA in Multilayered Thin Films*[a]***
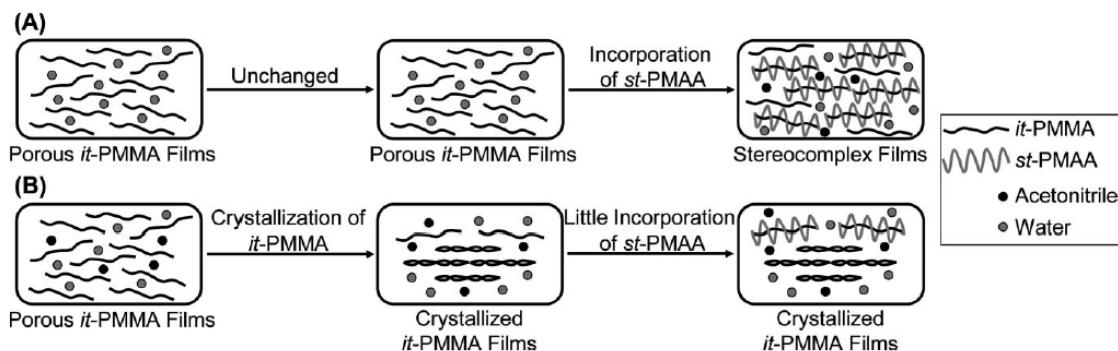


*[a]* Porous *it*-PMMA films, which were unchanged in water, selectively incorporated *st*-PMAA to form the stereocomplex (A). Crystallized *it*-PMMA films, which were prepared by immersion in acetonitrile/water (4/6, v/v), barely incorporated any *st*-PMAA (B).

It is believed that acetonitrile solvated the *it*-PMMA chains, and enhanced their molecular motion.[11,21] Therefore, the solvent effect of a *st*-PMAA solution during the incorporation stages was also investigated. Porous *it*-PMMA thin films were immersed into *st*-PMAA solutions with various ratios of acetonitrile/water (0.017 unitM). A *st*-PMAA solution with an acetonitrile content of more than 60 % was not examined because of the poor solubility of *st*-PMAA. Figure 2-6 shows the time dependence of the incorporation using various *st*-PMAA solutions. *st*-PMAA was barely incorporated into the porous *it*-PMMA films in water or acetonitrile/water (1/9, v/v) (Figure 2-6a, b), whereas the maximal incorporation increased significantly between 20 and 40 vol % of acetonitrile in the *st*-PMAA solution. From the fact that *st*-PMAA was slowly incorporated into the porous films (Figure 2-6c, d), it is believed that the *it*-PMMA chains in the film are slightly swollen by acetonitrile in the mixed solvents. At more

than 50 % of acetonitrile, the incorporation values saturated to about 80 % (Figure 2-6e, f, g). These results suggest that the *it*-PMMA chains could not move enough to change its conformation in water, and a certain degree of solvation in acetonitrile is necessary in order to incorporate *st*-PMAA. Acetonitrile is known as a strongly complexing solvent,[35] and would dynamically change the adsorbed *it*-PMMA chains from a random conformation into the proper shape for the stereocomplex formation at the stepwise assembly stages.[9,11] In contrast, the conformation of *it*-PMMA remained the same as that in the stereocomplex during the *st*-PMAA incorporation stages.[16] This enabled template polymerization to form the stereocomplex, even in water,[18,19] which is a nonsolvent for PMMA. Therefore, in the thin films, acetonitrile is not always necessary for stereocomplex formation, but is regarded as a solvent here to slightly solvate the *it*-PMMA chains. The solubilities of *st*-PMAA would not generate a significant effect, because the stereocomplex films did not dissolve in water. However, penetration of *st*-PMAA into the porous *it*-PMMA films is also necessary to form the stereocomplex. In Figure 2-7, the FT-IR/ATR spectra of the *st*-PMAA incorporated films with various mixed solutions were shown. The peak intensities of *st*-PMAA (1726 cm$^{-1}$) in the stereocomplexes increased with the acetonitrile content, which is in good agreement with the results of the QCM analyses (Figure 2-6). These observations also demonstrate that stereocomplex formation was promoted as the acetonitrile content increased in the *st*-PMAA solution. However, from Figure 2-7, the absorbance of *st*-PMAA for *it*-PMMA increased between acetonitrile/water (v/v) 4/6, 5/5, and 6/4, though these maximal incorporation were almost same (Figure 2-6). This might be because a mixture of the stereocomplexes with 1/1 and 2/1 (*st*-PMAA/*it*-PMMA) was formed as the original stereocomplex assembly. The IR carbonyl vibration of *it*-PMMA and *st*-PMAA

in a stereocomplex film with 1:1 stoichiometry are observed at 1731 and 1717 cm^{-1},[18] and 1:2 (*it*-PMMA:*st*-PMAA) stoichiometry are at 1737 and 1726 cm^{-1},[11] respectively. Thus, stereocomplexes with 1:2 stoichiometry were likely most formed using acetonitrile/water (6/4, v/v).
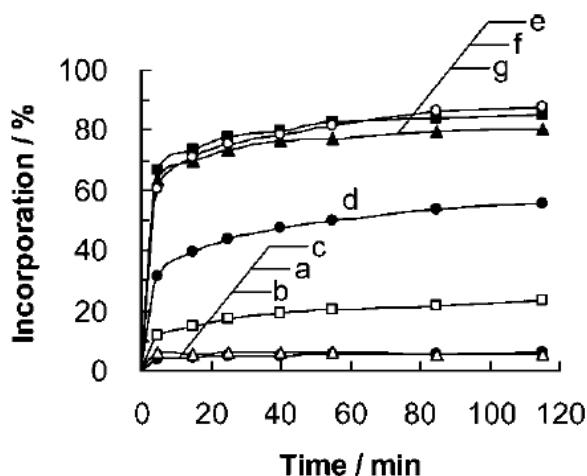


**Figure 2-6.** Time dependence of *st*-PMAA incorporation into porous *it*-PMMA films at a concentration of 0.017 unitM at 25 °C. The porous films were immersed into a *st*-PMAA soulution of mixed acetonitrile/water (v/v) solvents: (a) water, (b) 1/9, (c) 2/8, (d) 3/7, (e) 4/6, (f) 5/5, and (g) 6/4.

55
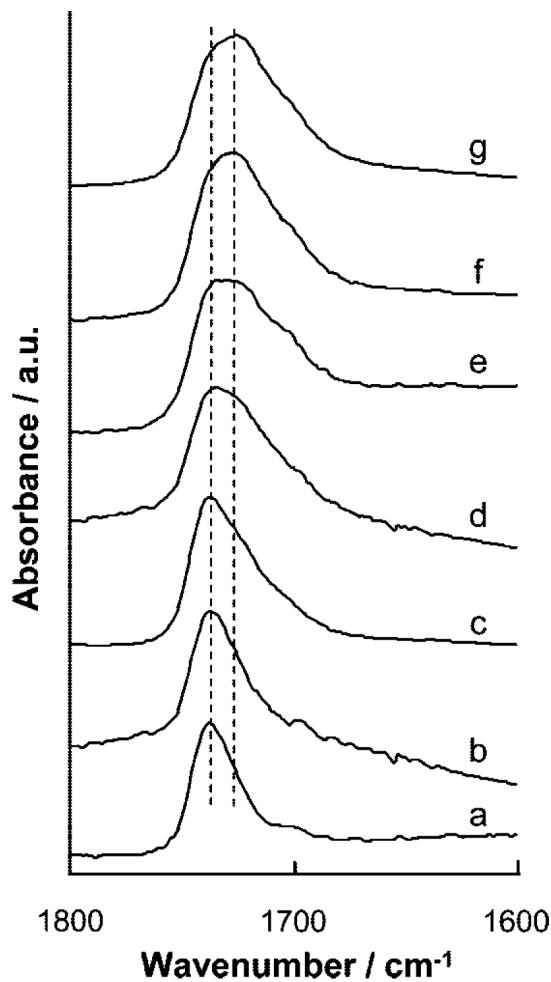
**Figure 2-7.** FT-IR/ATR spectra of *st*-PMAAincorporated films. The porous films were immersed into a *st*-PMAA soulution of mixed acetonitrile/water (v/v) solvents: (a) water, (b) 1/9, (c) 2/8, (d) 3/7, (e) 4/6, (f) 5/5, and (g) 6/4.

Film thickness would also affect the incorporation of *st*-PMAA into the porous *it*-PMMA thin films. Figure 2-8A shows the time dependence of the *st*-PMAA incorporation into porous *it*-PMMA thin films of varying thickness in a *st*-PMAA acetonitrile/water (4/6, v/v) solution. There was a tendency for *st*-PMAA to penetrate more slowly into the porous films as the amount of porous *it*-PMMA films was increasing. The thickness of the porous *it*-PMMA films, which corresponded to

56

approximately -800 Hz/QCM, was determined as 44 nm by AFM scratching mode in a previous study.[16] Therefore, the *it*-PMMA film thickness was calculated in this study according to an estimation of the increased thickness at a constant rate of 0.055nm/Hz (Figure 2-8B). The incorporation decreased to around 40 % with an increasing thickness of the porous *it*-PMMA films. Although it is difficult to explain why the decreasing behavior of the *st*-PMAA incorporation into the films became suppressed, the *it*-PMMA chains in the films would be evenly swollen by acetonitrile. Thus, it could be suggested that *st*-PMAA penetrated into the *it*-PMMA layer on the film surface easily, but more slowly inside the multilayered films due to entanglements with each polymer chain or interactions of the *it*-PMMA chains themselves.
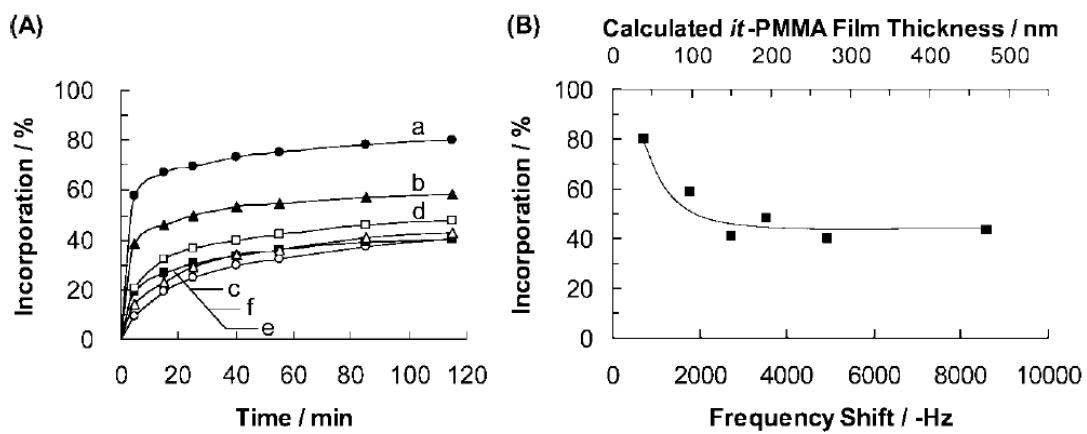


**Figure 2-8.** (A) Time dependence of *st*-PMAA incorporation into porous *it*-PMMA films prepared by LbL assembly for (a) 16-, (b) 24-, (c) 32-, (d) 40-, (e) 48-, and (f) 64-step assemblies in mixed acetonitrile/water (4/6, v/v) *st*-PMAA solutions at a concentration of 0.017 unitM at 25 °C. (B) Frequency shift dependence of the porous *it*-PMMA films for the incorporation of *st*-PMAA into the porous films.

## 2. 4 CONCLUSIONS

We investigated the structure of partially crystallized *it*-PMMA multilayered thin films and the mechanism of *st*-PMAA incorporation into the films. The XRD pattern of the *it*-PMMA thin films after immersion into acetonitrile/water (4/6, v/v) showed two peaks of a crystalline *it*-PMMA double-stranded helix ($2\theta = 9$ and $14°$). According to the FT-IR spectra, the *it*-PMMA chains maintained their conformations after the crystallization. Hemispherical outshoots with heights of several hundred nanometers were observed on the surface of crystallized *it*-PMMA films by AFM. The incorporation percentages of *st*-PMAA into the porous films decreased as the *it*-PMMA films crystallized, or with an increasing thickness of the porous *it*-PMMA films, probably due to the entanglement of *it*-PMMA chains. However, the incorporation into the porous films was gradually improved, when the acetonitrile contents of the *st*-PMAA solution increased from 20 to 40 vol %. In contrast, *it*-PMMA crystallization as well as *st*-PMAA incorporation did not occur using only water, which is a nonsolvent for *it*-PMMA. Thus, it can be concluded that the acetonitrile percentage in water is important for the dynamics of *it*-PMMA chains in porous thin films. We believe that these structural investigations and the incorporation behavior of the stereoregular host films also provide important insights for the analysis of template polymerization mechanisms.

## REFERENCES

1) J. D. Watson, F. H. C. Crick, *Nature* **1953**, *171*, 737.

2) J. Spevacek, B. Schneider, *Adv. Colloid Interface Sci.* **1987**, *27*, 81.

3) K. te Nijenhuis, *Adv. Polym. Sci.* **1997**, *130*, 67.

4) K. Hatada, T. Kitayama, *Polym. Int.* **2000**, *49*, 11.

5) E. Schomaker, G. Challa, *Macromolecules* **1989**, *22*, 3337.

6) J. Kumaki, T. Kawauchi, K. Okoshi, H. Kusanagi, E. Yashima, *Angew. Chem., Int. Ed.* **2007**, *46*. 5348.

7) J. Kumaki, T. Kawauchi, K. Ute, T. Kitayama, E. Yashima, *J. Am. Chem. Soc.* **2008**, *130*, 6373.

8) G. Decher, *Science* **1997**, *277*, 1232.

9) T. Serizawa, K.-i. Hamada, T. Kitayama, N. Fujimoto, K. Hatada, M. Akashi, *J. Am. Chem. Soc.* **2000**, *122*, 1891.

10) T. Kida, M. Mouri, M. Akashi, *Angew. Chem., Int. Ed.* **2006**, *45*, 7534.

11) T. Serizawa, K.-i. Hamada, T. Kitayama, K.-i. Katsukawa, K. Hatada, M. Akashi, *Langmuir* **2000**, *16*, 7112.

12) K.-i.Hamada, T. Serizawa, T. Kitayama, N. Fujimoto, K. Hatada, M. Akashi, *Langmuir* **2001**, *17*, 5513.

13) T. Serizawa, H. Yamashita, T. Fujiwara, Y. Kimura, M. Akashi, *Macromolecules* **2001**, *34*, 1996.

14) J. H. G. M. Lohmeyer, Y. Y. Tan, P. Lako, G. Challa, *Polymer* **1978**, *19*, 1171.

15) F. Bosscher, D. Keekstra, G. Challa, *Polymer* **1981**, *22*, 124.

16) T. Serizawa, K.-i. Hamada, T. Kitayama, M. Akashi, *Angew. Chem., Int. Ed.* **2003**, *42*, 1118.

17) H. Ajiro, D. Kamei, M. Akashi, *J. Polym. Sci., Part A: Polym. Chem.* **2008**, *17*, 5879.

18) T. Serizawa, K.-i. Hamada, M. Akashi, *Nature* **2004**, *429*. 52.

19) K.-i. Hamada, T. Serizawa, M. Akashi, *Macromolecules* **2005**, *38*, 6759.

20) F. Bosscher, G. ten Brinke, G. Challa, *Macromolecules* **1982**, *15*, 1442.

21) D. Kamei, H. Ajiro, C. Hongo, M. Akashi, *Chem. Lett.* **2008**, *37*, 332.

22) H. Kusanagi, H. Tadokoro, Y. Chatani, *Macromolecules* **1976**, *9*, 531.

23) A. de Boer, G. O. R. A. van Ekenstein, G. Challa, *Polymer* **1975**, *16*, 930.

24) K. Konnecke, G. Rehage, *Colloid Polym. Sci.* **1981**, *259*, 1062.

25) B. Schneider, J. Stokr, J. Spevacek, J. Baldrian, *Makromol. Chem.* **1987**, *188*, 2705.

26) K. Buyse, H. Berghmans, *Polymer* 2000, *41*, 1045.

27) *Polymer Handbook, 3rd ed.*, ed. by J. Brandrup, E. H. Immergut, John Wiley & Sons, New York, Chichester, Brisbane, Toronto, Singapore, **1989**.

28) J. Kumaki, T. Kawauchi, E. Yashima, *Macromolecules* **2006**, *39*, 1209.

29) J. Kumaki, T. Kawauchi, E. Yashima, *Macromol. Rapid Commun.* **2008**, *29*, 406.

30) M. Kamijo, N. Sawatari, T. Konishi, T. Yoshizaki, H. Yamakawa, *Macromolecules* **1994**, *27*, 5697.

31) K. Hatada, K. Ute, T. Tanaka, T. Kitayama, Y. Okamoto, *Polym. J.* **1985**, *17*, 977.

32) T. Kitayama, S. He, Y. Hironaka, T. Iijima, K. Hatada, *Polym. J.* **1995**, *27*, 314.

33) R. P. Kusy, *J. Polym. Sci., Part A: Polym. Chem.* **1976**, *14*, 1527.

34) G. Sauerbrey, *Z. Phys.* **1959**, *155*, 206.

35) E. J. Vorenkamp, F. Bosscher, G. Challa, *Polymer* **1979**, *20*, 59.

# Chapter 3

# Specific Recognition of Syndiotactic Poly(methacrylic acid) in Porous Isotactic Poly(methyl methacrylate) Thin Films Based on the Effects of Complexing Solvent, Temperature, and Stereoregularity

## 3. 1 INTRODUCTION

The stereocomplexation of poly(methyl methacrylate)s (PMMA) has received significant attention because stereocomplexes are unique structures composed of isotactic (*it*) and syndiotactic (*st*) PMMA chains bonded together by van der Waals forces.[1—3] These PMMA stereocomplexes form a multiple-stranded helical structure, which was demonstrated by X-ray[4] and atomic force microscopy.[5,6] Although the basic structure and mechanism of complex formation are still unclear, the formation of thermoreversible ion gels,[7] hollow capsules,[8] fibers,[9] and nano- or microstructures[10—13] via stereocomplexation have been reported recently as advanced materials. Numerous studies have also been performed on stereocomplex formation between *it*-PMMA and *st*-PMMA in solution,[14—18] bulk,[19] supercritical fluids,[20—22] and Langmuir-Blodgett films.[5,6,23—27] Furthermore, Challa *et al.* investigated the stereoselective association between *it*-PMMA and *st*-polymethacrylates in solution,[28—30] and the stereospecific polymerization of methacrylates in the presence of *it*-PMMA or *st*-PMMA.[31—33] However, there are few reports on stereocomplexes composed of *it*-PMMA and

*st*-poly(methacrylic acid) (PMAA).

In our laboratory, the layer-by-layer (LbL) assembly technique[34] has been employed to fabricate multilayered thin films composed of PMMA stereocomplexes on quartz crystal microbalance (QCM) substrates.[35—37] In particular, macromolecularly porous *it*-PMMA thin films obtained from *it*-PMMA/*st*-PMAA stereocomplex assemblies are very important from a scientific point of view, as will be described next. Porous *it*-PMMA films demonstrated the selective recognition of *st*-polymethacrylates,[38] and provided precise reaction fields for the perfectly controlled template polymerization of methacrylic acid (MAA),[39—41] because the van der Waals interactions were maximal, which contributes to stereocomplex formation due to suppressed molecular motion in the porous films as compared to in solution.[28—33]

More recently, we investigated the mechanisms responsible for this system, such as the recognition of similar guest molecules[42,43] or the structure of the porous *it*-PMMA films under specific conditions.[44—48] As a result, it is hypothesized that the template polymerization follows a pick up mechanism, in which the growing oligomer radical interacts with the porous *it*-PMMA films and MAA is freely supplied from the solution.[42] However, studies on the incorporation behaviors of *st*-PMAA with lower tacticities synthesized in the solution or at higher temperature conditions, in which the template polymerization was achieved,[39—41] are necessary not only to confirm the hypothesis but to get important insights into the regularity and stability of nanospaces in the *it*-PMMA films. In addition, it has been reported that acetonitrile content in the *st*-PMAA solution affects on the unit-molar ratio stoichiometry of *st*-PMAA/*it*-PMMA in the stereocomplex films[36] and the mobility of the *it*-PMMA polymer chains in the porous films.[45] Therefore, specific incorporation of *st*-PMAA into the porous *it*-PMMA

films depending on complexing solvents[29] would be achieved in this system.

In this study, we investigated the effects of stereoregularity, temperature, and solvent on *st*-PMAA incorporation into the porous *it*-PMMA films using QCM and infrared (IR) spectroscopy (Scheme 3-1).

**Scheme 3-1. Schematic Illustration of *st*-PMAA Extraction from Stereocomplex Films Composed of *it*-PMMA/*st*-PMAA, and Subsequent Specific *st*-PMAA Incorporation in Porous *it*-PMMA Films. Steregularity, Temperature, and Solvent Affect the *st*-PMAA Incorporation.**
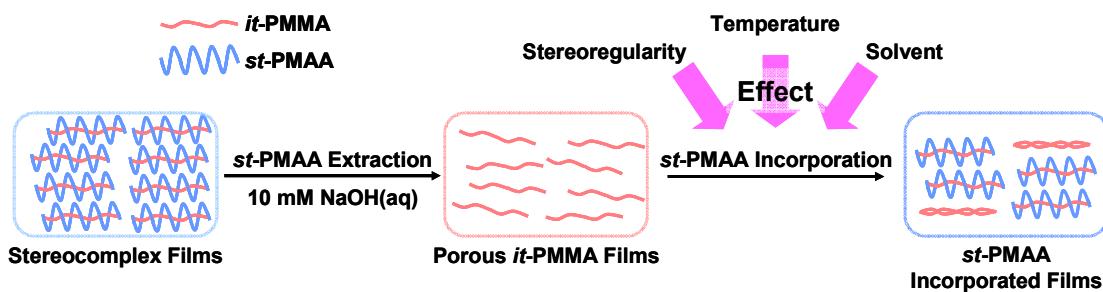


## 3. 2 EXPERIMENTAL

**Materials** *it*-PMMA and *st*-PMAA were synthesized by anionic polymerization in toluene at −78 ºC with *t*-C$_4$H$_9$MgBr[49] and *t*-C$_4$H$_9$Li[50] as initiators, respectively. *st*-PMAA of low tacticity was synthesized by radical polymerization in water at 40 ºC with 2,2'-azobis[2-(2-imidazolin-2-yl)propane] dihydrochloride as a water-soluble initiator. The number average molecular weights ($M_n$) and their distribution ($M_w/M_n$) were measured by size exclusion chromatography (Tosoh System HLC-8120GPC) with PMMA standards at 40 ºC in tetrahydrofuran. Their tacticities (*mm*:*mr*:*rr*) were analyzed from their α-methyl proton signals using 400-MHz NMR (nitrobenzene-$d_5$,

110 ℃). The characterization of *st*-PMAA was achieved after methylation of the carboxyl group to *st*-PMMA by a diazomethane solution. The characteristics of these polymers are summarized in Table 3-1, and the sample codes are abbreviated using the tacticity. Acetonitrile, *N,N*-dimethylformamide (DMF), and ethanol were purchased from Wako Pure Chemical Industries. Ultrapure distilled water was provided by the MILLI-Q labo.

**Table 3-1.** Stereoregular Polymethacrylates Synthesized in This Study

| Sample code | $M_n$ | $M_w/M_n$ | Tacticity / % | | |
|---|---|---|---|---|---|
| | | | *mm* | *mr* | *rr* |
| *it*-PMMA-96 | 22900 | 1.21 | 96 | 2 | 2 |
| *st*-PMAA-94 | 33700 | 1.45 | 1 | 5 | 94 |
| *st*-PMAA-73 | 36000 | 2.36 | 3 | 24 | 73 |
| *st*-PMAA-62 | 34200 | 2.25 | 5 | 33 | 62 |

**Quartz Crystal Microbalance** An AT-cut QCM with a parent frequency of 9 MHz was obtained from USI. The frequency was monitored by an Iwatsu frequency counter (Model 53131A). The quartz crystal (9 mm diameter) was coated on both sides with mirror-like polished gold electrodes (4.5 mm in diameter). QCM analysis enables us to calculate the amount of absorbed polymer at the nano gram order, $\Delta m$, by measuring the frequency decrease, $\Delta F$, using following equation.[51]

$$-\Delta F \text{ (Hz)} = 1.15\Delta m \text{ (ng)}$$

QCM electrode was cleaned three times with a piranha solution ($H_2SO_4$/40% $H_2O_2$ aqueous solution = 75/25, v/v) for 1 min each, followed by rinsing with ultrapure water and drying with $N_2$ gas. The cleaned substrate was immersed into an *it*-PMMA-96 acetonitrile solution at a concentration of 0.017 unitM for 5 min at 25 ℃. The substrate was then taken out, and rinsed thoroughly with acetonitrile. The QCM substrate was again immersed into a *st*-PMAA-94 acetonitrile/water (40/60, v/v) solution at a concentration of 0.017 unitM for 5 min at 25 ℃. The aforementioned procedure was repeated to fabricate stereocomplexes of *it*-PMMA/*st*-PMAA on the QCM substrate. This alternative deposition cycle was repeated for 16 steps. Then, porous *it*-PMMA thin films were prepared by the extraction of *st*-PMAA using 10 mM NaOH aqueous solution. Next, the porous *it*-PMMA films were immersed in each *st*-PMAA solution at a concentration of 0.017 unitM and rinsed with each solvent.

**Infrared Spectroscopy** Attenuated total reflection (ATR) IR spectra of the thin films were obtained with a Spectrum 100 FT-IR spectrometer (Perkin-Elmer). The interferograms were co-added 64 times and were Fourier transformed.

## 3. 3 RESULTS AND DISCUSSION

It has been previously reported that *st*-PMAA with low tacticity (*rr* = 58%) was not incorporated into macromolecularly porous *it*-PMMA films.[38] However, this study was not sufficient to study the specific recognition mechanism of the stereoregularities in this system, because the only one sample was tested. Therefore, *st*-PMAA with different stereoregularities (*rr* = 94, 73, and 62%, respectively) and almost same $M_n$ were synthesized to compare the incorporations under the same conditions (Table 3-1). When

the molecular weight of *st*-PMAA was appropriately twice that of *it*-PMMA, the incorporation constant of *st*-PMAA was maximal, as described in the previous paper.[40] The molecular weight distributions ($M_w/M_n$) of *st*-PMAA-62 and *st*-PMAA-73 were almost the same, although they were broader than that of *st*-PMAA-94 because of the differences of the polymerization methods or catalysts. Thus, it is indicated that the difference of the stereoregularities between *st*-PMAA-62 and *st*-PMAA-73 would directly affect on the incorporation behaviors, while the effect of molecular weight distribution should be taken into consideration in the case of *st*-PMAA-94. A mixed solvent of acetonitrile/water (40/60, v/v) was used as the solvent for the *st*-PMAA solution, and the porous *it*-PMMA films were immersed into the *st*-PMAA solutions for 115 min.[44—46] The incorporation of *st*-PMAA was calculated as a percentage of the incorporated *st*-PMAA weight against the extracted *st*-PMAA weight from QCM analyses, as previously reported.[45]

$$\text{Incorporation (\%)} = W_{\text{incorporation}}/W_{\text{extraction}} \times 100$$

Figure 3-1 shows the time dependence of the *st*-PMAA incorporation in porous *it*-PMMA films. The incorporation of *st*-PMAA-94 was almost saturated within 20 min, and the value reached a maximum around 80% (Figure 3-1a).[38,45] Note that *st*-PMAA-73 was incorporated in the porous *it*-PMMA films very slowly, and the incorporation was not saturated within 115 min (Figure 3-1b), whereas *st*-PMAA-62 was barely incorporated in the porous *it*-PMMA films even after 115 min (Figure 3-1c). Therefore, *it*-PMMA films were immersed in the *st*-PMAA-73 solution for 800 min, with the result that the incorporation value reached a maximum at approximately 60%, and became saturated. This indicates that the incorporation rates depended on the stereoregularity of *st*-PMAA, and that the porous *it*-PMMA films could not recognize

the *st*-PMAA obtained with conventional free radical polymerization at this dilute concentration (0.017 unitM). Indeed, the *st*-PMAA-62, employed in this study, was synthesized in an aqueous solution under the same conditions that the template polymerization was achieved in the porous *it*-PMMA films.[41] Thus, these results show a model for understanding the mechanism of template polymerization; the porous *it*-PMMA films selectively recognized growing PMAAs, not of lower tacticities but of higher tacticities (*rr* > 73%), synthesized in solution, although the incorporation of *st*-PMAA-94 was much faster than that of *st*-PMAA-73.
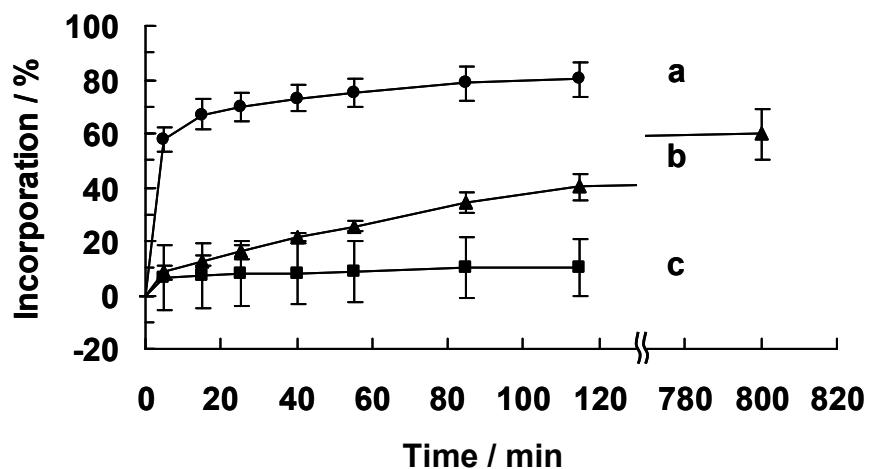


**Figure 3-1.** Time dependence of *st*-PMAA incorporation into porous *it*-PMMA films at a concentration of 0.017 unitM at 25 $^\circ$C. The porous films were immersed into a *st*-PMAA mixed acetonitrile/water (40/60, v/v) solution: (a) *st*-PMAA-94, (b) *st*-PMAA-73, and (c) *st*-PMAA-62 (the average value: *n* = 3).

FT-IR/ATR spectroscopy was used to evaluate the stereocomplex formation of *it*-PMMA/*st*-PMAA on a substrate.[36,38—40,42—48] The *it*-PMMA and *st*-PMAA peaks in the stereocomplexes were observed at 1737 and 1725 cm$^{-1}$, respectively, which

appeared on the *st*-PMAA-94 incorporated films after 115 min of immersion (Figure 3-2a). In contrast, the peak intensity of *st*-PMAA at the lower wavenumber was smaller on the *it*-PMMA/*st*-PMAA films after 800 min of immersion in the *st*-PMAA-73 solution (Figure 3-2b), as compared to the *st*-PMAA-94 incorporated films. In addition, there were almost no *st*-PMAA peaks on the *st*-PMAA-62 incorporated films (Figure 3-2c). These observations also demonstrated stereocomplex formation in the porous *it*-PMMA films, and supported the QCM results (Figure 3-1).
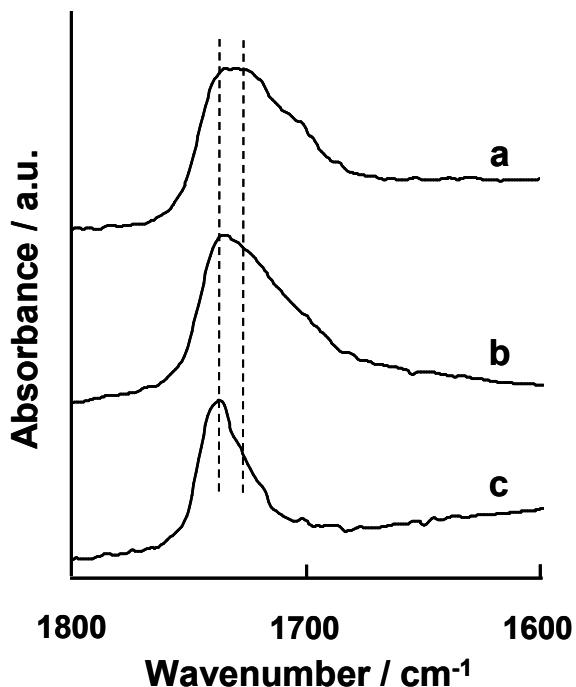


**Figure 3-2.** FTIR/ATR spectra of *st*-PMAA incorporated films. The porous films were immersed into a *st*-PMAA mixed acetonitrile/water (40/60, v/v) solution: (a) *st*-PMAA-94, (b) *st*-PMAA-73, and (c) *st*-PMAA-62.

Stereocomplex formation between *it*-PMMA and *st*-polymethacrylates in LbL films has been intensively investigated. However, almost all the reports were about the stereocomplexes with the highest stereoregularities.[35—41,44—48] Here, we reported the

first case of stereocomplex formation using *st*-PMAA with lower stereoregularity ($rr$ = 73%) in the LbL films (Figure 3-1b), although even *st*-PMMA with very low tacticity ($rr$ = 45%) was still able to form stereocomplexes with *it*-PMMA in solutions.[52] Furthermore, the multilayered thin films prepared by stepwise stereocomplex assembly of *it*-PMMA and *st*-PMAA-73 ($M_n$ = 50400, $M_w/M_n$ = 2.19) were successfully obtained, while the amount of the assemblies were about half that of *it*-PMMA and *st*-PMAA-94 (Figure 3-3). Note that the amount of *it*-PMMA films obtained by immersion of NaOH(aq) was almost the same as that of porous *it*-PMMA films using *st*-PMAA-94, because the amount of *st*-PMAA-73 at each step was much smaller compared with the case of *st*-PMAA-94, indicating that *st*-PMAA-73 only partially form stereocomplexes with *it*-PMMA. Therefore, *st*-PMAA-73 would form the stereocomplexes with *it*-PMMA more weakly than *st*-PMAA-94, which also affected on the incorporation rate in the porous *it*-PMMA films (Figure 3-1b). FT-IR/ATR spectrum of the assembled films composed of *it*-PMMA and *st*-PMAA-73 also demonstrated the stereocomplex formation, because its peak appeared at 1731 cm$^{-1}$ and shifted to a higher wavenumber compared to those of spin-coated *it*-PMMA (1725cm$^{-1}$) or *st*-PMAA films (1696 cm$^{-1}$).
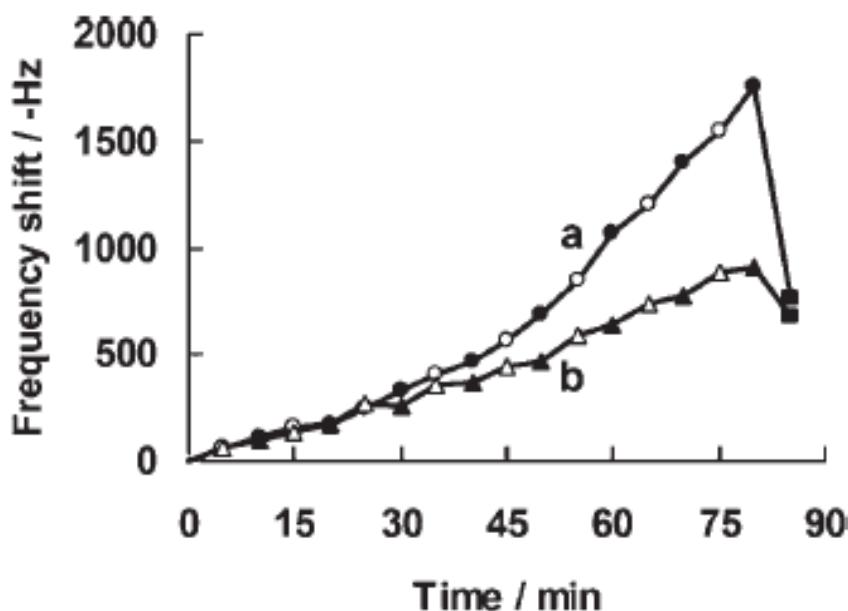
**Figure 3-3.** QCM analyses of 16-step assembly of *it*-PMMA in acetonitrile (whites) and *st*-PMAA (blacks) in acetonitrile/water (40/60, v/v) (*rr* = (a) 94 and (b) 73%, respectively) and subsequent selective extraction of *st*-PMAA using 10mM NaOH(aq) (black squares).

Next, the effects of temperature and solvent species on stereocomplex formation in porous *it*-PMMA films were investigated, and *st*-PMAA-94 was used to compare previous studies.[38,45] The maximum incorporation of *st*-PMAA is known to be around 80% in acetonitrile/water (40/60, v/v) at 25 ℃. However, we recently reported that the incorporation was variable when the acetonitrile content of the *st*-PMAA solution increased from 20 to 40 vol % at 25 ℃.[45] In order to observe slight changes from thermal effects on incorporation, we selected the solvent condition as acetonitrile/water (20/80, v/v), under which the maximum *st*-PMAA incorporation was approximately 20%.

*st*-PMAA was gradually incorporated into the porous *it*-PMMA films at 40 ℃, and the incorporation increased from 21% at 25 ℃ to 34% at 40 ℃ over 115 min (Figure

70

3-4b, c), suggesting that stereocomplexation is promoted with increasing temperature. However, there was almost no difference between 40 and 55 ºC, even after the porous it-PMMA films were immersed into st-PMAA solutions for 115 min (Figure 3-4a, b). Thus, these two films were also immersed for 800 min, with the result that there was not a significant difference considering the large margin of experimental error. It has been reported that competition between stereocomplex formation and it-PMMA crystallization occurred when the porous it-PMMA films were immersed into the st-PMAA solution.[44,45] Therefore, the it-PMMA crystallization would also be accelerated by an elevated temperature, and the stereocomplex formation might become progressively saturated. Figure 5 shows the FT-IR/ATR spectra of st-PMAA incorporated films at each temperature. Only one peak of it-PMMA (1737 cm$^{-1}$) was observed when the st-PMAA was incorporated at 25 ºC (Figure 3-5c), whereas the peak intensities of st-PMAA (1726 cm$^{-1}$) in the stereocomplexes increased with increasing incorporation of st-PMAA. Indeed, the maximum incorporation of the samples shown in Figure 3-4a, b were 60 and 50%, respectively.
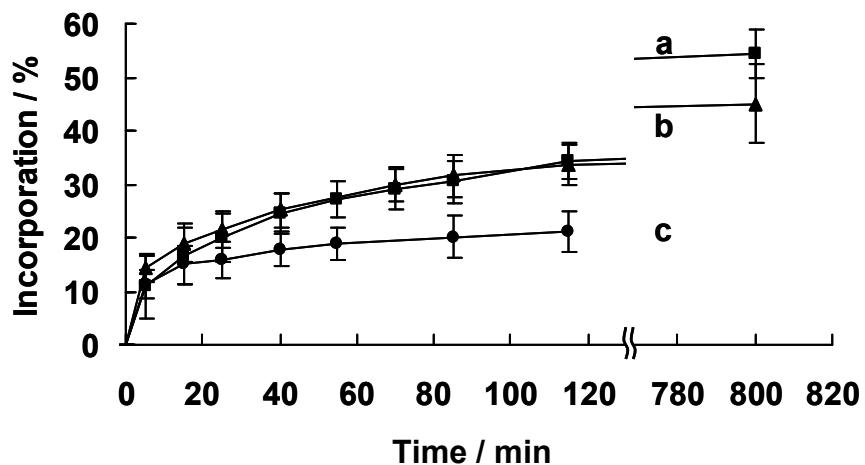
**Figure 3-4.** Time dependence of *st*-PMAA incorporation into porous *it*-PMMA films at a concentration of 0.017 unitM. The porous films were immersed into a *st*-PMAA mixed acetonitrile/water (20/80, v/v) solution at (a) 55 $^{\circ}$C, (b) 40 $^{\circ}$C, and (c) 25 $^{\circ}$C (the average value: $n = 3$).
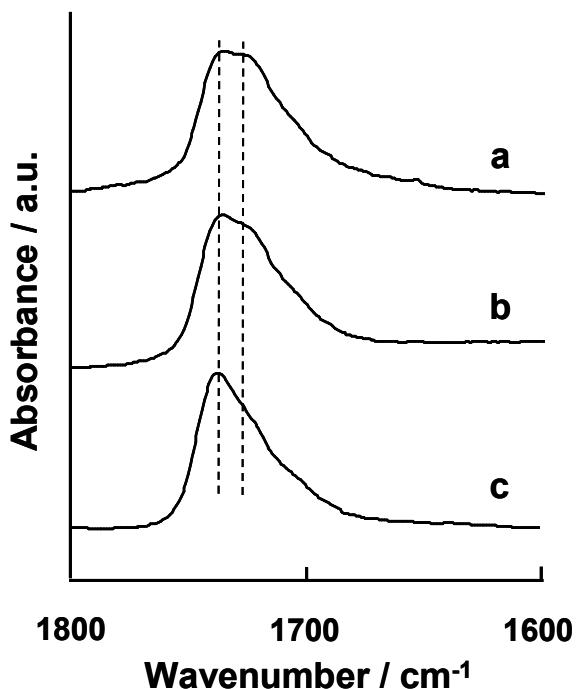


**Figure 3-5.** FTIR/ATR spectra of *st*-PMAA incorporated films. The porous films were immersed into a *st*-PMAA mixed acetonitrile/water (20/80, v/v) solution at (a) 55 $^{\circ}$C, (b) 40 $^{\circ}$C, and (c) 25 $^{\circ}$C.

72

We have previously studied *st*-PMAA incorporation in porous *it*-PMMA thin films using mixed solvents of acetonitrile/water.[38,42,44—46] However, other solvents such as DMF at 25 ℃,[28,29] ethanol/water (83/17, v/v) at 45 ℃,[29] and water at 70 ℃[39—41,43] have also been used as complexing solvents, although the *st*-PMAA synthesized in this study was not completely dissolved in DMF, likely due to differences in the tacticities or molecular weights. Thus, *st*-PMAA was dissolved in a mixed solvent of DMF/water (40/60, v/v) at 25 ℃, which has been employed for the LbL assembly of *it*-PMMA/*st*-PMAA.[39] *st*-PMAA incorporation in the porous films was then analyzed under these three conditions: ethanol/water (83/17, v/v) at 45 ℃, DMF at 25 ℃, and water at 70 ℃ at a concentration of 0.017 unitM.

The value of the incorporation at 5 min was −10% in ethanol/water (83/17, v/v) at 45 ℃ (Figure 3-6a), indicating that the films had peeled off in the mixed solvent. Indeed, porous *it*-PMMA films equivalent of about 50% incorporation were peeled off in 83 vol % ethanol/water at 45 ℃. However, the incorporation was improved from 15 min onward, and became almost saturated. The FT-IR/ATR spectrum of the films after 55 min immersion in ethanol/water (incorporation value: 13%) demonstrated the stereocomplex formation of *it*-PMMA/*st*-PMAA (Figure 3-7a). On the other hand, the incorporation in DMF/water (40/60, v/v) at 25 ℃ was approximately 8% at most (Figure 3-6b), although the porous films were not dissolved under these conditions. The IR spectrum also showed that almost no stereocomplexes were formed in the films in DMF/water (Figure 3-7b). It was reported that unit-molar ratio stoichiometry of *st*-PMAA/*it*-PMMA in the stereocomplex depended on the solvent species. The stereocomplex with 2/1 unit-molar stoichiometry (*st*-PMAA/*it*-PMMA) was formed in acetonitrile/water (40/60, v/v) at 25 ℃[36] or ethanol/water (83/17, v/v) at 70 ℃,[29] while

the stereocomplex with 1/1 unit-molar stoichiometry was formed in DMF/water (40/60, v/v) at 25 ºC.[39] Thus, these results suggest that *it*-PMMA in the porous films could only form the original 2/1 complex, in other word, rearrangement of the host *it*-PMMA from template of the 2/1 complex to the 1/1 complex could not happen. However, the mixed solvent of acetonitrile/water, which has also been employed for the LbL assembly of original stereocomplexes,[36,38,40—48] was most appropriate for *st*-PMAA incorporation in these porous *it*-PMMA films (Figure 3-1a).

Furthermore, the incorporation of *st*-PMAA in water at 70 ºC was around 5% (Figure 3-6c), and only the *it*-PMMA peak was observed by FT-IR (Figure 3-7c), although it was reported that porous *it*-PMMA films were not dissolved in the hot water over 3h.[43] We should also take into consideration the fact that the porous *it*-PMMA films incorporated the PMAA oligomers[42] instead of *st*-PMAA with a lower stereoregularity (*rr* = 62%) synthesized under the same conditions that template polymerization was achieved, and that the incorporation rates of *st*-PMAA depended on its tacticity (Figure 3-1). Therefore, this result strongly supports that the hypothesis that the mechanism of template polymerization is not *st*-PMAA incorporation in the porous films after polymerization of the MAA in solution, but rather oligomer incorporation with high tacticities from the aqueous solution and subsequent polymerization in the porous films.
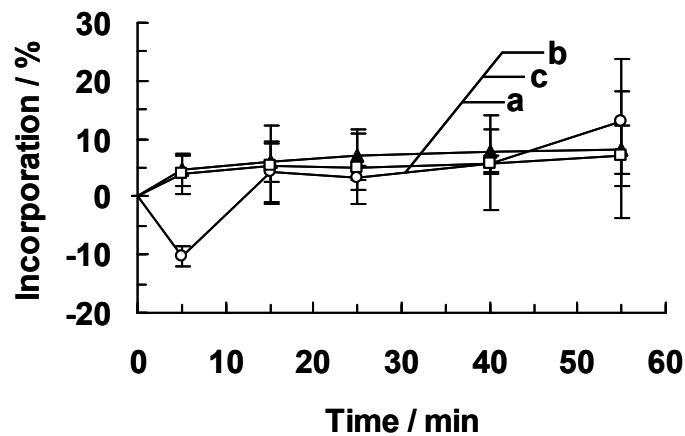
**Figure 3-6.** Time dependence of *st*-PMAA incorporation into porous *it*-PMMA films at a concentration of 0.017 unitM. The porous films were immersed into a *st*-PMAA solution: (a) ethanol/water (83/17, v/v) at 45 °C, (b) DMF/water (40/60, v/v) at 25 °C, and (c) water at 70 °C (the average value: $n = 3$).
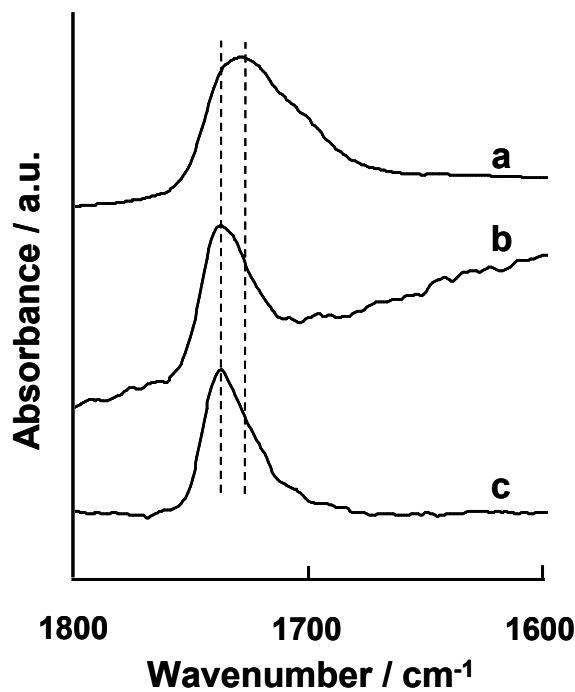


**Figure 3-7.** FTIR/ATR spectra of *st*-PMAA incorporated films. The porous films were immersed into a *st*-PMAA solution: (a) ethanol/water (83/17, v/v) at 45 °C, (b) DMF/water (40/60, v/v) at 25 °C, and (c) water at 70 °C.

## 3. 4 CONCLUSIONS

We demonstrated that *st*-PMAA incorporation in porous *it*-PMMA films depended on stereoregularity, temperature, and solvent using QCM and IR analyses. The first case of stereocomplex formation using *st*-PMAA with lower tacticity ($rr = 73\%$) in the LbL films was reported in this study, while *st*-PMAA obtained with conventional free radical polymerization ($rr = 62\%$) was barely incorporated into the porous *it*-PMMA films. It is recognized that van der Waals interactions between *it*-PMMA and *st*-PMAA at the interface were important, because the lack of stereoregularity of *st*-PMAA decreased the incorporation capability. In addition, the porous films could not incorporate *st*-PMAA ($rr = 94\%$) in water at 70 ºC. These investigations strongly support the hypothesis of template polymerization; the porous *it*-PMMA films would pick up growing PMAA with high tacticities from the aqueous solution and not *st*-PMAA. The maximum *st*-PMAA incorporation increased from 25 to 40 ºC, but there were almost no differences between at 40 ºC and at 55 ºC. This is likely because not only stereocomplex formation, but also *it*-PMMA crystallization, were promoted with increasing temperature. The porous *it*-PMMA films incorporated *st*-PMAA not in DMF/water (a complexing solvent of the 1/1 stereocomplex) but in acetonitrile/water or ethanol/water (complexing solvents of the 2/1 stereocomplex). These results could also shed light on the mechanism of the specific molecular recognition system.

## REFERENCES

1) J. Spevacek, B. Schneider, *Adv. Colloid Interface Sci.* **1987**, *27*, 81.

2) K. te Nijenhuis, *Adv. Polym Sci.* **1997**, *130*, 67.

3) K. Hatada, T. Kitayama, *Polym. Int.* **2000**, *49*, 11.

4) E. Schomaker, G. Challa, *Macromolecules* **1989**, *22*, 3337.

5) J. Kumaki, T. Kawauchi, K. Okoshi, H. Kusanagi, E. Yashima, *Angew. Chem., Int. Ed.* **2007**, *46*, 5348.

6) J. Kumaki, T. Kawauchi, K. Ute, T. Kitayama, E. Yashima, *J. Am. Chem. Soc.* **2008**, *130*, 6373.

7) T. Kawauchi, J. Kumaki, K. Okoshi, E. Yashima, *Macromolecules* **2005**, *38*, 9155.

8) T. Kida, M. Mouri, M.; Akashi, *Angew. Chem., Int. Ed.* **2006**, *45*, 7534.

9) M. Crne, J. O. Park, M. Srinivasarao, *Macromolecules* **2009**, *42*, 4353.

10) A. A. Kumar, K. Adachi, Y. Chujo, *J. Polym. Sci., Part A: Polym. Chem.* **2004**, *42*, 785.

11) T. Kawauchi, J. Kumaki, E. Yashima, *J. Am. Chem. Soc.* **2006**, *128*, 10560.

12) T. K. Goh, J. F. Tan, S. N. Guntari, K. Satoh, A. Blencowe, M. Kamigaito, G. G. Qiao, *Angew. Chem., Int. Ed.* **2009**, *48*, 8707.

13) N. C. Escude, E. Y. –X. Chen, *Chem. Mater.* **2009**, *21*, 5743.

14) H. Z. Liu, K. –J. Liu, *Macromolecules* **1968**, *1*, 157.

15) A. Boer, G. Challa, *Polymer* **1976**, *17*, 633.

16) E. Schomaker, G. Brinke, G.. Challa, *Macromolecules* **1985**, *18*, 1930.

17) E. Schomaker, E. J. Vorenkamp, G. Challa, *Polymer* **1986**, *27*, 256.

18) E. J. Lemieux, R. E. Prud'homme, *Polymer* **1998**, *39*, 5453.

19) E. Schomaker, G. Challa, *Macromolecules* **1988**, *21*, 2195.

20) T. Mizumoto, N. Sugimura, M. Moritani, Y. Sato, H. Masuoka, *Macromolecules* **2001**, *34*, 1291.

21) T. Mizumoto, N. Sugimura, M. Moritani, H. Yasuda, Y. Sato, H. Masuoka, *Macromolecules* **2001**, *34*, 5200.

22) S. Asai, T. Kawano, S. Hirota, Y. Tominaga, M. Sumita, T. Mizumoto, *Polymer* **2007**, *48*, 5116.

23) R. H. G. Brinkhuis, A. J. Schouten, *Macromolecules* **1992**, *25*, 2725.

24) R. H. G. Brinkhuis, A. J. Schouten, *Macromolecules* **1992**, *25*, 2732.

25) R. H. G. Brinkhuis, A. J. Schouten, *Macromolecules* **1993**, *26*, 2514.

26) J. Wang, D. Shen, S. Yan, *Macromolecules* **2004**, *37*, 8171.

27) J. Liu, Y. Zhang, J. Zhang, D. Shen, Q. Guo, I. Takahashi, S. Yan, *J. Phys. Chem. C* **2007**, *111*, 6488.

28) J. H. G. M. Lohmeyer, G. Kransen, Y. Y. Tan, G. Challa, *Polymer* **1975**, *13*, 725.

29) J. H. G. M. Lohmeyer, Y. Y. Tan, P. Lako, G. Challa, *Polymer* **1978**, *19*, 1171.

30) F. Bosscher, D. Keekstra, G. Challa, *Polymer* **1981**, *22*, 124.

31) R. Buter, Y. Y. Tan, G. Challa, *J. Polym. Sci., Part A: Polym. Chem.* **1972**, *10*, 1031.

32) R. Buter, Y. Y. Tan, G. Challa, *J. Polym. Sci., Part A: Polym. Chem.* **1973**, *11*, 1013.

33) J. H. G. M. Lohmeyer, Y. Y. Tan, G. Challa, *J. Macromol. Sci. Chem.* **1980**, *A14*, 945.

34) G. Decher, *Science* **1997**, *277*, 1232.

35) T. Serizawa, K.-i. Hamada, T. Kitayama, N. Fujimoto, K. Hatada, M. Akashi, *J. Am. Chem. Soc.* **2000**, *122*, 1891.

36) T. Serizawa, K.-i. Hamada, T. Kitayama, K.-i. Katsukawa, K. Hatada, M. Akashi, *Langmuir* **2000**, *16*, 7112.

37) K.-i. Hamada, T. Serizawa, T. Kitayama, N. Fujimoto, K. Hatada, M. Akashi, *Langmuir* **2001**, *17*, 5513.

38) T. Serizawa, K.-i. Hamada, T. Kitayama, M. Akashi, *Angew. Chem., Int. Ed.* **2003**, *42*, 1118.

39) T. Serizawa, K.-i. Hamada, M. Akashi, *Nature* **2004**, *429*, 52.

40) K.-i. Hamada, T. Serizawa, M. Akashi, *Macromolecules* **2005**, *38*, 6759.

41) H. Ajiro, D. Kamei, M. Akashi, *Polym. J.* **2009**, *41*, 90.

42) H. Ajiro, D. Kamei, M. Akashi, *J. Polym. Sci., Part A: Polym. Chem.* **2008**, *17*, 5879.

43) H. Ajiro, D. Kamei, M. Akashi, *Macromolecules* **2009**, *17*, 3019.

44) D. Kamei, H. Ajiro, C. Hongo, M. Akashi, *Chem. Lett.* **2008**, *37*, 332.

45) D. Kamei, H. Ajiro, C. Hongo, M. Akashi, *Langmuir* **2009**, *25*, 280.

46) D. Kamei, H. Ajiro, M. Akashi, *Polym. J.* **2010**, *42*, 131.

47) D. Kamei, H. Ajiro, M. Akashi, *J. Nanosci. Nanotech.* **2011**, *11*, 2545..

48) H. Ajiro, M. Maegawa, M. Akashi, *J. Polym. Sci., Part A: Polym. Chem.* **2012**, *50*, 1469.

49) K. Hatada, K. Ute, T. Tanaka, T. Kitayama, Y. Okamoto, *Polym. J.* **1985**, *17*, 977.

50) T. Kitayama, S. He, Y. Hironaka, T. Iijima, K. Hatada, *Polym. J.* **1995**, *27*, 314.

51) G. Sauerbrey, *Z. Phys.* **1959**, *155*, 206.

52) J. Spevacek, *Macomol. Chem.* **1987**, *188*, 861.

# Part 2 Morphological Observations of Porous Isotactic Poly(methyl methacrylate) Thin Films at Micrometer Scale

# Chapter 4

# Morphological Change of Isotactic Poly(methyl methacrylate) Thin Films by Self-organization and Stereocomplex Formation

## 4. 1 INTRODUCTION

Stereoregular poly(methyl methacrylate)s (PMMA) have attracted much attention because of their unique crystalline structure, morphology, and other particular properties since the first report by J. D. Stroupe *et al.*[1] Isotactic (*it*) PMMA and syndiotactic (*st*) PMMAcan self-aggregate either by themselves or as stereocomplexes. it-PMMA crystals form a double-stranded helical structure,[2] whereas *st*-PMMA does not crystallize, but includes specific organic solvents in a cavity within its single-stranded helix.[3] The stereoregular PMMA stereocomplex is a complementary helical structure formed on the basis of structural fitting between two chains of *it*-PMMA and *st*-PMMA.[4–6] Recently, the discussion has arisen on the basic structure of the PMMA stereocomplex by using X-ray[7] and atomic force microscopy (AFM),[8,9] although it was concluded that the structure of the stereocomplex is a helix with *it*-PMMA on the inside surrounded by *st*-PMMA.

Interfacial rearrangements of *it*-PMMA chains are expected to occur more easily than *st*-PMMA or atactic-PMMA chains, because the glass transition temperature of *it*-PMMA (~40 ℃) is significantly lower than that of *st*-PMMA or atactic-PMMA (around 105–135 ℃).[10] The crystallization of *it*-PMMA films has been researched by annealing at elevated temperatures for more than a few days, or under compression.[11–19] Most of these studies focused mainly on structural analyses of the crystals using infrared (IR) spectroscopy and X-ray diffraction (XRD), but the morphology of crystallized *it*-PMMA films has also been studied for a long time.[11,12,16,18] The film-formation methods used were either solvent evaporation from solution-cast films or the Langmuir–Blodgett technique as described below. Over 30 years ago, J. J. Klement and P. H. Geil[11] studied the lamellar growth of *it*-PMMA cast films annealed at a narrow temperature range (55–65 ℃) with electron microscopy, whereas G. Challa *et al.*[12] observed the macroscopic hexagonal structures of crystallized *it*-PMMA from casts at 90–130 ℃ using a polarization microscope. Later, R. H. R. Brinkhuis and A. J. Schouten[16] demonstrated the epitaxial crystallization in *it*-PMMA cast films covered by Langmuir–Blodgett overlayers. Recently, E. Yashima *et al.*[18] directly observed two-dimensional folded-chain crystals of *it*-PMMA monolayers obtained by Langmuir–Blodgett deposition using AFM.

In contrast, macromolecularly porous *it*-PMMA thin films have been studied as a scientifically important model, as they have strictly controlled nanospaces and were utilized for specific molecular recognition or precise reaction fields by forming stereocomplexes on substrates.[20–25] Porous *it*-PMMA thin films were prepared on quartzcrystal microbalance (QCM), silica or glass substrates through layer-by-layer (LbL) assembly[26] of *it*-PMMA/*st*-poly(methacrylic acid) (PMAA)[27–29] and the selective

extraction of *st*-PMAA from *it*-PMMA/*st*-PMAA stereocomplex films, taking advantage of the different solubilities of each component polymer. The *it*-PMMA/*st*-PMAA stereocomplex also forms a double-stranded helix similar to the aforementioned *it*-PMMA/*st*-PMMA stereocomplex.[30] In addition, porous films prepared by LbL assembly have been compared with spin-coated *it*-PMMA films. The spin-coated films showed neither the specific recognition of *st*-polymethacrylate[20] nor the template polymerization of methacrylic acid.[22] Thus, it is concluded that these phenomena are particular to the macromolecularly porous films.

More recently, we observed partial *it*-PMMA crystallization, as well as *st*-PMAA incorporation, into porous films by XRD analyses.[31,32] It was revealed that crystallized it-PMMA chains in films formed doublestranded helices.[2,33] The crystallization of *it*-PMMA occurred merely by immersing the porous films in a mixed solvent of acetonitrile/water (4/6, v/v) at room temperature, which is a different procedure and milder than conventional conditions.[11–19] Furthermore, *st*-PMAA incorporation into porous *it*-PMMA films was analyzed at the molecular level by QCM. Porous it-PMMA films incorporated *st*-PMAA with increasing acetonitrile content in the *st*-PMAA solution. Therefore, it was concluded that acetonitrile was important for *it*-PMMA chain motion in porous films. *st*-PMAA was also incorporated into *it*-PMMA films driven by stereocomplex formation, even after *it*-PMMA crystallized partially, although the amount of *st*-PMAA incorporated into crystallized films was reduced as compared with the incorporation into porous films.[32] However, both the changes in the morphology or properties of the films and the mechanisms responsible for these phenomena remained unclear.

In this study, we focused on the morphological changes of porous thin films during

*it*-PMMA crystallization and the subsequent *st*-PMAA incorporation. Films were characterized by scanning electron microscopy (SEM), AFM, X-ray photoelectron spectra and static contact angles. We also investigated whether the morphological changes of spin-coated films occur after immersion into a mixed solvent of acetonitrile/water in order to study the mechanisms of these interfacial rearrangements.

## 4. 2 EXPERIMENTAL

**Materials** *it*-PMMA34 ($M_n$ = 22 900, $M_w/M_n$ = 1.21, *mm:mr:rr* = 96:2:2) and *st*-PMAA35 ($M_n$ = 33700, $M_w/M_n$ = 1.45, *mm:mr:rr* = 1:5:94) were synthesized by conventional anionic polymerization. The number average molecular weights and distributions were measured by size exclusion chromatography using PMMA standards with a tetrahydrofuran eluant at 40 ºC and a flow rate of 0.6ml min$^{-1}$. Tacticities were analyzed from a-methyl proton signals using 400-MHz nuclear magnetic resonance (nitrobenzene-$d_5$, 110 ºC). Characterization of *st*-PMAA was achieved after the carboxyl group was methylated. Acetonitrile was purchased from Wako Pure Chemical Industries (Osaka, Japan). Ultrapure distilled water was provided by the MILLI-Q laboratory system (Millipore, Billerica, MA, USA).

**Film preparation** An AT-cut QCM with a parent frequency of 9 MHz was obtained from USI (Fukuoka, Japan) and used as the substrate. Frequency was monitored by an Iwatsu frequency counter (Model 53131A: Iwatsu Test Instruments Corp., Tokyo, Japan). The quartz crystal (9mm diameter) was coated on both sides with mirror-like polished gold electrodes (4.5mm in diameter). At first, the QCM electrode was cleaned three times with a piranha solution, a mixed aqueous solution of $H_2SO_4$/40% $H_2O_2$ (3/1, v/v) for 1min, followed by rinsing with ultrapure water and drying with $N_2$ gas. LbL

films were prepared as follows: the substrate was alternatively immersed into an *it*-PMMA acetonitrile solution and an *st*-PMAA acetonitrile/water (4/6, v/v) solution at a concentration of 0.017 unitM for 5 min at 25 ℃ each. The substrate was rinsed with each solvent, and dried with $N_2$ gas whenever it was taken out from each solution. This alternative deposition step was repeated 16 times to fabricate stereocomplexes of *it*-PMMA/*st*-PMAA on the substrates. Porous *it*-PMMA thin films were prepared by immersion into a 10mM NaOH aqueous solution. The

porous films were immersed in mixed solvents of acetonitrile/water (4/6, v/v) for 10 h, and then immersed in *st*-PMAA solutions of mixed acetonitrile/water (4/6, v/v) solvents for 115min.[32] Spin-coated *it*-PMMA films were prepared on the QCM at 1500 r.p.m. for 1 min with 0.051 unitM *it*-PMMA chloroform solutions. Acetonitrile was not used because it was a poor solvent for PMMA10 and could not dissolve *it*-PMMA completely at more than 0.017 unitM. Thus, chloroform, a good solvent for PMMA, was used to prepare the spin-coated films. The amount of *it*-PMMA adsorbed onto the substrate was approximately -1600 Hz per QCM. Spin-coated films were then immersed in acetonitrile/water (4/6, v/v) for 10 h.

**Measurements** SEM images were obtained with a JSM-6701F (JEOL, Akishima, Japan) at an acceleration voltage of 5 kV after osmium tetraoxide was spattered onto the surfaces of films at a thickness of approximately 5nm. AFM images were obtained with a JSPM-5400 (JEOL) that was operated in tapping mode in air at 25 ℃. Scanning was performed using silicon cantilevers (NSC35, μ-masch; resonance frequency: around 150 kHz; spring constant: $4.5Nm^{-1}$) within an area of 5×5 $\mu m^2$ with a 512 scan line and a scan speed of 5.0 $\mu m \ s^{-1}$. We did not perform any image processing other than the flat leveling. The mean square roughness ($R_a$) in the observed areas was estimated from the

following equation, where $F(x,y)$ is the surface relative to the center plane, which is a flat plane parallel to the mean plane, and $Lx$ and $Ly$ are the dimensions of the surface.

$$R_a = 1/(LxLy)\int_0^{Lx}\int_0^{Ly} \left| F(x,y) \right| \, dx \, dy$$

X-ray photoelectron spectroscopy (XPS) was obtained with a spectrometer (AXIS 165, Shimadzu-Kratos, Kyoto, Japan) using MgKa radiation. The typical operating conditions were as follows: X-ray gun, 12 kV, 10mA; takeoff angle, 90 ºC; pressure in the source chamber, ~$10^{-9}$ torr. The static contact angles of the thin films were measured by dropping ultrapure water on the films at 25 ºC with a DropMaster 500 (Kyowa InterFACE Science, Niiza, Japan). Contact angles were determined 10 s after applying the drop. The volume of water in the drop was 0.5 µl. All reported values represent the average of at least six measurements taken at different locations on the film surface.

## 4. 3 RESULTS AND DISCUSSION

We used QCM analysis to calculate the amount of $it$-PMMA assembled on the gold substrate by Sauerbrey's equation.[36] A typical QCM analysis is shown in Figure 4-1, and the time evolution means the period of immersion time in each solution or solvent. The stepwise stereocomplex assembly of $it$-PMMA/$st$-PMAA and the selective extraction of $st$-PMAA from assembled films were confirmed in previous papers.[20,23,25,32] Interestingly, the elution of porous $it$-PMMA thin films was barely observed after the films were immersed into acetonitrile/water (4/6, v/v) for 10 h, although the crystallized $it$-PMMA peaks were observed by XRD.[31,32] These results indicate that the interfacial rearrangements of $it$-PMMA chains that occurred in films were driven by the mixed solvent, whereas $it$-PMMA crystallization was driven by

annealing at high temperature or under compression in previous studies.[11–19] The crystallized *it*-PMMA thin films can incorporate *st*-PMAA, most likely because further interfacial rearrangements also occurred in these films. Therefore, the morphological changes of the porous thin films during *it*-PMMA crystallization and the subsequent *st*-PMAA incorporation were initially analyzed by SEM and AFM. The same crystallized *it*-PMMA films, which corresponded to approximately -1400 Hz per QCM, and the *st*-PMAA incorporated films were used in SEM and AFM observation.
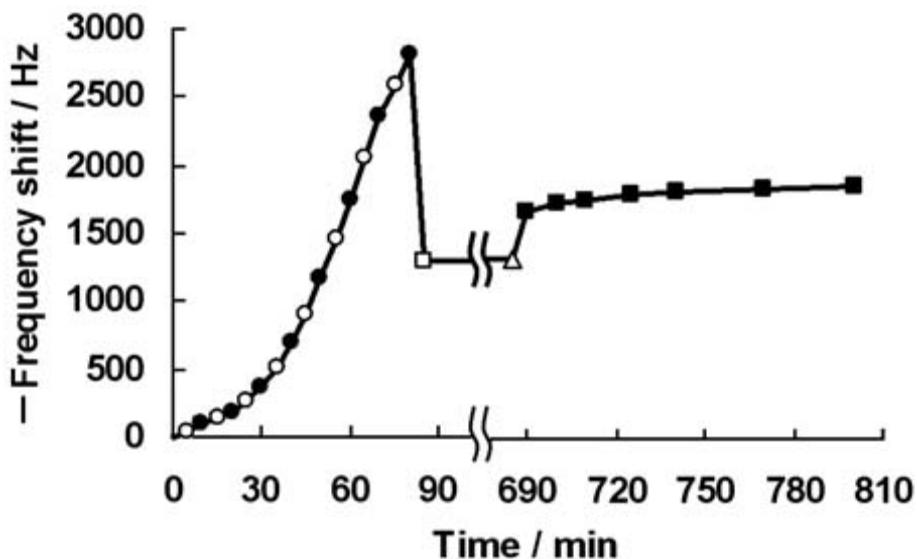


**Figure 4-1.** Typical QCM analysis of the LbL assembly, *st*-PMAA extraction, isotactic *it*-PMMA crystallization and subsequent *st*-PMAA incorporation. *it*-PMMA (white circles) in acetonitrile and st-PMAA (black circles) in acetonitrile/water (4/6, v/v) were alternately assembled on a QCM substrate at 0.017unitM at 25 °C. Porous it-PMMA films were prepared using 10mM NaOH(aq) (white square). The following *it*-PMMA crystallization occurred in a mixed solvent of acetonitrile/water (4/6, v/v) (white triangle). The last *st*-PMAA incorporation was observed at 0.017unitM at 25 °C (black squares).

We have observed several hemispherical outshoots on the surface of crystallized *it*-PMMA films by AFM,[32] which implies that the morphological changes of the films

86

occurred in a wide area as compared with the scanning area ($1 \times 1$ μm) used in previous studies.[20,29,32] Thus, SEM was used to observe the macroscopic deformation of porous thin films during *it*-PMMA crystallization and the subsequent *st*-PMAA incorporation. Figure 4-2 shows SEM images of crystallized *it*-PMMA films and *st*-PMAA incorporated films after 10 h of immersion in acetonitrile/water (4/6, v/v). Dotted aggregates of crystallized *it*-PMMA and networks of the *it*-PMMA/*st*-PMAA mixed assembly broadened evenly at the submillimeter scale (Figure 4-2a, b). The patterns were not observed on the surface of a bare QCM substrate and porous *it*-PMMA films. In the magnified view (tilted at 40-degree angles), some dots were connected to form big outshoots on the crystallized *it*-PMMA films (Figure 4-2c), and some isolated outshoots were also observed on *st*-PMAA incorporated films after *it*-PMMA crystallization (Figure 4-2d). However, most regions of the crystallized *it*-PMMA films and *st*-PMAA incorporated films formed dots and networks, respectively, although the configurations of these assemblies cannot be controlled yet. This morphological change from dots to networks likely resulted from an increased polymer density of films during the incorporation of *st*-PMAA.
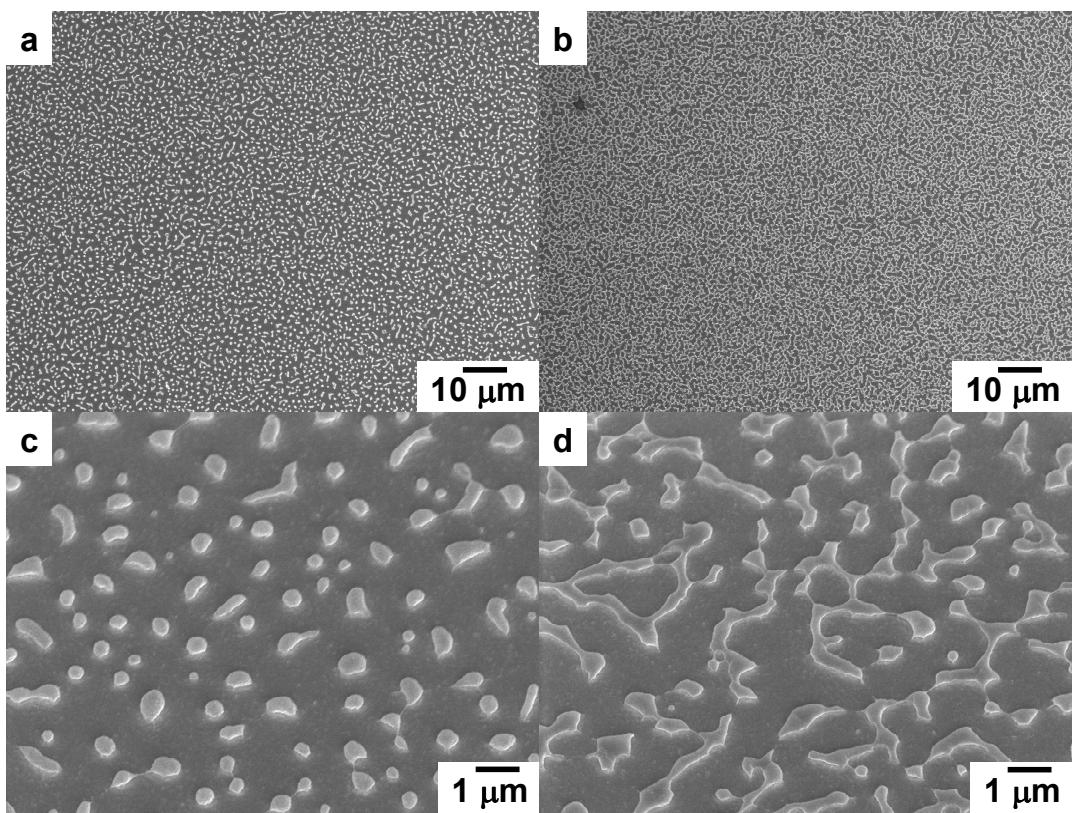
**Figure 4-2.** SEM images of (a, c) crystallized *it*-PMAA films and (b, d) *st*-PMAA incorporated films after 10h of immersion in acetonitrile/water (4/6, v/v). (a, b) Top view. (c, d) Tilted view.

AFM analysis was used to calculate both the height of the assemblies and the surface roughness of films, which was difficult to measure by SEM. Figure 4-3 shows AFM images of crystallized *it*-PMMA films and *st*-PMAA incorporated films after *it*-PMMA crystallization. Hemispherical outshoots of crystallized *it*-PMMA, which were several hundred nanometers high, were arranged in a dot pattern on films (Figure 4-3a), whereas porous films were relatively flat. The mean square roughness ($R_a$) of the crystallized *it*-PMMA films was 53 nm, although the $R_a$ of the smooth parts ($0.3\times0.3$ μm) of films was $3.3 \pm 0.2$ nm ($n = 3$). This value was more similar to that of a bare QCM substrate (3.1 nm) than that of porous *it*-PMMA films (17 nm), suggesting that the bare gold surface is exposed. In addition, the outshoots of crystallized *it*-PMMA

films, which corresponded to approximately -700 Hz per QCM, were smaller and more than that of the crystallized films in Figure 4-3a (-1400 Hz per QCM), which implies that film thickness is one of the important parameters for morphological changes of *it*-PMMA films. Furthermore, a similar dot pattern was also observed on crystallized *it*-PMMA (-700 Hz per QCM) after 40 h of immersion in acetonitrile/water (4/6, v/v). On the other hand, networks of agglomerates composed of crystallized *it*-PMMA and stereocomplexes were observed on the surface of *st*-PMAA incorporated films (Figure 4-3b), and the heights of these assemblies were not significantly different from that of crystallized *it*-PMMA films. Therefore, the polymer chains in films likely spread in a horizontal direction during *st*-PMAA incorporation. Indeed, the $R_a$ of *st*-PMAA-incorporated films was 46 nm, but the $R_a$ of the smooth parts ($0.3 \times 0.3$ μm) was $3.8 \pm 0.5$ nm ($n = 3$). This morphological change in films indicated that some noncrystalline parts of *it*-PMMA could incorporate *st*-PMAA, and that a rearrangement of the partially crystallized *it*-PMMA might occur on the film surface.
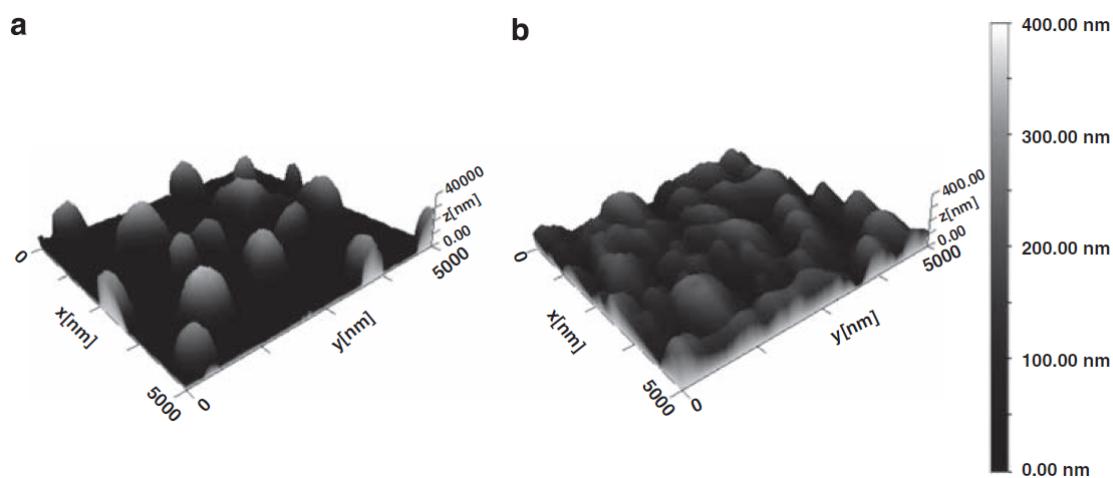


**Figure 4-3.** AFM images of (a) crystallized *it*-PMAA films and (b) *st*-PMAA incorporated films after 10h of immersion in acetonitrile/water (4/6, v/v).

Next, we were interested in the changes in properties of porous *it*-PMMA films. The deformation of films during *it*-PMMA crystallization would dynamically change the film thickness. XPS analysis is a common tool to confirm chemical bonds on a surface at ~10 nm of the measured depth. The XPS spectra of a bare QCM substrate, porous *it*-PMMA films and crystallized *it*-PMMA films are shown in Figure 4-4. Distinct Au 4f peaks at around 84.1 and 87.7 eV were observed on the QCM substrate (Figure 4-4a). In contrast, these Au peaks were not observed on the surface of porous films (Figure 4-4b), showing that the thickness of porous films was more than 10 nm, and that the substrate was evenly covered with film. In a previous paper,[20] the thickness of porous *it*-PMMA films was determined to be 44 nm by AFM scratching mode, which corresponded to approximately -800 Hz per QCM. Therefore, *it*-PMMA film thickness was calculated as 83 nm (-1500 Hz per QCM) in this study (Figure 4-1), according to a constant rate of 0.055 nm/Hz. Note that the intensity of Au 4f peaks on the surface of crystallized *it*-PMMA films was about two-thirds of that of the QCM substrate (Figure 4-4c), and that the heights of the outshoots on the crystallized *it*-PMMA films reached several hundred nanometers (Figure 4-3a), where Au peaks should not be detected. Thus, the film thickness of the smooth parts became less than 10nm after *it*-PMMA films were immersed in acetonitrile/water (4/6, v/v). These results confirmed that the homogeneously broadened *it*-PMMA in porous films became localized because of its crystallization, which brought about differences in the polymer density of films.
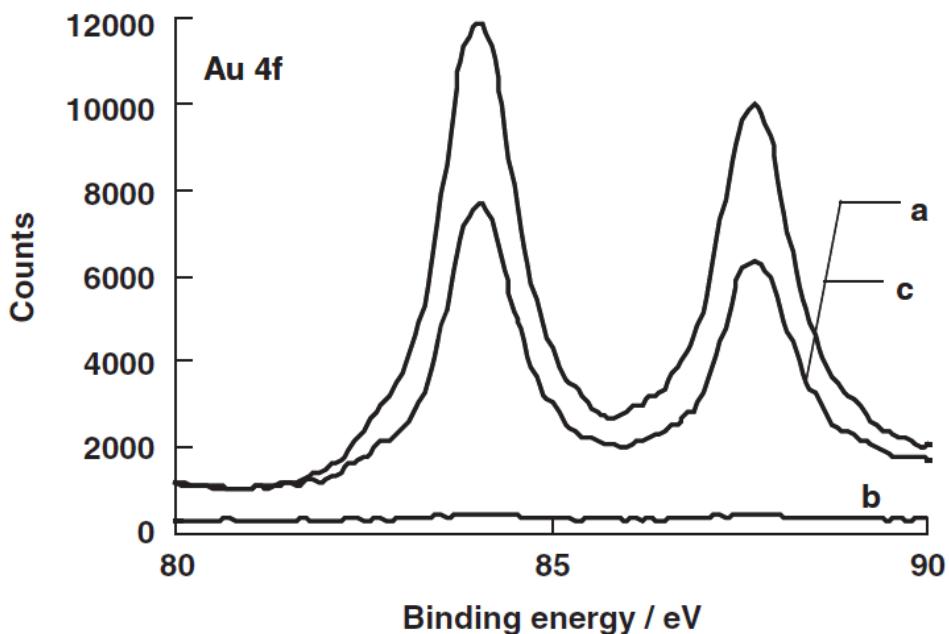
**Figure 4-4.** XPS in the region of the gold element of a bare quartz crystal microbalance substrate (a), porous *it*-PMMA films (b) and crystallized *it*-PMMA films (c) after 10h of immersion in acetonitrile/water (4/6, v/v).

Furthermore, film characteristics were analyzed on the millimeter scale with static contact angles, which have been used to confirm stepwise stereocomplex formation during LbL assembly.[29] We thought that the contact angles of each film would change according to its surface components or shapes. Figure 4-5 shows the dependence of static contact angles on various film surfaces. Surface components and polymer conformations were analyzed by attenuated total reflection-IR.[20] The mean angles of porous *it*-PMMA films as prepared and after 10 h of immersion in water were 49.2 ± 1.9º and 51.7 ± 1.0º, respectively (Figure 4-5a, b). This is reasonable because XRD analyses revealed that no structural changes of porous *it*-PMMA films occurred in water.[32] In contrast, the angles of crystallized *it*-PMMA films after 10 h immersion in acetonitrile/water (4/6, v/v) was 36.5 ± 1.6º (Figure 4-5c). These differences likely resulted from a surface morphology change of the thin films, because both films were

91

composed only of *it*-PMMA and the two porous films were smooth compared with crystallized films (Figure 4-3a). We should also consider that the film thickness of the smooth parts in crystallized *it*-PMMA films was less than 10 nm and the gold surface of QCM is exposed, according to XPS results (Figure 4-4c). Although the mean angle of a bare QCM substrate was 69.2 ± 1.4º, Z. Burton and B. Bhushan[37] reported that increasing roughness on hydrophilic surfaces, such as the patterned PMMA surface, decreased the contact angle, which was consistent with these results.
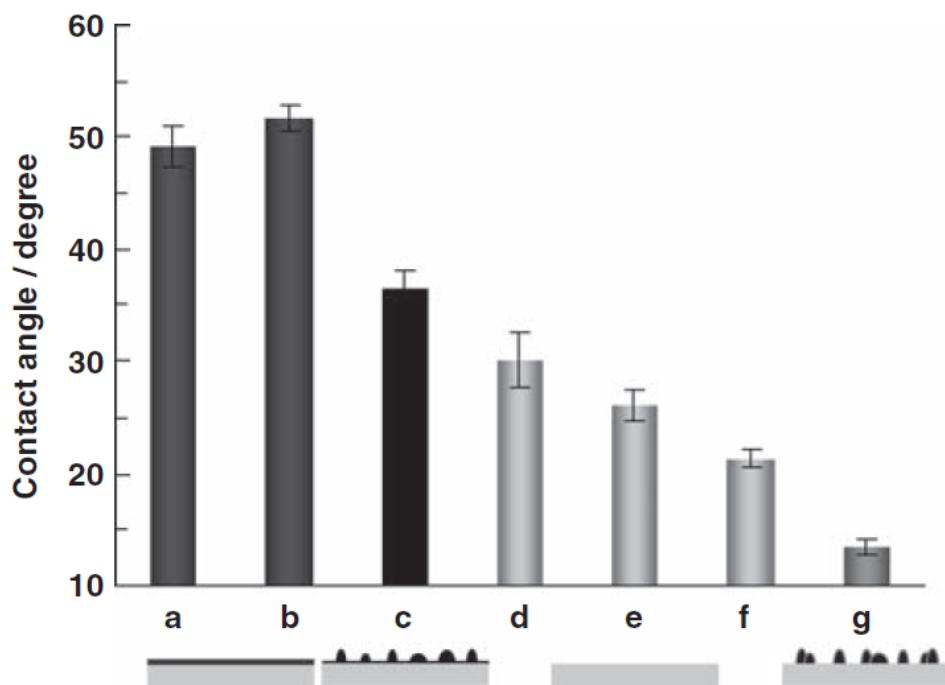


**Figure 4-5.** Static contact angles of porous *it*-PMMA films (a) as prepared and (b) after 10h of immersion in water, crystallized *it*-PMMA films (c) after 10h of immersion in acetonitrile/water (4/6, v/v), (d) stereocomplex films and *st*-PMAA incorporated films (e) just after *st*-PMAA extraction and (f) after 10h of immersion in water and (g) acetonitrile/water (4/6, v/v).

This tendency was also observed in the case of stereocomplex films. The contact angle of the original LbL films was 30.2 ± 2.5º, and the angles of *st*-PMAA

incorporated films after *st*-PMAA extraction and a subsequent 10 h of immersion in water were 26.4 ± 1.3º and 21.4 ± 0.8º, respectively (Figure 4-5d—f). The mean values of stereocomplex films were smaller than those of porous *it*-PMMA films,[29] because the hydrophobic *it*-PMMA is buried in the helical structure of hydrophilic *st*-PMAA in the stereocomplex model.[30] *st*-PMAA incorporated films remained flat, although the slow crystallization of *it*-PMMA also occurred during the incorporation of *st*-PMAA.[31] Therefore, the fast *st*-PMMA incorporation by stereocomplexation might prevent film deformation because of *it*-PMMA crystallization. On the other hand, the angle of *st*-PMAA incorporated films after *it*-PMMA crystallization was 13.6 ± 0.7º (Figure 4-5g). It is indicated that the surface of films was covered with stereocomplexes (Figure 4-6), although the *it*-PMMA inside the aggregates is densely packed and loses the ability to incorporate *st*-PMAA. It also remains unclear whether *st*-PMAA adsorbed both on the crystallized *it*-PMMA outshoots and on the smooth domains of films. These tendencies of static contact angles also corresponded to the relatively regular surface profile at the submillimeter scale, which was observed by SEM (Figure 4-2a, b).
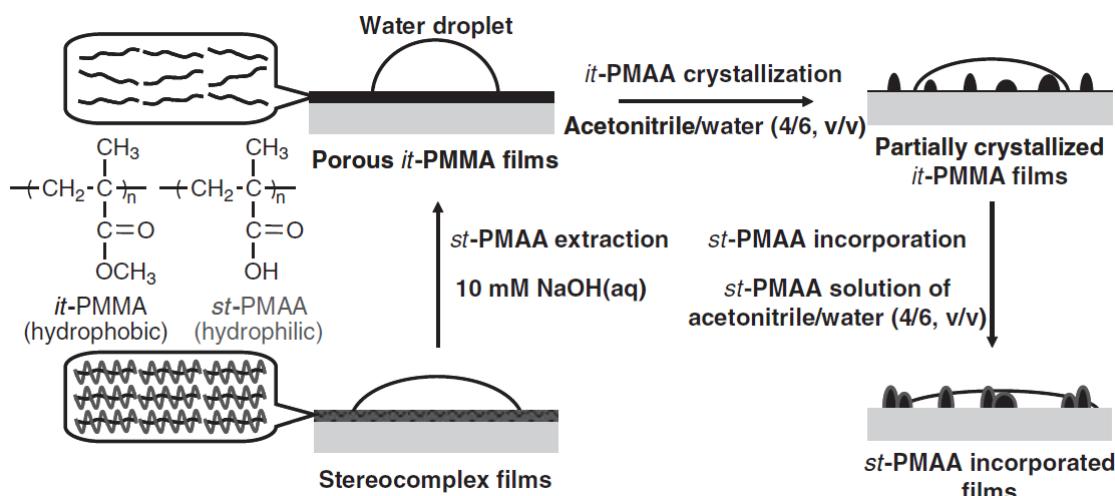
**Figure 4-6.** Schematic illustration of the morphological changes of macromolecularly porous thin films in *it*-PMMA crystallization and *st*-PMAA incorporation.

We were also interested in whether ordinary *it*-PMMA films would form outshoots after immersion into a mixed solvent of acetonitrile/water. Spin-coated *it*-PMMA films were prepared on the QCM substrate from the chloroform solution as described in the experimental procedure section. Figure 4-7 shows the AFM and SEM images of spin-coated *it*-PMMA films as prepared and after immersed in acetonitrile/water (4/6, v/v) for 10 h. The $R_a$ of spin-coated films was 8.4 nm and the film surface was relatively smooth (Figure 4-7a). A few big craters were formed on the films, most likely because of the evaporation of chloroform (Figure 4-7c). The QCM frequency shift was a few hertz after 10 h of immersion in acetonitrile/water (4/6, v/v), which implies that the spin-coated films did not dissolve in the mixed solvent either. Semispherical outshoots were also observed on films after immersion (Figure 4-7b), and dotted aggregates of *it*-PMMA broadened evenly at the submillimeter scale (Figure 4-7d). The same tendency of crystallized *it*-PMMA films was obtained by LbL assembly, even though the Ra of films (82 nm) was much greater than that of *it*-PMMA films from LbL

assembly (32 nm). The surface roughness derived by the crystallization of *it*-PMMA is dependent on the initial thickness, roughness or morphology of the films, such as the cratered surface. These results indicate that the formation of these hemispherical outshoots would occur by rearrangements of *it*-PMMA chains in thin films.
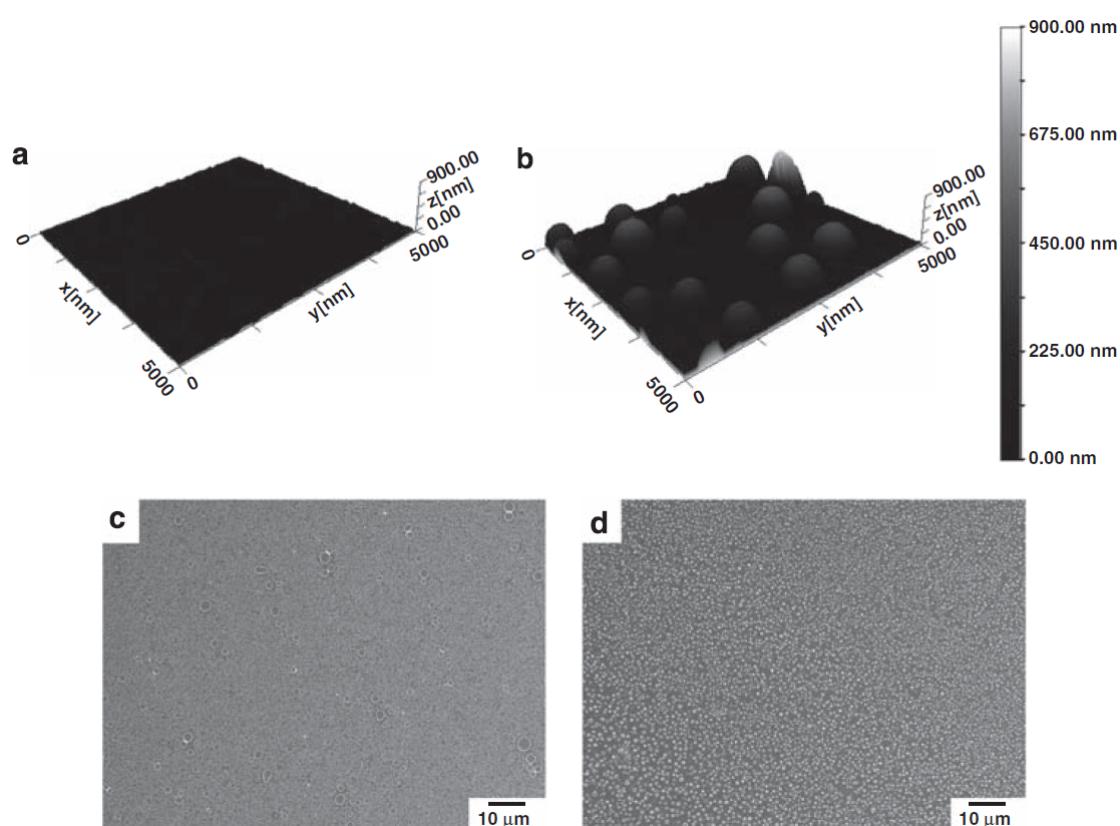


**Figure 4-7.** AFM and SEM images of spin-coated *it*-PMMA films (a, c) prepared from a chloroform solution and (b,d) after 10h of immersion in acetonitrile/water (4/6, v/v).

## 4. 4 CONCLUSIONS

We investigated the morphological changes of porous thin films on a QCM substrate during *it*-PMMA crystallization and the subsequent *st*-PMAA incorporation. Dotted aggregates of crystallized *it*-PMMA appeared on films on SEM and AFM images, although the films were not dissolved in a mixed solvent of acetonitrile/water. Gold substrate peaks were observed on crystallized *it*-PMMA films by XPS. Therefore, this indicated that the adsorbed *it*-PMMA spontaneously localized in films to reform the surface profile. These dotted *it*-PMMA aggregates were also observed when spin-coated films were immersed in the mixed solvent, suggesting that this immersion method is a simple and different approach to film deformation, as compared with previous studies. On the other hand, networks of crystallized *it*-PMMA and the stereocomplex appeared on *st*-PMAA-incorporated films. In this way, the design and restructuring of self-assembled films at the nano or micrometer scale were achieved through self-organization and stereocomplex formation of stereoregular polymethacrylates.

## REFERENCES

1) T. G. Fox, B. S. Garret, W. E. Goode, S. Grantch, J. F. Kincaid, A. Spell, J. D. Stroupe, *J. Am. Chem. Soc.* **1958**, *80*, 1768.

2) H. Kusanagi, H. Tadokoro, Y. Chatani, *Macromolecules* **1976**, *9*, 531.

3) H. Kusuyama, M. Takase, Y. Higashihata, H. T. Tseng, Y. Chatani, H. Tadokoro, *Polymer* **1982**, *23*, 1256.

4) J. Spevacek, B. Schneider, *Adv. Colloid Interface Sci.* **1987**, *27*, 81.

5) K. te Nijenhuis, *Adv. Polym. Sci.* **1997**, *130*, 67.

6) K. Hatada, T. Kitayama, *Polym. Int.* **2000**, *49*, 11.

7) E. Schomaker, G. Challa, *Macromolecules* **1989**, *22*, 3337.

8) J. Liu, Y. Zhang, J. Zhang, D, Shen, Q. Guo, I. Takahashi, S. Yan, S. *J. Phys. Chem. C* **2007**, *111*, 6488.

9) J. Kumaki, T. Kawauchi, K. Okoshi, H. Kusanagi, E. Yashima, *Angew. Chem., Int. Edn.* **2007**, 46, 5348.

10) *Polymer Handbook, 3rd ed.*, ed. by J. Brandrup, E. H. Immergut, John Wiley & Sons, New York, Chichester, Brisbane, Toronto, Singapore, **1989**.

11) J. J. Klement, P. H. Geil, *J. Macromol. Sci. B* **1972**, *6*, 31.

12) A. de Boer, G. O. R. A. van Ekenstein, G. Challa, *Polymer* **1975**, *16*, 930.

13) B. Schneider, J. Stokr, J. Spevacek, J. Baldrian, *Makromol. Chem.* **1987**, *188*, 2705.

14) J. Dybal, S. Krimm, *Macromolecules* **1990**, *23*, 1301.

15) R. H. R. Brinkhuis, A. J. Schouten, *Macromolecules* **1991**, *24*, 1496.

16) R. H. R. Brinkhuis, A. J. Schouten, *Macromolecules* **1992**, *25*, 2717.

17) D. Zhou, L. Li, B. Che, Q. Cao, Y. Lu, G. Xue, *Macromolecules* **2004**, *37*, 4744.

18) J. Kumaki, T. Kawauchi, E. Yashima, *J. Am. Chem. Soc.* **2005**, *127*, 5788.

19) J. Liu, J. Wang, H. Li, D. Shen, J. Zhang, Y. Ozaki, S. Yan, *J. Phys. Chem. B* **2006**, *110*, 738–742.

20) T. Serizawa, K.-i. Hamada, T. Kitayama, M. Akashi, *Angew. Chem., Int. Edn.* **2003**, *42*, 1118.

21) T. Serizawa, K.-i. Hamada, T. Kitayama, M. Akashi, *Nature* **2004**, *429*, 52.

22) K.-i. Hamada, T. Serizawa, M. Akashi, *Macromolecules* **2005**, *38*, 6759.

23) H. Ajiro, D. Kamei, M. Akashi, *J. Polym. Sci., Part A: Polym. Chem.* **2008**, *17*, 5879.

24) H. Ajiro, D. Kamei, M. Akashi, *Polym. J.* **2009**, *41*, 90.

25) H. Ajiro, D. Kamei, M. Akashi, *Macromolecules* **2009**, *42*, 3019.

26) G. Decher, *Science* **1997**, *277*, 1232.

27) J. H. G. M. Lohmeyer, G. Kransen, Y. Y. Tan, G. Challa, *Polym. Lett. Edn.* **1975**, *13*, 725.

28) J. H. G. M. Lohmeyer, Y. Y. Tan, P. Lako, G. Challa, *Polymer* **1979**, *19*, 1171.

29) T. Serizawa, K.-i. Hamada, T. Kitayama, K.-i. Katsukawa, K. Hatada, M. Akashi, *Langmuir* **2000**, *16*, 7112.

30) F. Bosscher, G. ten Brinke, G. Challa, *Macromolecules* **1982**, *15*, 1442.

31) D. Kamei, H. Ajiro, C. Hongo, M. Akashi, *Chem. Lett.* **2008**, *37*, 332.

32) D. Kamei, H. Ajiro, C. Hongo, M. Akashi, *Langmuir* **2009**, *25*, 280.

33) R. P. Kusy, *J. Polym. Sci., Part A: Polym. Chem.* **1976**, *14*, 1527.

34) K. Hatada, K. Ute, K. Tanaka, T. Kitayama, Y. Okamoto, *Polym. J.* **1985**, *17*, 977.

35) T. Kitayama, S. He, Y. Hironaka, T. Iijima, K. Hatada, *Polym. J.* **1995**, *27*, 314.

36) G. Sauerbrey, *Z. Phys.* **1959**, *155*, 206.

37) Z. Burton, B. Bhushan, *Nano Lett.* **2005**, *5*, 1607.

# Chapter 5

# Stability and Fusion of Porous Isotactic Poly(methyl methacrylate) Thin Films Fabricated on Silica Nanoparticles

## 5. 1 INTRODUCTION

Stereocomplexes of poly(methyl methacrylate) (PMMA) or poly(lactic acid) have received considerable interests not only due to their unique supramolecular structures but also because of their many applications in the biomedical field. Isotactic (*it*) PMMA and syndiotactic (*st*) PMMA form multiple-stranded helices,[1,2] and poly(L-lactide) and poly(D-lactide) form $3_1$-helix racemic crystals.[3,4] For example, multilayered thin films composed of the stereocomplexes fabricated by layer-by-layer (LbL) assembly[5—8] showed excellent performance for cell-adhesion and blood-coagulant,[9] or alkaline hydrolysis[10] as compared to spin-coated films composed of homopolymers. Furthermore, specific nanostructure formations such as spheres, networks, or hierarchical assemblies were achieved by stereocomplexation.[11—14]

In contrast, we demonstrated the macroscopic deformation of macromolecularly porous *it*-PMMA thin films prepared on a flat substrate with the stepwise stereocomplex assembly of *it*-PMMA/*st*-poly(methacrylic acid) (PMAA)[15] and *st*-PMAA extraction,[16] and the subsequent *it*-PMMA crystallization.[17—19] It was demonstrated that acetonitrile solvation promoted the crystallization of the porous *it*-PMMA films, whereas water maintained the polymer conformation of the films.[18] Furthermore, film crystallization induced the formation of nanoscale outshoots on the surface due to the easy

rearrangement of the polymer chains on the film by solvation without dissolution.[19] These dynamics of the *it*-PMMA polymer chains depending on the circumstances is interesting, but, the morphological changes all occurred on the same plane, and thus the effects of substrate geometry or static immersion on the outshoot formation remained unclear. Fusion based on the crystallization of *it*-polymethacrylates might create a specific nanostructure.[20]
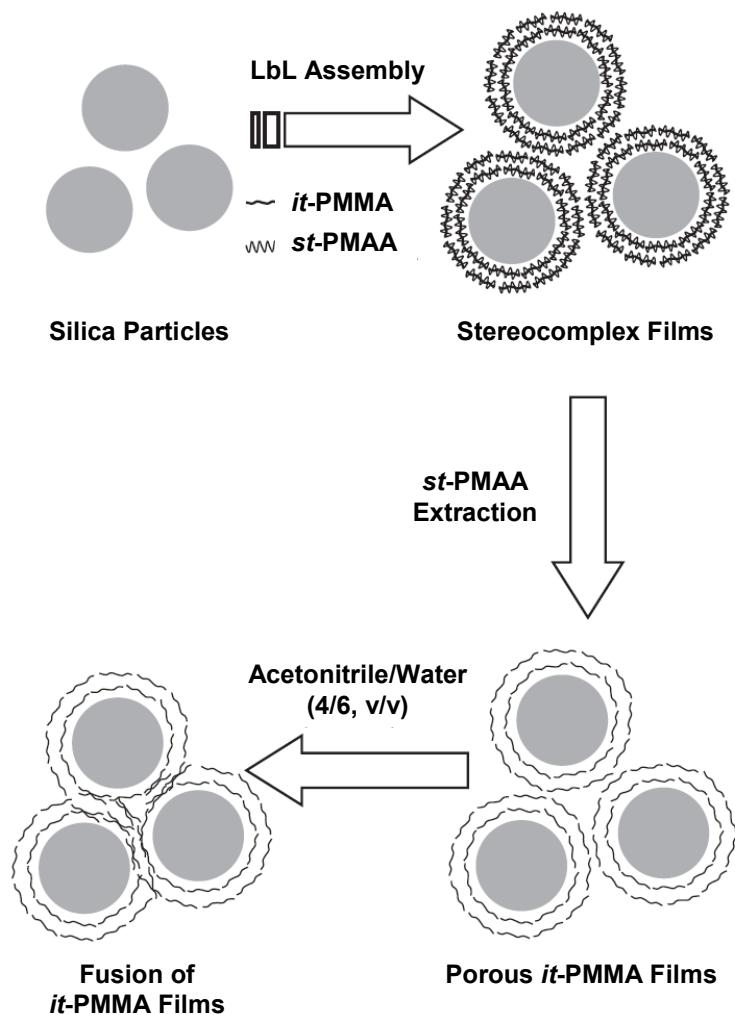


**Figure 5-1.** Schematic illustration of stereocomplex formation, the preparation of porous *it*-PMMA films, and the subsequent fusion of the *it*-PMMA films onto silica nanoparticles.

In this study, silica particles were employed as a model for multiple non-planar substrates, in contrast to previous studies with one planar substrate of glass or a quartz crystal microbalance (QCM).[15—19,21] Indeed, the film formation of stereocomplexes on various silica particles has been previously reported.[22—25] We selected silica nanoparticles of 330 nm in diameter[23] because the size of the hemispherical outshoots on the QCM substrate was several hundred nanometers,[18,19] as large as the silica nanoparticles. Therefore, the aggregation of the silica particles through fusion with the *it*-PMMA thin films would form a novel polymeric nanostructure (Figure 5-1), instead of the outshoot formation on the same plane. In addition, the particle structures under gentle stirring or static conditions were analyzed by dynamic light scattering (DLS) and scanning electron microscopy (SEM), respectively.

## 5. 2 EXPERIMENTAL

*it*-PMMA ($M_n$ = 22900, $M_w/M_n$ = 1.21, *mm:mr:rr* = 96:2:2)[26] and *st*-PMAA ($M_n$ = 33700, $M_w/M_n$ = 1.45, *mm:mr:rr* = 1:5:94)[27] were synthesized by conventional anionic polymerization. Silica nanoparticles with a diameter of 330 nm were alternately immersed into an acetonitrile solution of *it*-PMMA (1.7 mg ml$^{-1}$) and an acetonitrile/water (4/6, v/v) solution of *st*-PMAA (1.5 mg ml$^{-1}$) for 5 min at 25 °C under gentle shaking (each of solution volumes was 5 ml). After each immersion, the silica particles were rinsed with each solvent. The immersion process was continued for 16 steps to deposit the *it*-PMMA/*st*-PMAA stereocomplex films on the silica nanoparticles. Porous *it*-PMMA films were obtained by immersing the silica particles coated with the stereocomplex films in 10 mM NaOH(aq) for 30 min and rinsing with water. The

resulting particles were gently stirred in an aqueous or acetonitrile/water (4/6, v/v) solution for 10 h, which had been investigated in the previous articles.[18,19] The particle size distribution in aqueous solution was measured by the DLS method using a Zetasizer Nano ZS (Malvern Instruments, UK). The SEM images were obtained with a JSM-6701F (JEOL, Japan) after staining with osmium tetraoxide. A 10 μL aliquot from each solution was dropped onto poly(ethylene terephthalate) substrates on a SEM stage, and were dried at normal pressure at 25 ºC for 6 h.

## 5. 3 RESULTS AND DISCUSSION

Water and a mixed solvent of acetonitrile/water (4/6, v/v) were employed as proper solvents for the *it*-PMMA/*st*-PMAA stereocomplex films and porous *it*-PMMA films, because the effective LbL assembly of *it*-PMMA/*st*-PMAA was achieved[15—19,21,23—25] and neither of the films were dissolved in the solvents.[19,25] In addition, the conformational changes of the polymer chains in the porous *it*-PMMA films in water or acetonitrile/water (4/6, v/v) were investigated in previous studies.[17,18] Infrared (IR) spectroscopy was used to detect the polymer chain conformations on the silica nanoparticles. The LbL steps were continued for 40 steps for the IR analyses, because the carbonyl vibrations of a 16-step assembly[18,19] did not appear due to the thin film thickness.[25] The peaks of the alternative LbL assembly and *it*-PMMA films after 10 h of stirring in water or acetonitrile/water (4/6, v/v) appeared at around 1720 and 1730 cm$^{-1}$, respectively, whereas each cast film of *it*-PMMA and *st*-PMAA has a peak at 1726 and 1695 cm$^{-1}$, respectively. These results suggest that the stereocomplex films and the *it*-PMMA films remained on the silica particles after immersion.

Figure 5-2 shows the size distribution of the silica particles in distilled ultrapure water after gently shaking in each solution. The sizes of the bare silica nanoparticles, silica nanoparticles coated with the stereocomplex films after 10 h of stirring in water or acetonitrile/water (4/6, v/v), and porous *it*-PMMA films after 10 h of stirring in water were approximately 400, 420, 390, and 420 nm, respectively (Figure 5-2a—d). The layers of stereocomplexes or *it*-PMMA would not be detected by DLS, because all the values of the diameters of bare and coated silica particles were around 400 nm. On the other hand, the size of the silica particles coated with the *it*-PMMA films after 10 h of stirring in acetonitrile/water (4/6, v/v) was about 460 nm (Figure 5-2e), which was a little bigger than the other silica particles. Therefore, it was demonstrated that the stereocomplex films on the silica particles (Figure 5-2b, c) did not play a role in bonding the particles, whereas the *it*-PMMA chains on the silica particles, which were slightly solvated by acetonitrile, interacted with each other to form a couple of silica nanoparticles (Figure 5-2e). It is noteworthy that there was no adhesive effect on the silica particles, even when *it*-PMMA films were treated in water (Figure 5-2d). I expected that the *it*-PMMA chains would connect each of the silica particles to form an aggregate, although the *it*-PMMA adsorbed onto one planar substrate could move only on the surface. However, evident differences among these particles were not observed, most likely because the silica particles were gently shaken, whereas the self-assembly of *it*-PMMA on the QCM substrate occurred at rest in acetonitrile/water (4/6, v/v).[18,19]
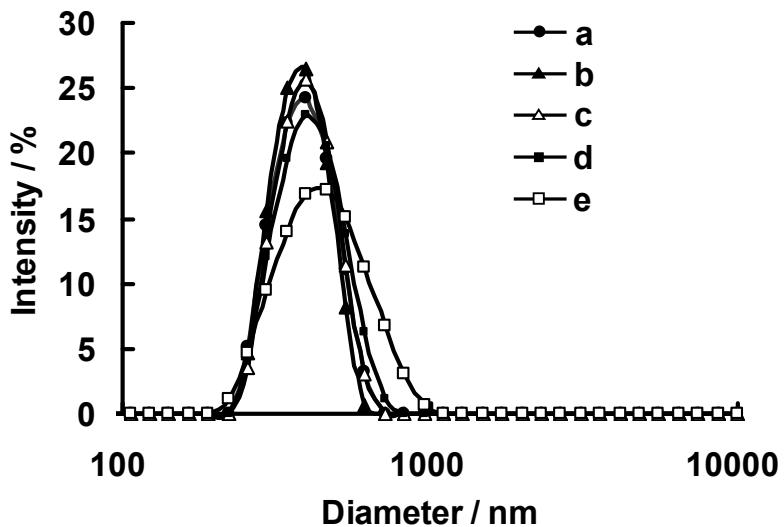
**Figure 5-2.** Size distribution of silica particles in distilled ultrapure water measured by DLS: (a) bare silica particles, (b, c) *it*-PMMA/*st*-PMAA stereocomplex film-coated silica particles, and (d, e) *it*-PMMA filmcoated silica particles.The polymer film-coated silica particles were gently shaken in (b, d) water and (c, e) acetonitrile/water (4/6, v/v) for 10 h, respectively.

Next, SEM images were observed after droplets from the silica suspensions were dried at rest. Although there was almost no fusion of the stereocomplex films on the silica nanoparticles after 10 h of stirring in water or acetonitrile/water (4/6, v/v), nor of the porous *it*-PMMA films after stirring in water (Figure 5-3a—d), only the *it*-PMMA films after 10 h of stirring in acetonitrile/water (4/6, v/v) fused to form nanostructured networks (Figure 5-3d). The aforementioned SEM observation was in good agreement of the results from Figure 5-2. In the magnified view of Figure 5-3d, almost all the *it*-PMMA films at contact points between the silica particles were extensively fused, indicating that the *it*-PMMA chains would infiltrate each layer of the films on the particles (Figure 5-1). Indeed, the thickness of the porous *it*-PMMA multilayered thin films prepared by LbL assembly for a 16-step assembly was estimated at approximately

44 nm, which was estimated by direct analyses of atomic force microscopy and approximate calculation by QCM analysis, as described in previous papers,[16,18] and also could be sketchily estimated at less than 50 nm in the magnified view of Figure 5-3d. Furthermore, QCM analysis also revealed that the porous *it*-PMMA films were not peeled off after immersion in acetonitrile/water (4/6, v/v).[19] Thus, the fusion of the *it*-PMMA films occurred not by the dissolution of *it*-PMMA in the mixed solvent, but rather by an interaction of the *it*-PMMA chains driven by the slight solvation of acetonitrile without dissolution. Furthermore, it is expected that the removal of silica particles[23] from the *it*-PMMA/silica assemblies will lead to novel nanostructures[28] composed of only *it*-PMMA.
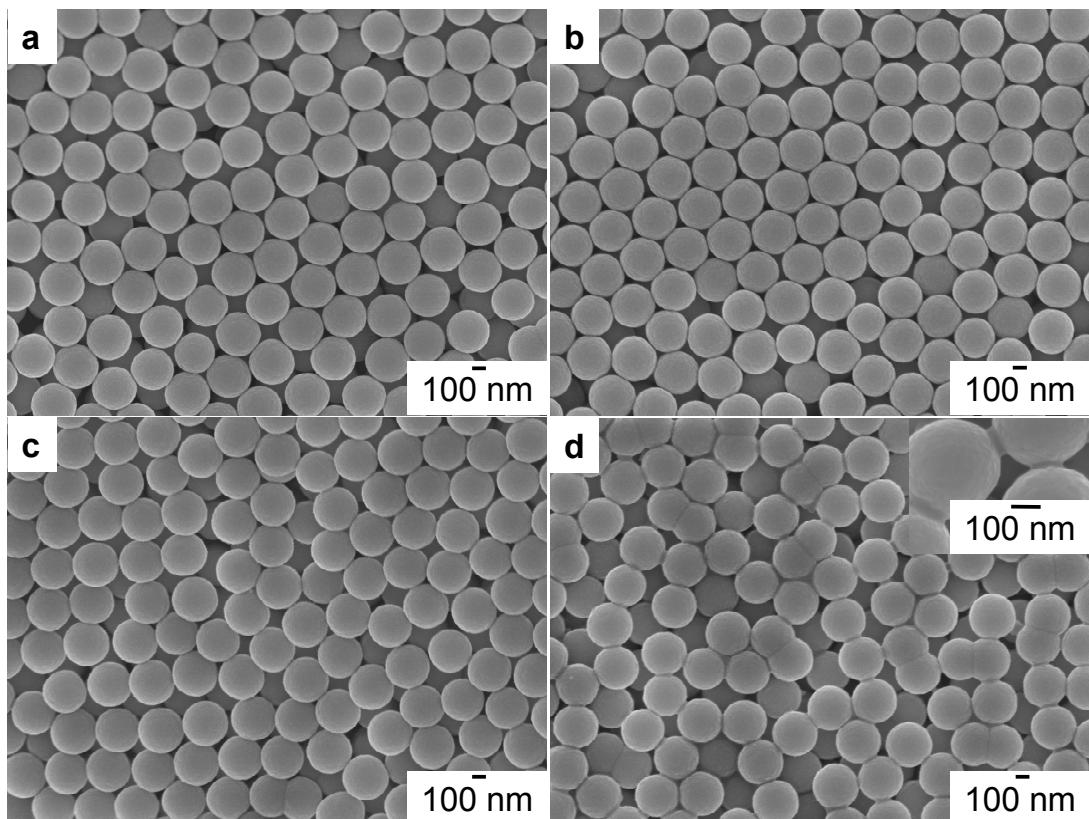


**Figure 5-3.** SEM images of silica particles coated with (a, c) *it*-PMMA/*st*-PMAA stereocomplex films and (b, d) porous *it*-PMMA films after 10 h of immersion in (a, b) water and (c, d) acetonitrile/water (4/6, v/v).

## 5. 4 CONCLUSIONS

The fusion of porous *it*-PMMA thin films prepared on silica nanoparticles was observed after gentle shaking in acetonitrile/water (4/6, v/v) and subsequent drying on a SEM stage, although DLS showed only a few aggregates of the silica particles in the solution. These results suggest that leaving the solution at rest is important for film fusion on the particles, and that multiple spherical substrates would promote the cross-linking of the *it*-PMMA chains on the particles.

## REFERENCES

1) E. Schomaker, G. Challa, *Macromolecules* **1989**, *22*, 3337.

2) J. Kumaki, T. Kawauchi, K. Okoshi, H. Kusanagi, E. Yashima, *Angew. Chem., Int. Edn.* **2007**, *46*, 5348.

3) T. Okihara, M. Tsuji, A. Kawaguchi, and K. Katayama, *J. Macromol. Sci. Phys*. **1991**, *B30*, 119.

4) D. Brizzolara, H. J. Cantow, K. Diederichs, E. Keller, A. J. Domb, *Macromolecules* **1996**, *29*, 191.

5) G. Decher, *Science* **1997**, *277*, 1232.

6) Y. Wang, A. S. Angelatos, F. Caruso, *Chem. Mater.* **2008**, *20,* 848.

7) E. Kharlampieva, V. Kozlovskaya, S. A. Sukhishvili, *Adv. Mater*. **2009**, *21*, 3053.

8) S. Mandal, M. V. Lee, J. P. Hill, A. Vinu, K. Ariga, *J. Nanosci. Nanotechnol.* **2010**, *10*, 21.

9) T. Serizawa, K. Yamashita, M. Akashi, *J. Biomater. Sci., Polym. Edn.* **2004**, *15*, 511.

10) T. Serizawa, Y. Arikawa, K. Hamada, H. Yamashita, T. Fujiwara, Y. Kimura, M. Akashi, *Macromolecules* **2003**, *36*, 1762.

11) T. Kawauchi, J. Kumaki, E. Yashima, *J. Am. Chem. Soc.* **2006**, *128*, 10560.

12) G. T. Tor, J. F. Tan, S. N. Guntari, K. Satoh, A. Blencowe, M. Kamigaito, G. G. Qiao, *Angew. Chem., Int. Ed.* **2009**, *48*, 8707.

13) N. C. Escude, E. Y.-X. Chen, *Chem. Mater.* **2009**, *21*, 5743.

14) S. H. Kim, F. Nederberg, L. Zhang, C. G. Wade, R. M. Waymouth, J. L. Hedrick, *Nano Lett.* **2008**, *8*, 294.

15) T. Serizawa, K.-i. Hamada, T. Kitayama, K.-i. Katsukawa, K. Hatada, M. Akashi, *Langmuir* **2000**, *16*, 7112.

16) T. Serizawa, K.-i. Hamada, T. Kitayama, M. Akashi, *Angew. Chem., Int. Edn.* **2003**, *42*, 1118.

17) D. Kamei, H. Ajiro, C. Hongo, M. Akashi, *Chem. Lett.* **2008**, *37*, 332.

18) D. Kamei, H. Ajiro, C. Hongo, M. Akashi, *Langmuir* **2009**, *25*, 280.

19) D. Kamei, H. Ajiro, M. Akashi, *Polym. J.* **2010**, *42*, 131.

20) H. Ajiro, M. Akashi, *Macromol. Rapid Commun.* **2010**, *31*, 714.

21) H. Ajiro, D. Kamei, M. Akashi, *J. Polym. Sci., Polym. Chem. Ed.* **2008**, *46*, 5879.

22) T. Serizawa, K.-i. Hamada, M. Akashi, *Nature* **2004**, *429*, 52.

23) T. Kida, M. Mouri, M. Akashi, *Angew. Chem., Int. Edn.* **2006**, *45*, 7534.

24) H. Ajiro, D. Kamei, M. Akashi, *Polym. J.* **2009**, *41*, 90.

25) H. Ajiro, D. Kamei, M. Akashi, *Macromolecules* **2009**, *42*, 3019.

26) K. Hatada, K. Ute, K. Tanaka, T. Kitayama, Y. Okamoto, *Polym. J.* **1985**, *17*, 977.

27) T. Kitayama, S. He, Y. Hironaka, T. Iijima, K. Hatada, *Polym. J.* **1995**, *27*, 314.

28) Y. Arikawa, T. Serizawa, T. Mukose, Y. Kimura, M. Akashi, *Polym. Prep. Jpn.* **2006**, *55*, 4040.

# Part 3 Mechanistic Studies on Template Polymerization in Porous Isotactic Poly(methyl methacrylate) Thin Films

# Chapter 6

# Methacrylic Acid and Methyl Methacrylate Oligomers Adsorbed to Porous Isotactic Poly(methyl methacrylate) Ultrathin Filims

## 6. 1 INTRODUCTION

Natural polymers, such as DNA and proteins, are synthesized with extremely precise structures, controlled at main chain configurations, and contain arrays of different kinds of monomers and higher order structures. This almost perfect selectivity is achieved by template effects based on interactions between polymers. Controlling polymer structure is essential for synthetic polymers, because the chemical and physical characteristics of a polymer strongly depend on stereoregularity and molecular weight. Usually, synthetic polymers are mixtures of various stereochemistries and conformations, possessing molecular weight distributions. Thus, a huge amount of research has been put into controlling polymeric structure. For example, the design of polymerization catalysts, proper additives, and the design of monomer structures provides narrow molecular weight distributions and stereocontrol.[1–5]

The template effect during polymerization is also known as a synthetic method to

control molecular weight and increase the polymerization rate, which leverages interactions with the mold (template) polymer.[6] Radical template polymerization on methacrylate and acrylate using poly(vinyl pyrolidone) has been widely investigated. Although most studies concentrate on the kinetics and molecular weight distributions of complex formation,[7–12] S. Kitagawa and T. Uemura recently achieved a topotactic selective polymerization in porous inorganic materials with a radical method.[13,14]

Stereocomplexes, such as enantiomeric poly(lactide)s and syndiotactic (*st*) poly(methyl methacrylate) (PMMA)/isotactic (*it*) PMMA, are an attractive materials from the aspect of creating of molecularly stereocontrolled templates.[15] The discussion arose on the basic structure of the PMMA stereocomplex, by commonly using X-rays.[16–18] More recently, the visual images of stereocomplex were captured by AFM.[19,20] With their different approach, both G. Challa and E. Yashima concluded that the structure of the PMMA stereocomplex is a helix with *it*-PMMA inside surrounded by *st*-PMMA, which supports the possibility for stereospecific template polymerization. G. Challa *et al*. also reported the stereocontrol of PMMA. They polymerized methyl methacrylate (MMA) radically in the presence of stereoregular *it*-PMMA or *st*-PMMA, which resulted in syndiotactic or isotactic enriched polymers, respectively, because of the formation of stereocomplexes during the polymerization.[21–23] However, it was difficult to draw out the effect of the template to its maximum so that polymers existed under thermal motion in solutions.

Complex formation on substrates by alternatively dipping into each polymer solution was explored, and this procedure provides ultrathin films composed of polycations/polyanions.[24] Polymer–polymer interactions were usually electrostatic in nature; however, van der Waals interactions were applied toward *it*-PMMA/*st*-PMMA

stereocomplex formation.[25] The amount of PMMA stereocomplex assembled could be controlled by solvents, polymer concentration, and molecular weight, which enabled the preparation of desirable stereocomplex ultrathin film on substrates. With this LbL assembly technique, a variety of stereocomplex ultrathin films was also prepared, such as *st*-poly(methacrylic acid) (PMAA)/*it*-PMMA stereocomplexes[26] and *st*-poly(alkyl methacrylate)/*it*-PMMA stereocomplexes.[27] It is noteworthy that the LbL assembly technique is a general procedure for PMMA stereocomplex derivatives with different solubilities and bulkiness.

A revolutionary invention with this method is the preparation of porous *it*-PMMA ultrathin films as templates, achieved by the selective extraction of *st*-PMAA from *st*-PMAA/*it*-PMMA stereocomplex films.[28] Furthermore, the subsequent incorporations of *st*-PMAA or *st*-PMMA were confirmed, implying the existence of stereoregular nanospaces and possible stereospecific polymerization. In fact, free radical polymerization of MMA within nanospaces of *st*-PMAA ultrathin films was achieved. Surprisingly, the radically synthesized polymer showed high isotacticity ($mm = 97$, $M_n = 68500$, $M_w/M_n = 2.4$), and *st*-PMAA was similarly formed from methacrylic acid (MAA) with a radical method within porous *it*-PMMA ultrathin films ($rr = 98$, $M_n = 19200$, $M_w/M_n = 2.1$).[29] The molecular weight was also controlled, as shown by one-pot polymerization with various molecular weight templates.[30] It was a significant phenomenon, because molecular weight control with a radical method is usually difficult to achieve, due to side reactions, such as disproportionation and radical coupling reactions of active radical species.

Highly tactic and molecular weight controlled PMMAs have been synthesized by anionic polymerization;[31,32] however, a strict water-free condition and organometallic

compounds are needed. Template polymerization in porous ultrathin films by radical methods provides the possible manufacture of precise controlled PMMAs.

On the other hand, the detailed mechanism for radical template polymerization remains unclear in porous ultrathin films. Thus, mechanistic investigations could be essential for understanding the quite rare stereospecific living radical polymerization system and to expand its possible applications toward various vinyl monomers. In general, pick-up and zip mechanisms are known as template polymerization mechanisms, depending on interaction behaviors between template polymer and reacting monomers or oligomers.[6] Therefore, if the interacting species are determined with the template polymer one could reveal the template polymerization mechanism. At present, the adsorption behavior of *st*-PMAA toward porous *it*-PMMA ultrathin films and various compounds toward PMMA stereocomplexes have been investigated.[28,33] However, adsorption behaviors of oligomers and monomers toward porous *it*-PMMA ultrathin films have not been characterized on well-controlled template polymerization systems.[34]

In this study, we focused on porous *it*-PMMA ultrathin films to reveal molecular weight control during the template polymerization.[30] Previously, the interactions of *it*-PMMA with *st*-PMMA using various molecular weight,[25] *st*-PMAA,[26] atactic-PMAA, *st*-poly(ethyl methaclyrate), and *st*-poly(propyl methacrylate)[28] have been studied; however, no data are available about the intermediate species of template polymerization. Thus, we paid attention to vinyl monomers (MAA and MMA) and their oligomers, as models of active radical intermediate species during template polymerization (Scheme 6-1), to investigate their interactions on a quartz crystal microbalance (QCM), together with ATR-IR spectral analyses.

**Scheme 6-1. Preparation of Porous *it*-PMMA Ultrathin Film and Incorporation of Monomers and Oligomers.**
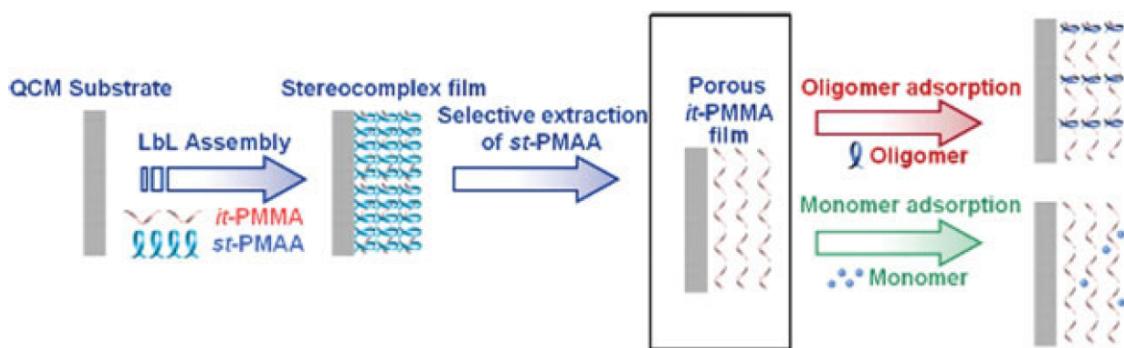


## 6. 2 EXPERIMENTAL

**Materials** Methyl methacrylate (MMA) (Tokyo Chemical Industry Co.), trimethylsilylmethacrylate (Aldrich), and toluene (Tokyo Chemical Industry Co.) were distilled with calcium hydride just before use. *it*-PMMA in this study was synthesized by anionic polymerization of MMA in toluene at 78 ℃ for 5 days with *t*-BuMgBr[31] (*mm*:*mr*:*rr* = 96:2:2, $M_n$ = 22900, $M_w/M_n$ = 1.21 were used for oligomer adsorption. *mm*:*mr*:*rr* = 96:3:1, $M_n$ = 36000, $M_w/M_n$ = 1.20 were used for monomer adsorption). *st*-PMAA was synthesized by anionic polymerization of trimethylsilylmethacrylate with *t*-BuLi/Bis(2,6-di-tert-butylphenoxy)methyl aluminum,[32] and the obtained polymer was methylated by diazomethane to be characterized (*mm*:*mr*:*rr* = 1:5:94, $M_n$ = 33700, $M_w/M_n$ = 1.45 were used for oligomer adsorption. *mm*:*mr*:*rr* = 1:6:93, $M_n$ = 32400, $M_w/M_n$ = 1.59 were used for monomer adsorption). Tacticities of polymers were determined by ^{1}H NMR spectra of alpha methyl protons in nitrobenzene-$d_5$ at 110 ℃. Molecular weights and polydispersities were determined by SEC in THF at 40 ℃ with PMMA standard. PMAA oligomers were obtained by radical polymerization with

113

azobisisobutylonitrile and purified with fractionation by THF and benzene. Trimer of PMMA was prepared by anionic polymerization with NaOMe.[35]

**Quartz Crystal Microbalance** An AT-cut quartz crystal with a parent frequency of 9 MHz was obtained from USI (Japan). A crystal (9 mm in diameter) was coated on both sides with gold electrodes 4.5 mm in diameter, which was of mirror like polished grade. The frequency was monitored by an Iwatsu frequency counter (Model SC7201) and was recorded manually. The leads of the quartz crystal microbalance (QCM) were sealed and protected with a rubber gel to prevent degradation as a result of the solvent contact during immersion in organic solutions. The amount of polymers adsorbed, $\Delta m$, could be calculated by measuring frequency decreases in the QCM, $\Delta F$, using Sauerbrey's equation[36] as follows:

$$\Delta F = 2F_0{}^2/(A\rho_q\mu_q)^{1/2} \times \Delta m$$

where $F_0$ is the parent frequency of the QCM (9 MHz), $A$ is the electrode area (0.159 cm$^2$), $\rho_q$ is the density of the quartz (2.5 g cm$^{-3}$), and $\mu_q$ is the shear modulus (2.95 × 10$^{11}$ dyn cm$^{-2}$). This equation was reliable when measurements were made in air as described in this study, because the mass of solvent is never detected as frequency shifts, and the effect of the viscosity of the absorbent on the frequency can be ignored.

## 6. 3 RESULTS AND DISCUSSION

Stereocomplexes were prepared using the combinations between $it$-PMMA ($M$n = 22900) and $st$-PMAA ($M$n = 33,700), or $it$-PMMA ($M$n = 36000) and $st$-PMAA ($M$n = 32400). A typical QCM analysis is shown in Figure 6-1. The porous $it$-PMMA ultrathin film was prepared as follow: 16-step alternative immersions into $it$-PMMA in

acetonitrile and *st*-PMAA in acetonitrile/water (4/6, v/v) with 0.017 unit M were achieved to form stereocomplexes of *st*-PMAA/*it*-PMMA on a QCM substrate at 25 ºC. Then, 0.01 M NaOHaq. was used to extract *st*-PMAA from the stereocomplex, which results in the *it*-PMMA ultrathin film with stereoregular (*st*-PMAA) nanospace, analyzed by AFM[28] and XRD.[37] The reduced weight at this point showed the total amount of adsorbed *st*-PMAA in the alternative assembly. Using the obtained porous *it*-PMMA ultrathin films on the QCM substrate, vinyl monomers and oligomers were adsorbed and their behaviors were observed. To clarify the adsorption amounts and the relationship among various kinds of compounds in this study, the complexing efficiency (CE) was defined as:

$$CE\ (\%) = W_{incorp.} \times (M_{st}/M_{incorp.})/\{2 \times W_{it} \times (M_{st}/M_{it})\} \times 100$$

where $W_{incorp.}$ is the increased weight at incorporation stages, $W_{it}$ is the remaining *it*-PMMA weight on the QCM substrate, $M_{incorp.}$ is the unit molecular weight of the incorporation compound, $M_{st}$ is the unit molecular weight of *st*-PMAA (86.09 g mol$^{-1}$), and $M_{it}$ is the unit molecular weight of *it*-PMMA (100.12 g mol$^{-1}$), assuming 2:1 *st*-PMAA/*it*-PMMA stoichiometry. $W_{incorp.}$ was calculated by the change of frequency ($\Delta F$) in formula (6-1).
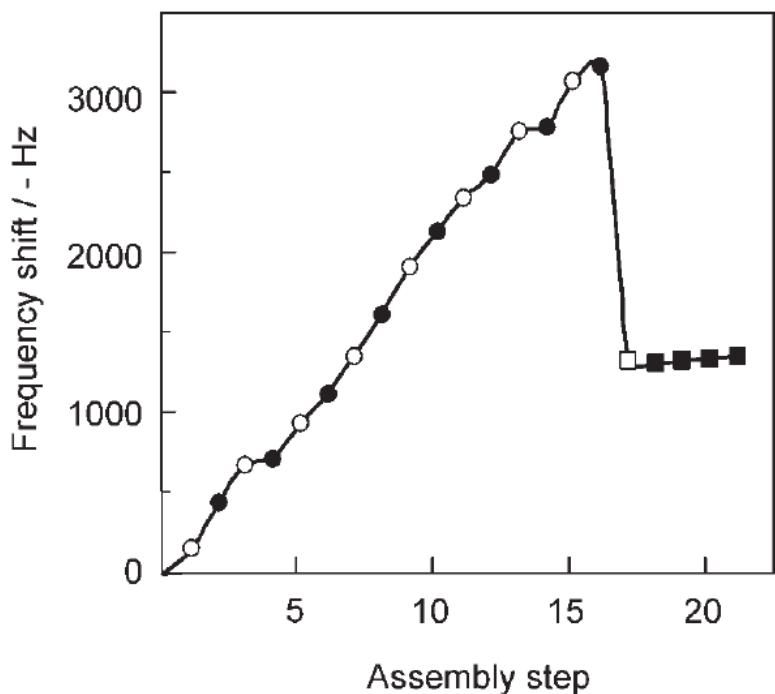
**Figure 6-1.** Typical frequency shift of QCM by the stepwise assembly: *it*-PMMA (open circle) in acetonitrile and *st*-PMMA (filled circle) in acetonitrile/water (4/6, v/v). The LbL alternative assembly was achieved for 16-steps on the QCM substrate at the concentration of 0.017 unit M at 25 °C and *st*-PMAA was selectively extracted by NaOH(aq) (open square). The following subsequent MMA (filled square) incorporation was achieved at the concentration of 0.13 mol L$^{-1}$ at 25 °C.

At first, we were interested in the structure of the trimer as the smallest stereoregular unit (*mm*, *mr*, and *rr*), which is possibly small enough to enter into the stereoregular nanospace, with little tacticity variation and a short sequence. Thus, the PMMA trimer was prepared by anionic polymerization initiated by sodium methoxide[35] and distilled under vacuum. On the other hand, it was difficult to purify the PMAA trimer from oligomers after radical polymerization with azobisisobutylonitrile, and a mixture of oligomers was used. Both oligomer ending structures were derived from each initiator and were confirmed by mass spectra (Figure 6-2).

116
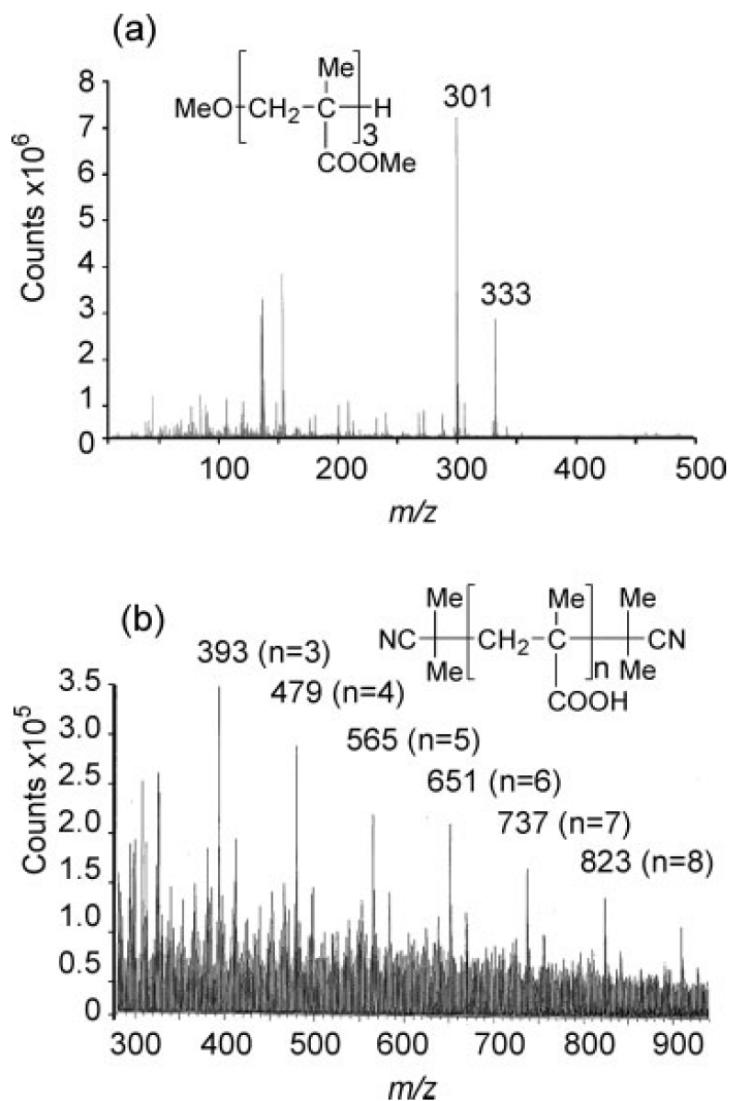
**Figure 6-2.** FAB mass spectra of (a) poly(methyl methacrylate) trimer and (b) poly(methacrylic acid) oligomers.

Figure 6-3 shows CE (%) of the adsorbed PMMA trimer toward porous *it*-PMMA ultrathin films, accompanied with those of *st*-PMMA and MMA. As reported, the *st*-PMMA adsorbed around 30% from acetonitrile solution, indicating quick stereocomplex formation on the surface, otherwise the *it*-PMMA on the QCM was dissolved by acetonitrile [Figure 6-2(a)].[28] In fact, MMA and PMMA trimers were not able to keep *it*-PMMA on the QCM under the same conditions, and whole polymers

flowed, when employed for adsorption compounds. To estimate their adsorption behavior, MeOH/water (1/1, v/v) was selected since it does not destroy the ultrathin film and the PMMA trimer and MMA demonstrate good solubility in this solvent. The results are depicted in Figure 6-2(b,c) with a concentration of 0.1 mol $L^{-1}$ at 25 ºC. Although the MMA monomer does not stayin the film at all, the PMMA trimer is adsorbed with around 5% CE immediately and sustains this value. Surprisingly, this value approximates the ideal value, when stereocomplex formation is achieved by st-PMAA/*it*-PMMA = 2. In other words, considering the amount (about 1800 Hz) and molecular weight of the *it*-PMMA on the ultrathin film ($M$n = 22900), the ratio of (PMMA trimer)/(*it*-PMMA) was calculated to be about 6. The aforementioned indicates approximately 230 ng of the PMMA trimer is trapped inside the porous *it*-PMMA film, whereas over 70000 times (17 mg) of the PMMA trimer exists in solution. This suggests that the possible adsorption spot in the porous *it*-PMMA film is limited, even when a large excess of *rr*-, mr-, and *mm*-isomers should exist. Probably, the different structure from the polymer chain, such as the ending group, would contribute the stable adsorption. The smaller bulkiness of the methoxy group, the ending group in the PMMA trimer, rather than the isobutyl group, which is used in actual radical polymerization might allow the PMMA trimer to enter the porous *it*-PMMA ultrathin film. To add to this, the length and angle of C—C bonds in PMMA trimers were altered from vinyl monomer structures, affecting favorable van der Waals interactions.
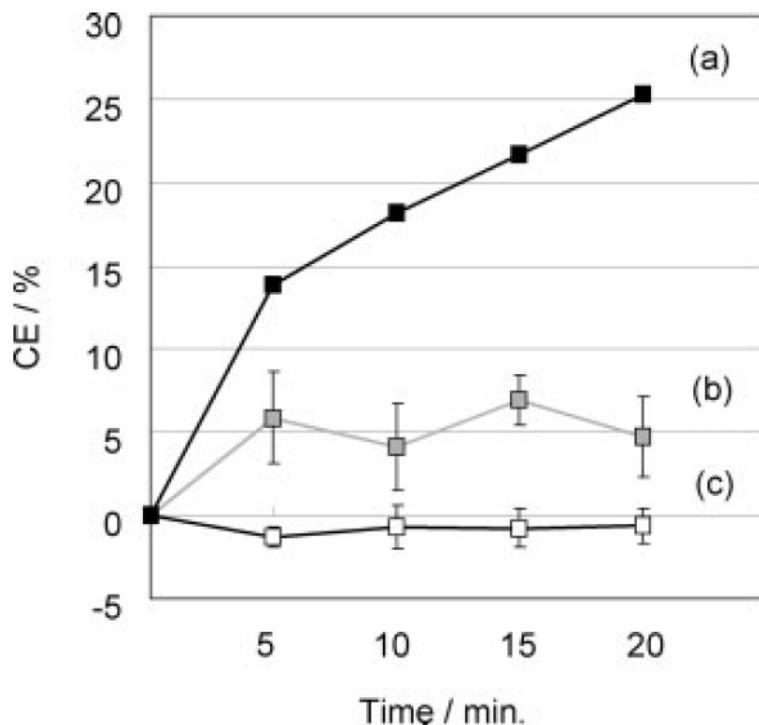
**Figure 6-3.** Complexing efficiency of *st*-PMMA (a), PMMA-trimer (b), and MMA (c) with *it*-PMMA in MeOH/H$_2$O (1/1, v/v) at 0.1 mol L$^{-1}$ (the average value; $n$ = 3).

ATR-IR spectra of the QCM surface covered with ultrathin films are shown in Figure 6-4 and correspond to carbonyl groups of *it*-PMMA and PMMA trimers. Since the pattern of carbonyl groups have been assigned to conformations of each stereoregular PMMA and PMAA, detectionof the difference give us insight into the nanostructure of each polymer.[28] Compared with the peak top around 1739 cm$^{-1}$ of porous *it*-PMMA [Figure 6-4(c)], the shift to 1737 cm$^{-1}$ was observed in the spectrum of the *it*-PMMA/PMMA trimer 5% CE, accompanied with a slight shoulder pattern around 1730 cm$^{-1}$ [Figure 6-4(b)]. This suggests that PMMA trimer is incorporated into the porous *it*-PMMA film, to maintain the internal main chain conformation.
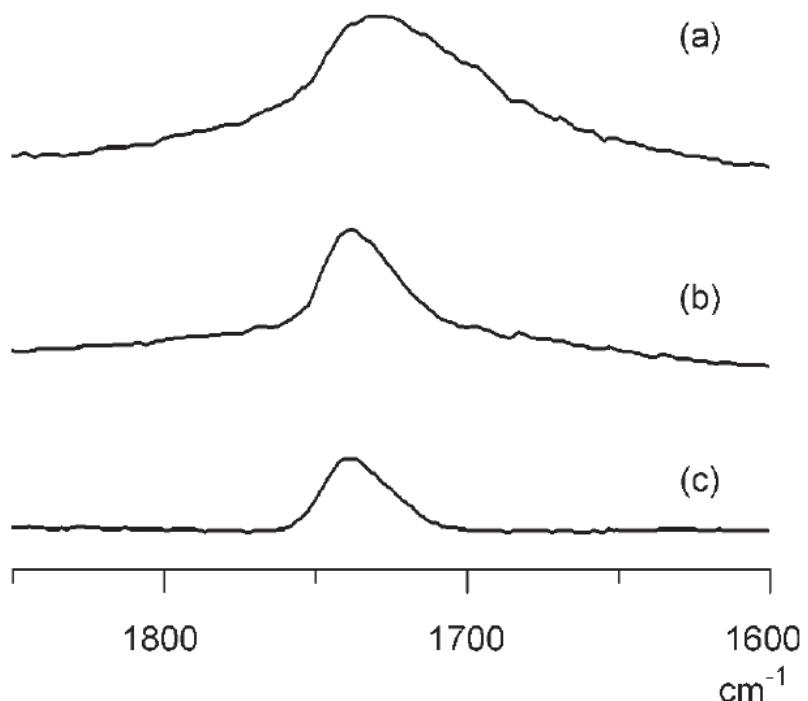
**Figure 6-4.** ATR-IR spectra of (a) stereocomplex, (b) complex of porous *it*-PMMA and PMMA trimer, and (c) porous *it*-PMAA film.

The space of the porous *it*-PMMA ultrathin film should fit into the *st*-PMAA structure rather than the *st*-PMMA, which possesses bulky methyl groups. Next we might try the PMAA trimer, however, synthetic difficulties and a small amount incorporation of PMMA trimers, which made it difficult to analyze ATR-IR spectra, further hampered the research. The radical oligomerization of methacrylic acid (MAA) and solvent fractionation by THF and benzene provided the mixture of PMAA trimer and several oligomers with isobutylonitrile groups at the ends [Figure 6-2(b)]. Thus, we used the PMAA oligomer, which consisted of a mixture of trimer to octamer.
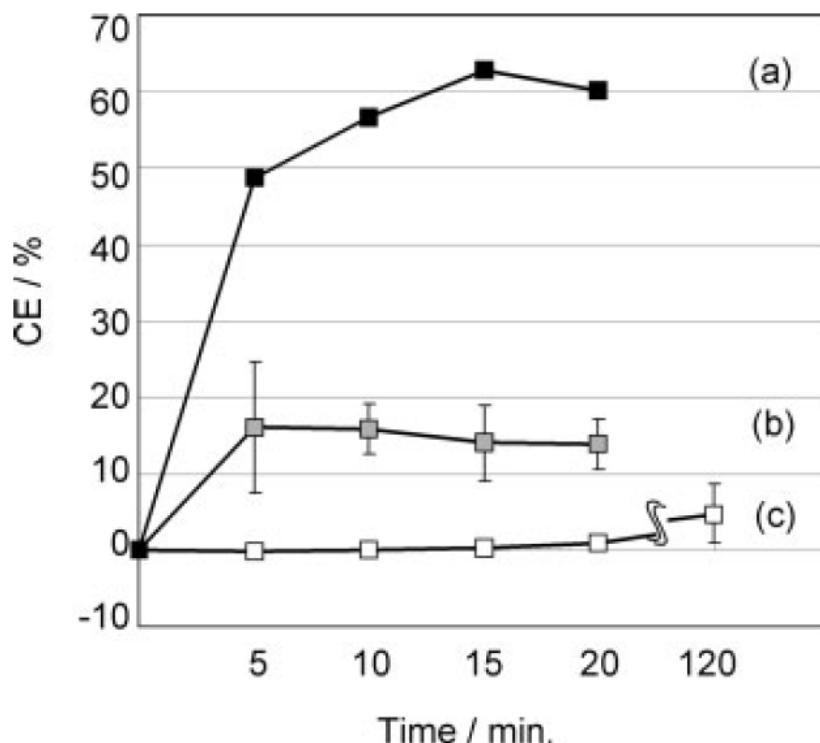
**Figure 6-5.** Complexing efficiency of (a) *st*-PMAA in MeCN/$H_2O$ = 4/6 at 0.017 unit M, (b) PMAA-oligomer in $H_2O$ at 0.13 unit M, and (c) MAA in $H_2O$ at 0.13 unit M with *it*-PMMA (the average value; $n$ = 3).

The general tendency of the adsorption behavior using PMAA oligomer was the same as that using PMMA trimer (Figure 6-5). Namely, *st*-PMAA and PMAA oligomers were absorbed nearly 60 and 15% CE, respectively, but no monomer (MAA) adsorption was observed at 20 min. Incorporated amounts of *st*-PMMA in Figure 6-3 and *st*-PMMA in Figure 6-5 decreased when compared with reported values, probably because of different stereocomplex ratios during the preparation of porous *it*-PMMA films in this study.[28] MAA looks like it is being incorporated gradually, however, a significant difference is still recognized between monomer and oligomer 2 h later. Besides, atactic PMAA could not be incorporated into the porous *it*-PMMA ultrathin film as reported.[28] On the other hand, PMAA oligomer entered into the porous film very

quickly at the initial stage, and the value did not change at all, in spite of the abundant amount of PMAA oligomer around the film [Figure 6-5(b)]. This implies a limited adsorption site exists in porous *it*-PMMA ultrathin films for the oligomer under these conditions and supports the reason why the living nature of active radical species in the ultrathin film and why molecular weight control was achieved in template polymerization using the radical method. Monomer could move in and out of the film to contribute to polymer growing reactions, and the total shape of the polymer should be syndiotactic as shown by polymer incorporation [Figure 6-5(a)]. atactic-PMAA oligomer (radical), which would be formed during the template polymerization at the same time, would not be able to enter into the *it*-PMMA ultrathin film, so radical concentration should extremely decrease in the *it*-PMMA ultrathin film. Therefore, we suggest that the limitedincorporation of oligomer is a reasonable model of radical species and provides a mechanism for the reported template polymerization. Polymer carbonyl peaks were confirmed by ATR-IR spectra, and slight peak top shifts from 1739 cm$^{-1}$ to 1737 cm$^{-1}$ were confirmed (Figure 6-6).
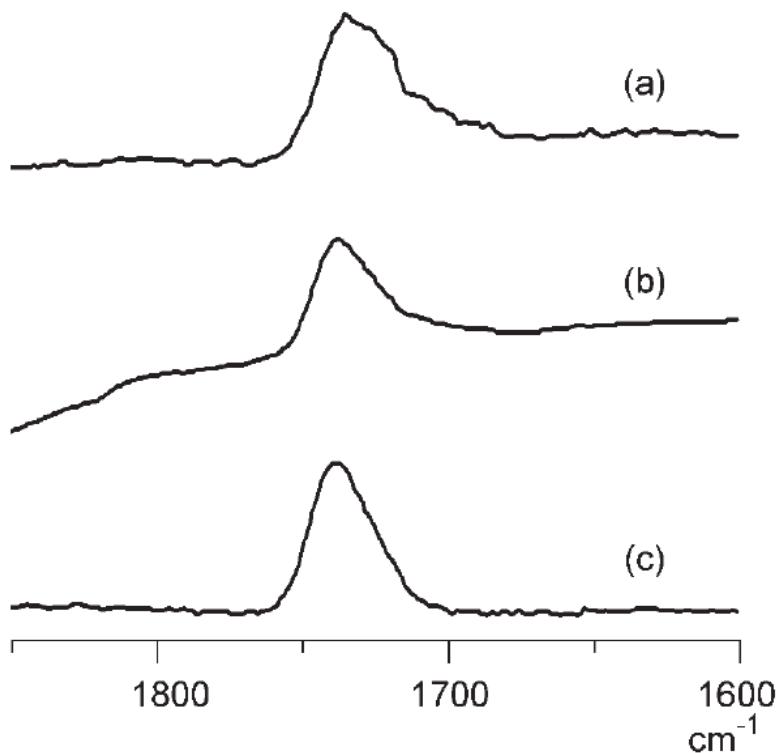
**Figure 6-6.** ATR-IR spectra of (a) complex of PMAAoligomer and *it*-PMMA film after extraction of *st*-PMMA (50% CE), (b) complex of PMAA-oligomer and *it*-PMMA film after extraction of *st*-PMMA (15% CE), and (c) porous *it*-PMMA film.

The monomer concentration used for adsorption was 0.1 mol L$^{-1}$, which was also used for template polymerization (Figure 6-3, 6-5). However, MAA was slightly incorporated after 2 h, which lead to more investigations with vinyl monomers under 20-fold concentrated conditions. Results from MAA, methacryl amide, and acrylic acid are shown in Figure 6-7. van der Waals interactions between methyl ester groups of *it*-PMMA and alpha methyl groups of *st*-poly(alkyl methacrylate) contribute to the stereocomplex formation.[38,39] Under concentrated conditions, MAA was moderately adsorbed into porous *it*-PMMA films [Figure 6-7(b)]; however, acrylic acid which does not possess alpha methyl groups was not adsorbed at all, as expected from the conventional idea regarding van der Waals interactions [Figure 6-7(c)]. Interestingly,

methacrylamide was adsorbed with almost the same value as that of MAA, implying the porous *it*-PMMA ultrathin films do not really recognize MAA, the monomer which gave rise to template polymerization. This result is reasonable, because the template space accommodated the polymer but not the monomer, even if the monomer was the source for template polymerization. In other words, the mechanism of the template polymerization follows a pick up mechanism, whose association with the template polymer is the oligomer but not the monomer. Compound angles and bond lengths are important factors to fit template structure.
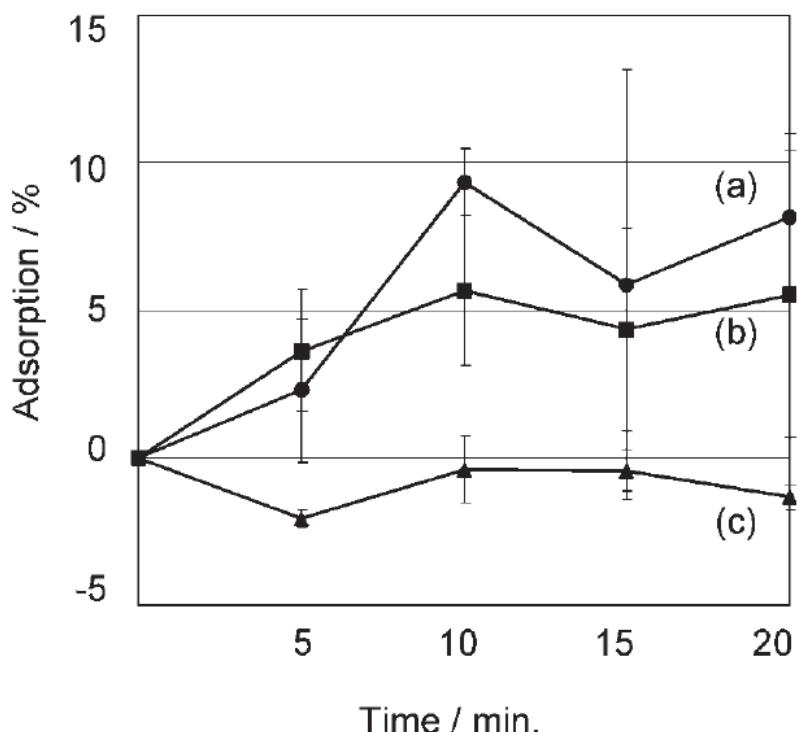


**Figure 6-7.** Adsorption efficiency of (a) methacryl amide, (b) methacrylic acid, and (c) acrylic acid in $H_2O$ at 2 mol $L^{-1}$ (the average value; $n = 3$).

## 6. 4 CONCLUSIONS

The mechanism for the stereoregular living polymerization of MAA on porous *it*-PMMA template film was investigated, using oligomers as active intermediate model species. When we combined results from monomeric and oligomeric adsorption behaviors, template polymerization follows a pick up mechanism, in which the growing oligomer radical interacts with the template polymer and monomer is freely supplied. The adsorbed PMMA trimer and PMAA oligomer amounts are limited to 5 and 15% CE toward the porous *it*-PMMA film, respectively. These results support a reason for molecular weight control during template polymerization, because the concentration of the growing radical species in the porous *it*-PMMA ultrathin film would be determined at initial stage by small amount of oligomers to the stable value. No further atactic oligomer radical could enter the ultrathin reaction field to prevent side reactions, such as radical coupling termination. Thus, the synthesized molecular weight of PMAA on the template polymerization in the porous *it*-PMMA ultrathin film should be controlled. Basic information regarding vinyl monomer adsorption under condensed conditions might provide further applications for the porous *it*-PMMA ultrathin films.

## REFERENCES

1) M. Kamigaito, T. Ando, M. Sawamoto, *Chem. Rev.* **2001**, *101*, 3689.

2) K. Matyjaszewski, J. Xia, *Chem. Rev.* **2001**, *101*, 2921.

3) G. W. Coates, *Chem. Rev.* **2000**, *100*, 1223.

4) S. D. Ittel, L. K. Johnson, M. Brookhart, *Chem. Rev.* **2000**, *100*, 1169.

5) T. Nakano, Y. Okamoto, *Chem. Rev.* **2001**, *101*, 4013.

6) S. Polowinski, *Prog. Polym. Sci.* **2002**, *27*, 537.

7) J. Ferguson, S. Shah, *Eur. Polym. J.* **1968**, *4*, 343.

8) J. -C. Matuszweska, S. Polowinski, *Eur. Polym. J.* **1998**, *34*, 557.

9) R. Muramatsu, T. Shimidzu, *Bull. Chem. Soc. Jpn.* **1972**, *45*, 2538.

10) V. Y. Baranovskii, A. A. Litmanovich, I. M. Papisov, V. A. Kabanov, *Eur. Polym. J.* **1981**, *17*, 969.

11) J. Smid, Y. Y. Tan, G. Challa, *Eur. Polym. J.* **1983**, *19*, 853.

12) K. Fujimori, G. T. Trainor, M. J. J. Costigan, *Polym. Sci., Polym. Chem. Ed.* **1984**, *22*, 2479.

13) T. Uemura, D. Hiramatsu, Y. Kubota, M. Takata, S. Kitagawa, *Angew. Chem., Int. Ed.* **2007**, *46*, 4987.

14) T. Uemura, K. Kitagawa, S. Horike, T. Kawamura, S. Kitagawa, M. Mizuno, K. Endo, *Chem. Commun.* **2005**, 5968.

15) W. R. Mariott, N. C. Escudé, E. Y. -X. Chen, *J. Polym. Sci., Part A: Polym. Chem.* **2007**, *45*, 2581.

16) A. M. Liquori, G. Anzuino, V. M. Coiro, M. D'Alagni, P. De Santis, M. Savino, *Nature* **1965**, *206*, 358.

17) E. Schomaker, G. Challa, *Macromolecules* **1989**, *22*, 3337.

18) T. Kida, M. Mouri, M. Akashi, *Angew. Chem., Int. Ed.* **2006**, *45*, 7534.

19) J. Kumaki, T. Kawauchi, K. Okoshi, H. Kusanagi, E. Yashima, *Angew. Chem., Int. Ed.* **2007**, *46*, 5348.

20) J. Liu, Y. Zhang, J. Zhang, D. Shen, Q. Guo, I. Takahashi, S. Yan, *J. Phys. Chem. C* **2007**, *111*, 6488.

21) R. Buter, Y. Y. Tan, G. Challa, *J. Polym. Sci., Part A-1: Polym. Chem.* **1972**, *10*,

1031.

22) R. Buter, Y. Y. Tan, G. Challa, *J. Polym. Sci., Polym. Chem. Ed.* **1973**, *11*, 1013.

23) J. H. G. M. Lohmeyer, Y. Y. Tan, G. Challa, *J. Macromol. Sci., Chem. A* **1980**, *14*, 945.

24) G. Decher, *Science* **1997**, *277*, 1232.

25) T. Serizawa, K.-i. Hamada, T. Kitayama, N. Fujimoto, K. Hatada, M. Akashi, *J. Am. Chem. Soc.* **2000**, *122*, 1891.

26) T. Serizawa, K.-i. Hamada, T. Kitayama, K.-i. Katsukawa, K. Hatada, M. Akashi, *Langmuir* **2000**, *16*, 7112.

27) K.-i. Hamada, T. Serizawa, T. Kitayama, N. Fujimoto, K. Hatada, M. Akashi, *Langmuir* **2001**, *17*, 5513.

28) T. Serizawa, K.-i. Hamada, T. Kitayama, M. Akashi, *Angew. Chem., Int. Ed.* **2003**, *42*, 1118.

29) T. Serizawa, K.-i. Hamada, M. Akashi, *Nature* **2004**, *429*, 52.

30) K.-i. Hamada, T. Serizawa, M. Akashi, *Macromolecules* **2005**, *38*, 6759.

31) K. Hatada, K. Ute, K. Tanaka, T. Kitayama, Y. Okamoto, *Polym. J.* **1985**, *17*, 977.

32) T. Kitayama, S. He, Y. Hironaka, T. Iijima, K. Hatada, *Polym. J.* **1995**, *27*, 314.

33) T. Serizawa, K. Yamashita, M. Akashi, *Polym. J.* **2006**, *38*, 503.

34) T. Serizawa, M. Akashi, *Polym. J.* **2006**, *38*, 311.

35) A. Laguerre, J. P. Busnel, C. M. Bruneau, *Makromol. Chem. Rapid. Commun.* **1984**, *5*, 21.

36) G. Sauerbrey, *Z. Phys.* **1959**, *155*, 206.

37) D. Kamei, H. Ajiro, C. Hongo, M. Akashi, *Chem. Lett.* **2008**, *37*, 332.

38) J. H. G. M. Lohmeyer, Y. Y. Tan, P. Lako, G. Challa, *Polymer* **1978**, *19*, 1171.

39) F. Bosscher, D. Keekstra, G. Challa, *Polymer* **1981**, *22*, 124.

# Chapter 7

# Macroporous Silicagel Substrate for Stereoregular Template Polymerization of Methacrylic Acid Using Stereocomplex Assembled Thin Films

## 7. 1 INTRODUCTION

Controlling polymer structure is important, because the chemical and physical characteristics of a polymer depend on its molecular weight distribution and stereoregularity. Polymer-polymer interactions have received much attention due to the possible application as a precise reaction control. For example, isospecific and syndiospecific template polymerizations of methyl methacrylate (MMA) have been reported with the use of stereocomplex formation in the presence of one stereoregular polymer.[1,2] However, van der Waals interactions between isotactic (*it*) and syndiotactic (*st*) poly(methyl methacrylate)s (PMMA) exert an unfavorable effect against the formation of a stereoregular polymer during radical polymerization in solution, because the polymer chain moves constantly with thermal motion. Recently, molecularly porous thin films were employed for stereoregular template polymerization, which were prepared by the alternative layer-by-layer assembly of *it*-PMMA/*st*-poly(methacrylic acid) (PMAA) and the subsequent extraction of one polymer from the stereocomplex film.[3,4] It was a breakthrough for the precise control of radical polymerization on MMA and methacrylic acid (MAA). This new stereocontrol approach is significant, because conventional anionic polymerization requires restricted polymerization conditions and

organometal reagents. Porous *it*-PMMA thin film formation, *st*-PMAA recognition, and stereoregular template polymerization of MAA were investigated preliminarily on a quartz crystalline microbalance (QCM) substrate at the nano gram order. In order to manufacture stereoregular PMMAs with the aforementioned template polymerization method, a more efficient reaction field is crucial. Although silica gel (diameter: 1.6 mm) was used as a substrate because of its larger surface area,[3] the issues still remain. For example, the aggregation of the silicagels bearing thin polymer films prevents good dispersion, which is required for an efficient reaction field. The smaller the silicagel is, the greater the reaction efficiency, but this makes it difficult to recover the silicagels completely by centrifugation after several dozen alternative immersion steps.

Therefore, we selected a macroporous silicagel (diameter: 7 μm, pore: 100 nm) as a suitable substrate for template polymerization in this study. Macroporous silicagel is widely used, for example as the supporting for material of a stationary phase in high-performance liquid chromatography (HPLC).[5] Packed column is possible to be applied for repeatedly available polymerization container. Herein, we report the template polymerization of MAA on a porous *it*-PMMA thin film formed on macroporous silicagels, and discuss the curvature effect and reproducibility.

## 7. 2 EXPERIMENTAL

**Materials** Macroporous silicagel (diameter: 7 mm, pore: 100 nm) was purchased from Daiso, Co., LTD. MMA (Tokyo Chemical Industry Co., LTD.), MAA (Tokyo Chemical Industry Co., LTD.), trimethylsilylmethacrylate (Aldrich), toluene (Tokyo Chemical Industry Co., LTD.) were distilled with calcium hydride. 2,2'-Azobis(2-methylpropionamidine) dihydrochloride (V-50) (Wako) was used

without further purification. *it*-PMMA for Layer-by-layer assembly in this study was synthesized by anionic polymerization of MMA in toluene at 78 °C for 5 d with *t*-BuMgBr[6] (*mm*:*mr*:*rr* = 96:3:1, $M_n$ = 36000, $M_w/M_n$ = 1.20). *st*-PMAA for Layer-by-layer assembly was synthesized by anionic polymerization of trimethylsilylmethacrylate with *t*-BuLi/bis(2,6-di-tert-butylphenoxy)methyl aluminum,[7] and the obtained polymer was methylated by diazomethane to be characterized (*mm*:*mr*:*rr* = 1:5:94, $M_n$ .33700, $M_w/M_n$ = 1.45). Tacticities of polymers were determined by ^{1}H NMR spectra of alpha methyl protons in nitrobenzene-$d_5$ at 110 °C. Molecular weights and polydispersities were determined by SEC in THF at 40 °C with PMMA standard.

**Preparation of Porous *it*-PMMA Thin Film** Stereocomplex was prepared using *it*-PMMA ($M_n$ = 36000) and *st*-PMAA ($M_n$ = 32400), which were obtained by anionic polymerizations. The porous *it*-PMMA thin film on macroporous silicagel was typically prepared as follow. In plastic tube with cap, a 2 g of macroporous silicagel was introduced. 40 mL of *it*-PMMA in acetonitrile with 0.017 unitM was then introduced into the tube to rotate mildly for 15 min. After centrifugation, supernatant polymer solution was separated from macroporous silicagel, and washed with acetonitrile twice. Similarly, *st*-PMAA in acetonitrile/water (4/6, v/v) with 0.017 unitM was treated to form stereocomplexes of *st*-PMAA/*it*-PMMA on macroporous silicagel substrate. Those alternative immersions were repeated twenty cycles (Table 7-1, entry 1–4). The same procedure was achieved to prepare the other stereocomplex on macroporous silicagel, except for *st*-PMAA in acetonitrile/water (2/8, v/v) and washing water for *st*-PMAA steps (Table 7-1, entry 5). Then, 0.01M NaOH(aq) was used to extract *st*-PMAA from

131

the both stereocomplex, which results in the *it*-PMMA ultrathin film with stereoregular (*st*-PMAA) nanospace. The extraction was confirmed by the IR spectral change of carboxyl group.

**Table 7-1.** Template polymerization of methacrylic acid[a]

| Entry | Solvent for *st*-PMAA MeCN:water | Reuse cycle | Yield[c] mg (%) | Tacticity[d] *mm:mr:rr* | $M_n$[e] $\times 10^3$ | PDI[e] |
|-------|-------|-------|-------|-------|-------|-------|
| 1 | 40:60 | — | 44 (5%) | 1:10:89 | 29.5 | 2.84 |
| 2[b] | 40:60 | Second | 28 (3%) | 1:11:88 | 28.9 | 2.53 |
| 3[b] | 40:60 | Third | 36 (4%) | 1:11:88 | 30.7 | 2.72 |
| 4[b] | 40:60 | Fourth | 28 (3%) | 1:8:91 | 31.2 | 2.66 |
| 5 | 20:80 | — | 36 (4%) | 3:8:89 | 28.4 | 2.30 |

[a]Methacrylic acid = 0.9 mL. Initiator = 0.143 g. Solvent = water, 300 mL. Temp. = 40 °C. Time = 2 h. [b]Same silica gel was used as a recycle three times. [c]Recovered as a NaOH aq.-soluble part. [d]Determined by ^{1}H NMR of alpha-methyl group of PMMA, which was derived from the obtained PMAA. [e]Determined by SEC with PMMA standard in THF after methylation.

**Template Polymerization** 0.9mL of MAA was dissolved in ultrapure water, and the porous *it*-PMMA thin film on macroporous silicagel were introduced. Dry nitrogen gas was handled for more than 15 min before use, and then V-50 was added under nitrogen atmosphere to heat at 40 °C for 2 h. The mixture was cool down to stop reaction. Macroporous silicagel was washed by water to recover PMAA, which was produced in solution. Then PMAA which was synthesized in porous *it*-PMMA thin film was extracted by 0.01M NaOH(aq). The macroporous silicagel with porous thin film was used for three times.
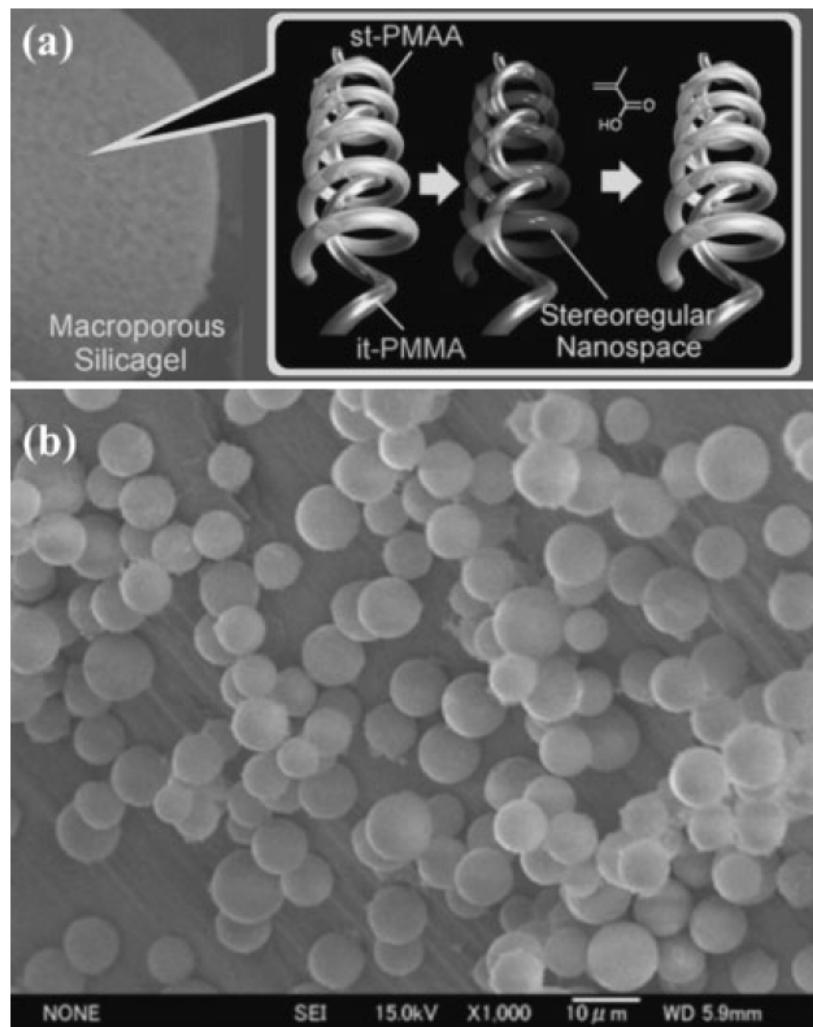
**Figure 7-1.** Schematic illustration of (a) stereoregular template preparation for *st*-PMAA and (b) a SEM image of the macroporous silicagel with *it*-PMMA/*st*-PMAA stereocomplex films. White bar indicates 10 μm.

## 7. 3 RESULTS AND DISCCUSION

Figure 7-1 shows a schematic illustration of stereocomplex (*it*-PMMA/*st*-PMAA) formation, porous *it*-PMMA film preparation, and the subsequent template polymerization of MAA, together with SEM images of the silicagel. After 10 cycles of

133

alternative immersion between the *it*-PMMA and *st*-PMAA solution, the *it*-PMMA/*st*-PMAA stereocomplex would be present on the surface. It is not surprising that holes in the silicagel could still be clearly observed, because the width of *it*-PMMA/*st*-PMMA stereocomplex is around 2 nm as reported elsewhere.[8] These holes were also recognized even after 20 cycles of alternative immersion, although very small amount of polymer which are not adsorbed onto the silicagel was also observed. Due to the washing processes of silicagel against the existing *it*-PMMA or *st*-PMAA, these polymers were assumed to be stereocomplexes. During the *st*-PMAA template (porous *it*-PMMA film) preparation with the subsequent extraction of *st*-PMAA, the holes in the silicagel were not completely covered with the polymers, but the silicagel surface became smoother and the hole size tended to be smaller; these findings were confirmed by SEM. This suggests that the polymer solution could permeate inside each silicagel particle, and a template field could also be created inside the macroporous silicagel.

The syndiospecific template polymerization of MAA with the *it*-PMMA film on the silicagel was successfully achieved (Table 7-1).[3] The template polymerization with twenty cycles of alternative assembly on 2 g of macroporous silicagel resulted in 44 mg (5% yield) of PMAA, whereas 740 mg of PMAA (81% yield) was recovered from the solution. Previously, it has been reported that about $1.4 \times 10^{-6}$ mg (1600 Hz) of *it*-PMMA/ *st*-PMAA stereocomplex was adsorbed onto a QCM (9 mm diameter) at 5 cycles of assembly.[9] Assuming that the same amount of stereocomplex was adsorbed onto the macroporous silicagel, 2.6 g was estimated as the amount of stereocomplex film in this study, because a 60 m$^2$ surface area of macroporous silicagel (30m$^2$/g, 2 g) was used for 20 cycles of assembly. Taking the 1/2 ratio of *it*-PMMA/*st*-PMAA into account, the efficiency of the template polymerization was calculated to 3%. However,

the amount adsorbed onto the silicagel should be much smaller than the theoretical value, because the surface energy of glass on macroporous silicagel is much smaller than that of gold on a QCM. Furthermore, the molecular weight ($M_n$ = 26000) during the extraction procedure was smaller than that of $st$-PMAA used during stereocomplex formation, and the molecular weight of synthesized PMAA was similar to that of the extracted PMAA. Taken together, these findings imply that not all stereocomplex film were effective for template field creation deep inside the pores, however, the template polymerization proceeded along the nanospace.

A lack of syndiotacticity was observed in PMMA recovered from supernatant in the previously reported template polymerization,[3] which was considered to be a result of the excess adsorption of $rr$-triads to the template thin film. However, the tacticity of the PMAA collected from solution in this study was atactic after treatment with diazomethane (Figure 7-2c), which is a similar value as the typical PMAAs obtained with radical methods. This is likely the result of the large amount of monomer polymerized as compared to the template thin film. On the other hand, PMAA synthesized on the macroporous silicagel was confirmed as highly syndiotactic (Figure 7-2d), suggesting that the stereoregularity of the PMAA was influenced by the $it$-PMMA film on the macroporous silicagel. The molecular weight of PMAA synthesized on the macroporous silicagel ($M_n$ = 28000) was similar to the initially extracted $st$-PMAA ($M_n$ = 26000), and smaller than that collected from solution ($M_n$ = 46000), which implies that the polymerization circumstances were quite different.
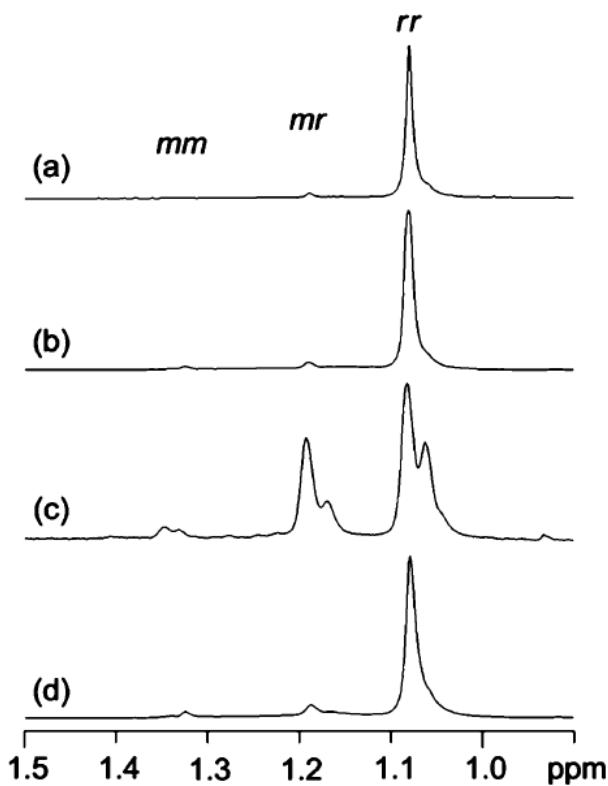
**Figure 7-2.** $^1$H NMR spectra of synthesized poly(methacrylic acid) at 110 $^o$C in nitrobenzene-*d* after methylation with diazomethane. (a) *st*-PMMA obtained by anionic polymerization, (b) PMMA extracted from stereocomplex thin film on macroporous silicagel at preparation of template reaction field, (c) PMMA collected from solution after polymerization, and (d) PMMA synthesized with porous *it*-PMMA on silicagel.

Next, the macroporous silicagel was maintained at 20 $^o$C for 2 d, and then the template polymerization was repeated two times (Table 7-1, entries 2, 3, Figure 7-3a, 3b). Another 13 d late, the template polymerization was performed again (Table 7-1, entry 4, Figure 7-3c). These results demonstrate that the polymerization field was stable for recycled use, because the highly syndiotactic selective polymerization was repeatedly observed.
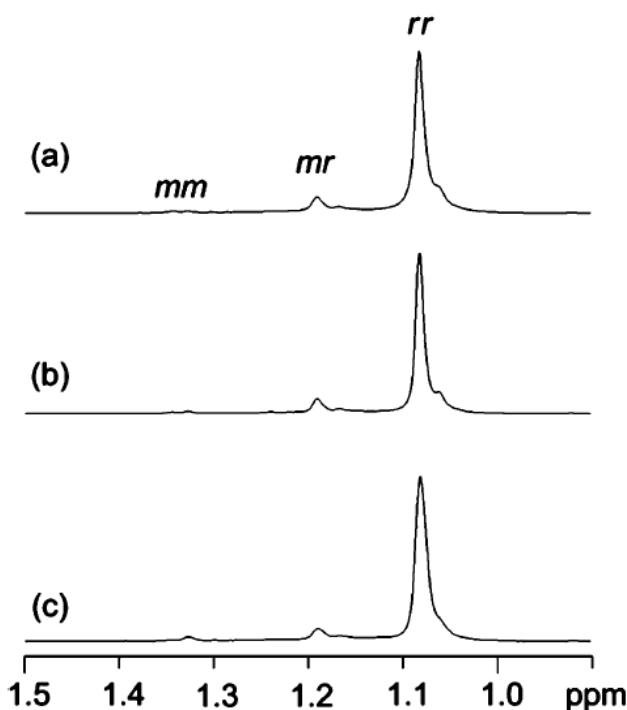
**Figure 7-3.** $^1$H NMR spectra of synthesized poly(methacrylic acid) on the reused *it*-PMMA film after methylation by diazomethane (in nitrobenzene-*d*, 110 $^{\circ}$C). (a) Secondly synthesized PMAA, (b) thirdly synthesized PMAA, and (c) fourthly synthesized PMAA.

Finally, the alternative assembly of *it*-PMMA/*st*-PMAA onto macroporous silicagel with 40 cycles was examined with acetonitrile/water (2/8, v/v) for the *st*-PMAA solvent (Table 7-1, entry 5). The reused template polymerization on the macroporous silicagel provided almost the same yield. Solvent effect on the amount of stereocomplex formation by layer-by-layer was reported.[10] When acetonitrile/water (3/7, v/v) was employed, the stereocomplex amount decrease almost two-thirds of that with acetonitrile/water (4/6). Thus, the result (Table 7-1, entry 5) is understandable because of the solvent effect and twice layer-by-layer assembly. The molecular weights were controlled, and they were highly syndiotactic (*rr* = 90%) as measured by $^1$H NMR after methylation with diazomethane for all of the obtained PMAAs (Table 7-1). These

reproducible results suggest that the template polymerization of methacrylic acid with *it*-PMMA/macroporous silicagels has practical applications for manufacturing using HPLC systems.

## REFERENCES

1) R. Buter, Y. Y. Tan, G. Challa, *J. Polym. Sci.: Part A-1* **1972**, *10*, 1031.

2) R. Buter, Y. Y. Tan, G. Challa, *J. Polym. Sci., Polym. Chem. Ed.* **1973**, *11*, 1003.

3) T. Serizawa, K.-i. Hamada, M. Akashi, *Nature* **2004**, 429, 52.

4) T. Serizawa, M. Akashi, *Polym. J.* **2006**, *38*, 311.

5) Y. Okamoto, E. Yashima, *Angew. Chem., Int. Ed.* **1998**, *37*, 1020.

6) K. Hatada, K. Ute, K. Tanaka, T. Kitayama, Y. Okamoto, *Polym. J.* **1985**, *17*, 977.

7) T. Kitayama, S. He, Y. Hironaka, T. Iijima, K. Hatada, *Polym. J.* **1995**, *27*, 314.

8) J. Kumaki, T. Kawauchi, K. Okoshi, H. Kusanagi, E. Yamshima, *Angew. Chem., Int. Ed.* **2007**, 46, 5348.

9) T. Serizawa, K.-i. Hamada, T. Kitayama, M. Akashi, *Angew. Chem., Int. Ed.* **2003**, 42, 1118.

10) T. Serizawa, K.-i. Hamada, T. Kitayama, K.-i. Katsukawa, K. Hatada, M. Akashi, *Langmuir* **2000**, *16*, 7112.

# Chapter 8

# Template Polymerization in Porous Isotactic Poly(methyl methacrylate) Thin Films by Radical Polymerization and Post-polymerization of Methacrylate Derivatives

## 8. 1 INTRODUCTION

The development of controlled polymerization methods is an important research area because physical and chemical characters of polymers are influenced by their structures, such as molecular weight and stereoregularity. G. Challa *et al.* investigated the stereospecific polymerization of methyl methacrylate (MMA)[1,2] and methacrylic acid (MAA)[3] in the presence of stereoregular poly(methyl methacrylate) (PMMA) because isotactic (*it*) PMMA and syndiotactic (*st*) PMMA form stereocomplexes whose structures were reported as double-stranded helices by X-ray[4] and triple-stranded helices by AFM measurements.[5] In 2004, almost perfectly controlled radical polymerizations of methacrylates were reported in porous thin films.[6,7] Surprisingly, free radical polymerization principally controlled both molecular weights and stereoregularities, although little stereoregularity control was achieved in solution. Therefore, the elucidation of template polymerization mechanisms in thin films would provide significant finds. These aforementioned complexes were prepared by layer-by-layer (LbL) assembly as a critical approach.

LbL assembly, which is achieved by simple alternative immersions, was first reported by G. Decher *et al.*[8,9] as a convenient technique for fabricating thin films using

polycation-polyanion interactions. Because of its simplicity and high applicability, the LbL assembly method is applied to a wide research area such as multilayer preparations,[10] metal particles,[11] virus,[12] proteins,[13] silica colloids,[14] and so on. However, weak polymer-polymer interactions, such as van der Waals interactions of *it*-PMMA and *st*-PMMA in stereocomplex formation,[15] were applied to LbL assembly by our group.[16] Then, thin films were successfully fabricated on quartz crystal microbalance (QCM) substrates by *it*-PMMA/*st*-poly(alkyl methacrylate) stereocomplexes[17] as well as *it*-PMMA/*st*-PMMA stereocomplexes. Among the successive research, *it*-PMMA/*st*-poly-(methacrylic acid) (PMAA) stereocomplex formation[18] was the most important because the polymer possesses quite differentsolubilities in organic/alkali water solvents, which enabled us to extract only one component from stereocomplex thin films. Therefore, porous *it*-PMMA thin films were prepared, bearing *st*-PMAA-shaped nanospaces inside,[19-21] to lead the isospecific polymerization of MMA with porous *st*-PMAA thin films6 and the syndiospecific polymerization of MAA.[7]

To investigate the mechanism of template polymerization, molecular weight growth during polymerization was monitored,[6] and oligomeric adsorption behaviors in porous *it*-PMMA thin films were analyzed.[22] These studies showed that the system proceeds in a living radical polymerization manner; however, the stereospecific mechanism has attracted attention for the possibility of stereocontrol of other polymers bearing similar structures.

Usually, molecular designs of monomers, catalysts, and additives are important to achieve stereospecific polymerization, which is why the molecular design of substituents[23-26] and the structural design of catalyst ligands[27-30] has been intensively researched for controlled polymerization. The use of porous reaction fields is another

important approach for the controlled polymerization.[31-33] Basically, the aforementioned strategies are based on constructing and curving nanospaces at the molecular level along polymer main chains. In previous work, it was reported that porous *it*-PMMA thin films could partially associate with *st*-PMAA derivatives, such as *st*-PMMA, *st*-poly(ethyl methacrylate), and *st*-poly(propyl methacrylate).[19] Therefore, the application of other vinyl monomer polymerization to the template polymerization system would provide useful information on the mechanism.

In this study, we first confirmed the living manner in porous *it*-PMMA thin films by postpolymerizing of MAA on QCM substrates. Then, radical polymerizations were performed on MAA, MMA, acrylic acid (AA), and methacrylamide (MAm) with *it*-PMMA thin films on QCM substrates (Scheme 8-1). The polymerizability was compared on QCM, and $^1$H NMR spectra were measured for the obtained PMMA to discuss the template polymerization mechanism.

**Scheme 8-1. Preparation of Porous *it*-PMMA Thin Film and Post-Polymerization of Methacrylic Acid and Its Derivatives**
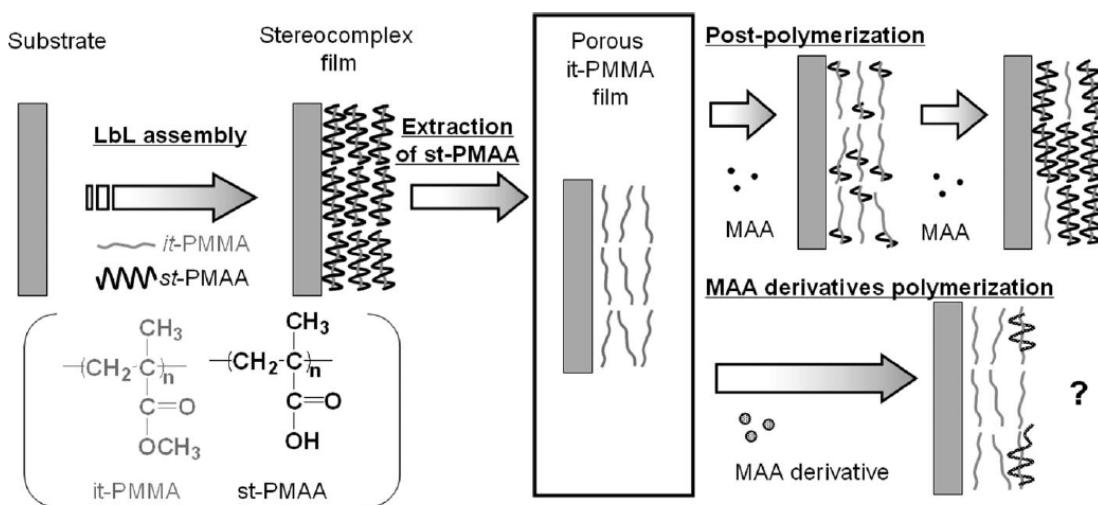
## 8. 2 EXPERIMENTAL

**Materials** MMA (Tokyo Chemical Industry), MAA (Tokyo Chemical Industry), AA (Tokyo Chemical Industry), trimethylsilylmethacrylate (Aldrich), and toluene (Tokyo Chemical Industry) were distilled just before use. MAm (Tokyo Chemical Industry), anhydrous acetonitrile (Wako Pure Chemical Industries, Japan), and anhydrous methanol (Wako Pure Chemical Industries, Japan) were used without further purification. Ultrapure distilled water was provided by the MILLI-Q laboratory (MILLIPORE). *it*-PMMA in this study was synthesized by anionic polymerization of MMA in toluene at -78 °C for 5 days with *t*-BuMgBr[34] (*mm*:*mr*:*rr* = 96:3:1, $M_n$ = 36000, $M_w/M_n$ = 1.20 was used for QCM substrate, *mm*:*mr*:*rr* = 96:2:2, $M_n$ = 22900, $M_w/M_n$ ) 1.21 was used for silica gels substrate). *st*-PMAA was synthesized by anionic polymerization of trimethylsilylmethacrylate with *t*-BuLi/Bis(2,6-di*tert*-butylphenoxy)-methyl aluminum,[35] and the obtained polymerwas methylated by diazomethane to be characterized (*mm*:*mr*:*rr* =1:6:93, $M_n$ = 32400, $M_w/M_n$ = 1.59 was used for QCM substrate, *mm*:*mr*:*rr* = 1:5:94, $M_n$ = 33700, $M_w/M_n$ = 1.45 was used for silica gels substrate). Tacticities of polymers were determined by ^{1}H NMR spectra of alpha methyl protons in nitrobenzene-$d_5$ at 110 °C.

**Polymerization on a Quartz Crystal Microbalance Substrate** The preparation of porous *it*-PMMA thin films on a QCM by LbL assembly and the subsequent template polymerization on a QCM were conducted as reported in the literature.[6,7] A typical experimental procedure of postpolymerization is described for the polymerization in MAA. A QCM substrate was immersed in an *it*-PMMA solution in acetonitrile (0.017 unitM) for 5 min at 25 °C, washed gently with acetonitrile, and dried with nitrogen gas to measure the frequency. The substrate was immersed in a *st*-PMAA solution in

acetonitrile/water (4:6 v/v; 0.017 unitM) for 5 min at 25 °C. Alternate immersions were repeated for 16 steps (8 cycles); the selective extraction of *st*-PMAA in a 10 mM NaOH aqueous solution for 5 min was performed to obtain the porous *it*-PMMA film as a template polymerization field. This film was immersed in 6.8 mL of degassed ultrapure water with 85 mg MAA (1 mmol) in a glass vial capped by a septum rubber for 30 min at room temperature; then, 3.2 mL of radical initiator VA-044 (16.5 mg, 0.05 mmol) solution in the degassed ultrapure water was combined to heat up to 70 °C for polymerization reactions. The additional 2.5 mL of MAA solution in ultrapure water (8.5 mg/mL) was introduced to the reaction glass vial after 30 min and kept at 70 °C for more than 2.5 h. The QCM substrate was gently washed by ultrapure water to measure frequency.

**Polymerization on Macroporous Silica Gels** The preparation of porous *it*-PMMA thin films on silica gels, and subsequent template polymerizations on silica gels were conducted as reported in the literature.[6,36] LbL-assembled *it*-PMMA/*st*-PMAA stereocomplex on macroporous silica gels (2.0 g) was introduced to 300 mL of ampule, and 250 mL of aqueous 10 mM NaOH solution was introduced to purge nitrogen for 2 h. After removed of NaOH solution by syringe, the silica gels were washed by ultrapure watertwice to obtain porous *it*-PMMA film on silica gels. MeOH (50 mL) and ultra pure water (50 mL) were then combined with silicagels in ampule, and MMA (0.3 mL, 2.8 mmol) was introduced and nitrogen was purged for 1.5 h. VA-044 (37.9 mg, 0.14 mmol) was added to the mixture, and an additional 10 min of nitrogen purge was performed. The polymerization was initiated by heating up to 40 °C. After 3 h of reaction and removal of the supernatant solution, the ampule was cooled to room temperature, and silica gels were washed by 40 mL of acetonitrile three times. After

centrifugation, the separated silica gels were then washed by 40 mL of chloroform three times again. The recovered solutions by each step were condensed to obtain polymers: the extracted NaOH(aq) soluble part, 318 mg (100 mg NaCl was included); supernatant solution part, 35 mg; acetonitrile soluble part, 71.3 mg; chloroform soluble part, 95.4 mg.

**Quartz Crystal Microbalance** An AT-cut quartz crystal with a parent frequency of 9 MHz was obtained from USI (Japan). A crystal (9 mm in diameter) was coated on both sides with gold electrodes 4.5 mm in diameter, which was of mirrorlike polished grade. The frequency was monitored by an Iwatsu frequency counter (model SC7201) and was recorded manually. The amount of polymers adsorbed, $\Delta m$, could be calculated by measuring frequency decreases in the QCM, $\Delta F$, using Sauerbrey's equation[37] as follows

$$\Delta F = 2F_0^2/(AF_q\,\mu_q)^{1/2})\Delta m$$

where $F_0$ is the parent frequency of the QCM (9 MHz), $A$ is the electrode area (0.159 cm$^2$), $F_q$ is the density of the quartz (2.5 g cm$^{-3}$), and $\mu_q$ is the shear modulus (2.95 × 1011 dyn cm$^{-2}$). This equation was reliable when measurements were made in air as described in this study because the mass of solvent is never detected as frequency shifts, and the effect of the viscosity of the absorbent on the frequency can be ignored.

**Measurements** Attenuated total reflection (ATR) IR spectra of the thin films were obtained with a Spectrum 100 FT-IR spectrometer (Perkin-Elmer). The interferograms were coadded 64 times and were Fourier transformed. $^1$H NMR spectra were measured by JNMGSX400 system (JEOL, Japan). Static contact angles were measured using an automatic contact angle meter apparatus (Drop Master 100, Kyowa Interface Science, Japan) at room temperature. A drop of ultrapure water was introduced to the film using

a microsyringe.


## 8. 3 RESULTS AND DISCUSSION

The stereospecific template polymerization of methacrylates using the complementary interaction of stereocomplex formation is significant because of the simple free-radical polymerization without any harmful organometal reagents under strict polymerization conditions.[6] However, the stereocomplex film formation prior to the polymerization by LbL assemblies was affected by subtle condition changes such as molecular weights of template polymers, the combination of polymers, concentrations, solvents, temperatures, and so on. On the research series of polymerization mechanistic studies, we initially had difficulties in controlling and estimating polymerizations. Besides, *it-* PMMA and *st*-PMAA did not form clear 2:1 stereocomplexes on the QCM in all cases, but $1.22 \pm 0.34{:}1$ ($n = 29$), implying a mixture of 2:1 and 1:1 stereocomplexes.[15,18,38] Therefore, the complex efficiency (C.E.) was determined to evaluate the polymerization value in this study as the following

C.E. = (increased weight after polymerization)/(extracted *st*-PMAA weight) × 100

The results of template polymerization of methacrylate derivatives are listed in Table 8-1.

**Table 8-1.** Radical Polymerization with Porous *it*-PMMA Film on QCM[a]

| run | monomer | concn (mol/L) | temp (°C) | polymerization $t_1$ (h) | time $t_2$ (h) | C.E.[b] (%) |
|---|---|---|---|---|---|---|
| 1[c] | MAA | 0.1 | 70 | 3 | 0 | −3 |
| 2[d] | | | 70 | 3 | 0 | −4 |
| 3 | MAA | 0.02 | 40 | 2 | 0 | 2 |
| 4 | MAA | 0.02 | 70 | 2 | 0 | 2 |
| 5 | MAA | 0.1 | 70 | 3 | 0 | 27 |
| 6 | MAA | 0.1 | 70 | 3 | 3 | 50 |
| 7 | MAA | 0.1 | 70 | 4 | 2 | 65 |
| 8 | MAA | 0.1 | 70 | 0.5 | 2.5 | 59 |
| 9 | MAm | 0.1 | 70 | 2 | 0 | 8 |
| 10 | MAm | 0.1 | 70 | 0.5 | 2.5 | 12 |
| 11 | AA | 0.1 | 70 | 2 | 0 | 66 |
| 12 | AA | 0.1 | 70 | 0.5 | 2.5 | 71 |
| 13[e] | MMA | 0.1 | 70 | 0.5 | 2.5 | 90 |

[a] Solvent: water. After the reaction for $t_1$ (h) was initiated, monomer solution (1.0 M, 2.5 mL) was added for postpolymerization for $t_2$ (h). [b] Yields were determined as complex efficiency (C.E.). [c] Blank polymerization without VA-044. [d] Blank polymerization without monomer. [e] MeOH/water (1:1 v/v) was used as solvent.

Because every LbL assembly step and extraction step differed for each substrate, it would be difficult to compare polymerizabilities with frequency changes when only small amounts of monomer polymerized. For this reason, blank polymerizations were run to check if the defined C.E. formula (8-1) was appropriate for evaluations. Following the reported polymerization conditions,[7] MAA in ultrapure water (0.1 mol/L) was heated to 70 °C for 3 h on QCM substrates with porous *it*-PMMA films without an azo-initiator (VA-044) (Table 8-1, entry 1). The resulting QCM analysis showed a -3% C.E. value, suggesting that there was no polymerized PMAA incorporated into the porous *it*-PMMA film and that very slight *it*-PMMA peeled on the substrate. The aforementioned tendency was also confirmed under conditions with an azo-initiator but without an MAA monomer to obtain -4% C.E., as depicted in Figure 8-1a (Table 8-1, entry 2). These data show that porous *it*-PMMA thin films are relatively stable, and most host template polymers remained on QCM substrates.
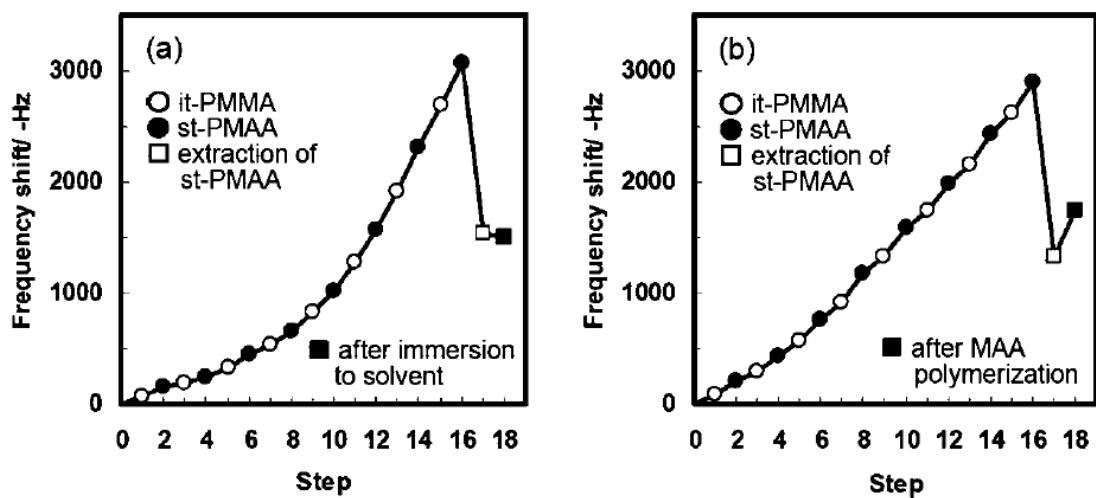
**Figure 8-1.** QCM analyses of LbL assembly, selective extraction, and template polymerization with (a) blank (Table 8-1, entry 2) and (b) 27% yield (Table 8-1, entry 5).

First, MAA polymerizations were performed under diluted conditions (0.02 M) for the purpose of polymerization analyses with low conversions. At both 40 and 70 °C, 2% C.E. valueswere observed (Table 8-1, entries 3 and 4). Considering the slight *it*-PMMA peeling (Table 8-1, entries 1 and 2) and oligomer adsorptions,[22] the C.E. values were appropriate to the explanation that the initially generated oligomers immediately adsorbed into porous *it*-PMMA thin films, and there were no further polymerizations that proceeded in the film, whereas the MAA monomer was consumed in solution. Under five times concentrated conditions (0.1 M), the increased value was apparently confirmed with 27% C.E., which demonstrated that actual polymerizations in films had taken place. (Table 8-1, entry 5). In Figure 8-2, the speculation of FT-IR/ATR spectra of the films with 27% C.E. are shown and compared with those of porous *it*-PMMA films and *st*-PMAA cast films.

147
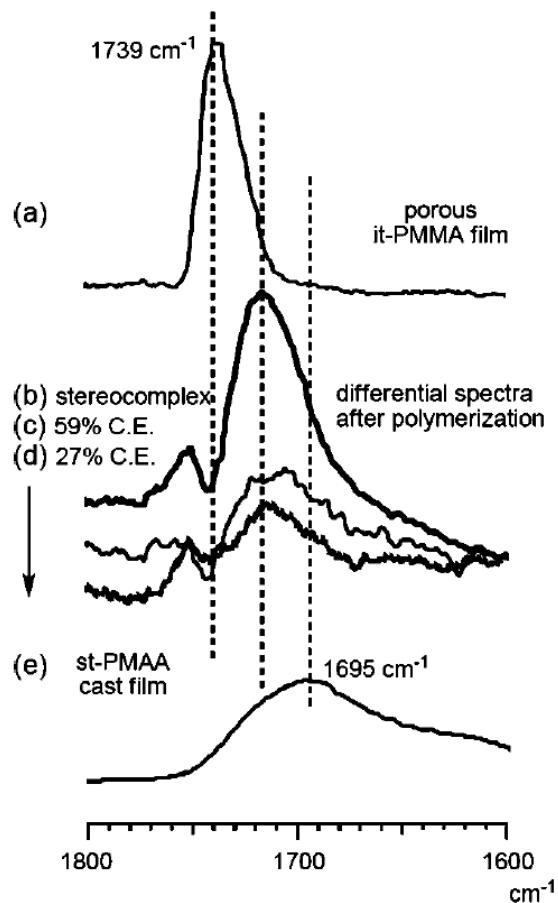
**Figure 8-2.** (a) FT-IR/ATR spectrum of the porous *it*-PMMA. The differential FT-IR/ATR spectra of (b) *it*-PMMA/*st*-PMAA, (c) MAA polymerized on *it*-PMMA film with 59% C.E. (Table 8-1, entry 8), and (d) MAA polymerized on *it*-PMMA film with 27% C.E. (Table 8-1, entry 5), which were obtained by the subtraction of the porous *it*-PMMA (a). (e) FT-IR/ATR spectrum of the *st*-PMAA cast film.

Because of the fact that the amount of polymerized MAA was smaller than that of originally attached *it*-PMMA films, it was difficult to find changes in spectral patterns. Then, the differential spectrum (Figure 8-2d) was compared with that of *it*-PMMA/*st*-PMAA stereocomplex films (Figure 8-2b), which were obtained by subtracting the IR spectrum of porous *it*-PMMA films (Figure 8-2a) from those of originally measured IR spectra. Whereas the spectrum of *st*-PMAA cast film, which should possess a random conformation, showed a peak at 1695 cm$^{-1}$, differential spectra

of both template polymerized films (27% C.E., Figure 8-2d) and stereocomplexes (Figure 8-2b) exhibited peaks at around 1720 cm$^{-1}$. This result shows that the circumstances of carbonyl groups of the obtained PMAA are similar to those of stereocomplexes, suggesting that stereocomplex formation is achieved during MAA polymerization.

However, the C.E. value in this study remained lower than that in a previously reported case,[7] probably because different stereoregular polymers were employed for stereocomplex formation and because the structure of the resulting porous *it*-PMMA film had variant balances of the oligomer adsorption, the mobility of *it*-PMMA chains, and the porosity that allowed monomer supply. In the solid polymer matrix, it is known that radicals are entrapped and gradually react.[39] To investigate the possibility of further polymerization, postpolymerization was applied because the polymerization system was reported in a living radical polymerization manner.

Additional MAA solution (2.5 mL, 8.5 mg/mL) was added 3 h, 4 h, and 0.5 h after initiation, respectively (Table 8-1, entries 6-8). In all cases, increased weights compared with that without added monomer were observed. Because no increasing weights were observed without radical initiators (Table 8-1, entry 1), 50% C.E. (Table 8-1, entry 6), 65% C.E. (Table 8-1, entry 7), and 59% C.E. (Table 8-1, entry 8) increasing weights should be attributed to the postpolymerization in porous *it*-PMMA thin films, implying that polymer radicals inside *it*-PMMA films still possessed reactivity and were ready to react if monomers were supplied (Figure 8-3a). To add to this, the intensity of differential IR spectra increased from that with 27% C.E. (Figure 8-2c,d). Furthermore, the contact angle on the surface changed from 49.2 ± 1.9 to 36.7 ± 2.8° compared with porous *it*-PMMA thin films, which hint that the surface hydrophilicity change came

149

from stereocomplex formation. Therefore, postpolymerization would be a good approach to improving C.E. in this template polymerization system.
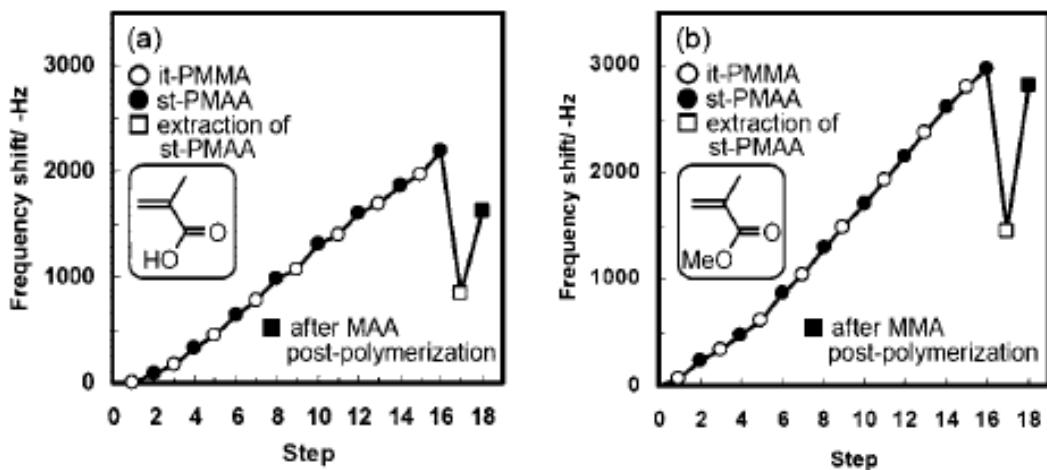


**Figure 8-3.** (a) QCM analyses of LbL assembly, selective extraction, and template polymerization of methacrylic acid with C.E. ) 59% (Table 8-1, entry 8) and (b) template polymerization of methyl methacrylate with C.E. ) 90% (Table 8-1, entry 13).

Another approach to investigating polymerization mechanisms is to change monomer structures and evaluate the effects of substituent bulkiness and polarities. Especially in this template polymerization system, van der Waals interactions were considered to be strong driving forces in stereocomplex formation, in which the molecular shape is very important. Porous *it*-PMMA thin films have incorporated *st*-PMAA derivatives to some extent,[19] and MAm and MMA were absorbed and acrylic acid (AA) was not absorbed into *it*-PMMA thin films when vinyl monomer concentrations were condensed (2 M).[22] Therefore, those MAA derivatives were applied to template polymerization of *it*-PMMA/*st*-PMAA systems (Table 8-1, entries 9-13).

MAm is a monomer with similar adsorption into porous *it*-PMMA thin films as MAA[22] because of its structural similarity with R-methyl groups, which should be

associated with *it*-PMMA polymer chains.[40] However, the result of radical polymerization resulted in 8% C.E. (Table 8-1, entry 9), and it was slightly improved to 12% C.E., even when a postpolymerization was applied (Table 8-1, entry 10). It would be difficult for nonstereocomplex formation polymer combinations, such as *it*-PMMA/poly(MAm), to polymerize, although the monomer and limited oligomers were able to be incorporated. Reversely, polymerization using a smaller vinyl monomer, AA, made the weight increase to 71% C.E. (Table 8-1, entry 12), although AA itself did not incorporate into porous *it*-PMMA thin films.[22] Therefore, the size of porosity might strictly affect the polymerizability of MAA derivatives. However, a slightly bigger structure, MMA is expected to completely polymerize because of *it*-PMMA/*st*-PMMA stereocomplex formation as a driving force. After polymerization of MMA on QCM substrates, C.E. was 192% C.E. at first because of the adsorption of atactic (*at*) PMMA synthesized in MeOH/water (1:1, v/v). When the QCM substrate was rinsed with acetonitrile, which dissolved not only at-PMMA but also *it*-PMMA on the QCM, polymer still remained with 90% C.E., and it was stable in acetonitrile at 25 °C overnight (Figure 8-3b; Table 8-1, entry 13). Because *it*-PMMA/*st*-PMMA stereocomplexes do not dissolve in acetonitrile, the template polymerization of MMA in porous *it*-PMMA thin films was suggested.

To study the stereoregularity of obtained polymers, we chose the MMA polymerization on macroporous silica gels because the tacticity study of poly(AA) was difficult. Prior to the polymerization, we investigated the effect of steps in stereocomplex formation on silica gels by FT-IR/ATR spectra (Figure 8-4).
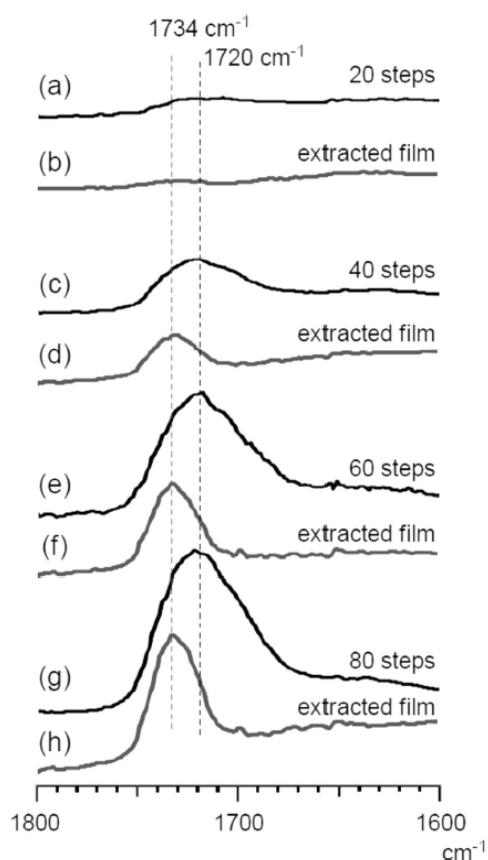
**Figure 8-4.** FT-IR/ATR spectra of *it*-PMMA/*st*-PMAA stereocomplex film on silica gels and the porous *it*-PMMA films on silica gels with (a,b) 20 steps, (c,d) 40 steps, (e,f) 60 steps, and (g,h) 80 steps.

On the basis of the absorption intensity of silica gels at 1057 cm$^{-1}$, the relative IR intensity of carbonyl groups at 1720 cm$^{-1}$ proportionally grows, depending on the number of the alternative LbL assembly steps (Figure 8-4a,c,e,g), whereas each cast film of *it*-PMMA and *st*-PMAA has a peak at 1726 and 1695 cm$^{-1}$, respectively. The peak at each LbL step shifted to 1721 cm$^{-1}$ with the same spectral patterns (Figure 8-4b,d,f,h), showing that the complete extraction of *st*-PMAA at each step and that the porous *it*-PMMA thin film do not depend on the thickness of the film. The stepwise weight increase to 80 steps was also confirmed by QCM analysis.

MMA was then polymerized with porous *it*-PMMA thin films on 2 g of macroporous silica gels, prepared by an 80 step LbL assembly. The polymerization was conducted in MeOH/water (1:1 v/v) at 40 °C for 3 h. After polymerization, the supernatant was removed, and the polymer films on silica gels were washed with acetonitrile because at-PMMA and *it*-PMMA are soluble in acetonitrile, but the stereocomplex is insoluble. After it was separated from acetonitrile solution, the silica gel was then washed with chloroform to recover the rest of the polymers as an acetonitrile insoluble part. In this way, the reaction mixture was fractionated and separately analyzed as (1) the supernatant solution part, (2) the acetonitrile-soluble part, and (3) the chloroform-soluble part. Prior to the polymer analyses, the reaction was monitored by FT-IR/ATR spectra, as shown in Figure 8-5. The IR intensity of the polymer film on silica gels after MMA polymerization apparently increased compared with that of initial porous *it*-PMMA thin films on silica gels (Figure 8-5b). Silica gels with polymers were washed by 40 mL of acetonitrile three times, and IR spectra were measured again for carbonyl peaks in PMMA to see if they remained (Figure 8-5d), whereas initial porous *it*-PMMA films on macroporous silica gels totally washed away. This result indicates thesynthesized PMMA formed stereocomplex with the initial porous *it*-PMMA. Finally, 40 mL of chloroform was used to recover PMMAs from silica gels (95 mg).
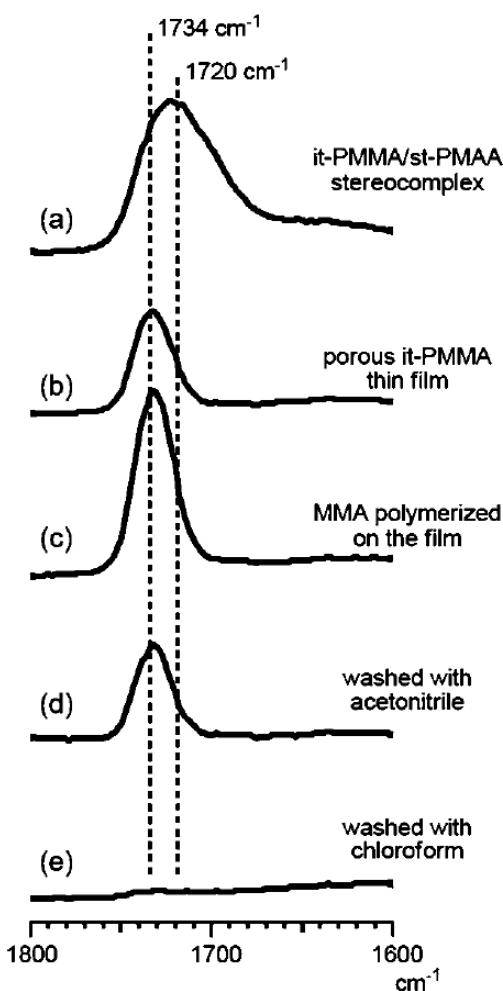
**Figure 8-5.** FT-IR/ATR spectra of the polymer film on silica gels, whose intensity corresponded at 1057 cm$^{-1}$: (a) *it*-PMMA/*st*-PMAA stereocomplex, (b) porous *it*-PMMA film, (c) MMA polymerized in the porous *it*-PMMA film, (d) acetonitrile insoluble part after the MMA polymerization in the porous *it*-PMMA film, and (e) after washing with chloroform on silica gels.

$^1$H NMR spectra of fractionated PMMAs are depicted in Figure 8-6. Together with a slight amount of *it*-PMMA, PMMAs recovered from supernatant solution showed typical at-PMMA (Figure 8-6a). However, the acetonitrile soluble part showed only *it*-PMMA, which was used to build the porous *it*-PMMA host film (Figure 8-6b). At last, $^1$H NMR spectra of the rest of the film, collected as an acetonitrile-insoluble and chloroformsoluble part, showed that the equivalent amount of *it*-PMMA existed as

slightly syndiotactic enriched PMMA (Figure 8-6c). The chloroform-soluble part (*mm*:*mr*:*rr* = 49:22:29) includes the synthesized PMMA with radical method and the original *it*-PMMA host as template film. The aforementioned experimental data suggest that enough MMA could be polymerized in *it*-PMMA film nanospaces and that the partially stereocomplex formed to change the total solubility in acetonitrile. However, taking the amount of *it*-PMMA host into account, the syndiotactic selectivity in Figure 8-6c was not so high, although almost perfect selectivities were achieved in the previous work.[6,7] The reason why selectivities varied between MMA and MAA polymerizations is that MMA possesses abulky methyl group. Stereospecific template polymerization has been achieved only when the same polymer was synthesized as the polymer extracted from stereocomplex.[6,7] In this study, the porous nanostructure was created not by PMMA but by PMAA. In short, the porous nanostructure itself played an important role in stereoregulation in addition to stereocomplex formation. The substituent effect is supported by the fact that the porous *it*-PMMA film can incorporate *st*-PMAA with around 80% C.E., whereas *st*-PMMA and *st*-poly(ethyl methacrylate) are incorporated with only 43 and 8% C.E., respectively.[19,22] Therefore, the strict stereoregular control of PMMA during the polymerization was difficult under the present conditions. It is noteworthy that MMA was also polymerized in acetonitrile/water (4:6 v/v) and resulted in the same insoluble PMMA (13 mg), which was equivalent to the remaining *it*-PMMA.
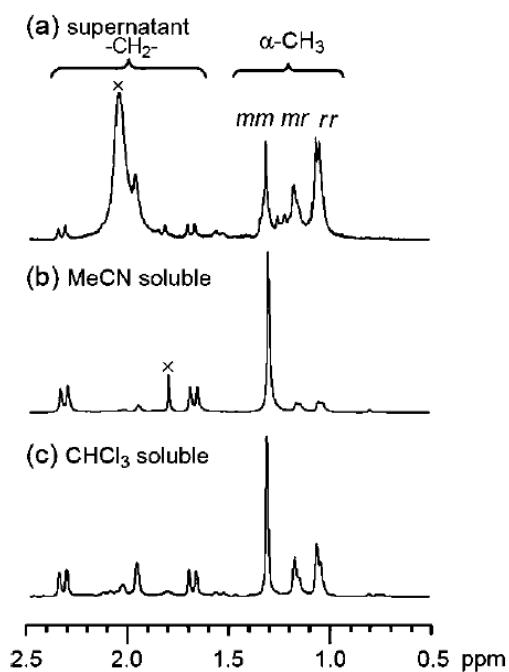
**Figure 8-6.** ^{1}H NMR spectra of PMMA obtained with *it*-PMMA thin film on macroporous silica gels in MeOH/water (1:1 v/v). (a) The supernatant solution part of the template polymerization, (b) the acetonitrile-soluble part of the host *it*-PMMA, and (c) the acetonitrileinsoluble and CHCl$_3$-soluble part of the obtained PMMA with the host *it*-PMMA (400 MHz, in nitrobenzene-*d* at room temperature).

SEC charts of the resulting polymers are shown in Figure 8-7. The SEC analysis of the acetonitrile-soluble part depicted a unimodal pattern ($M_n$ = 11000), indicating *it*-PMMA host in accord with ^{1}H NMR spectrum (Figure 8-7b). However, bimodal distribution was observed from the analysis of the chloroformsoluble part ($M_n$ = 330000, $M_n$ = 18000) (Figure 8-7c). The low-molecular-weight part ($M_n$ = 18000), attributed to the rest amount of the *it*-PMMA host and associated with the synthesized PMMA, and the high-molecular-weight part ($M_n$ = 330000) could be assigned to the synthesized PMMA. The value does not correspond to the expected molecular weight when the 1:2 stereocomplex formed with the *it*-PMMA host, suggesting that the methyl group of the MMA monomer also disturbed the molecular weight control in the template

156

polymerization system as well as stereoregulation. Therefore, strict monomer structure is necessary for stereoregular control and molecular weight control at the same time, although the active living radicals cause postpolymerization.
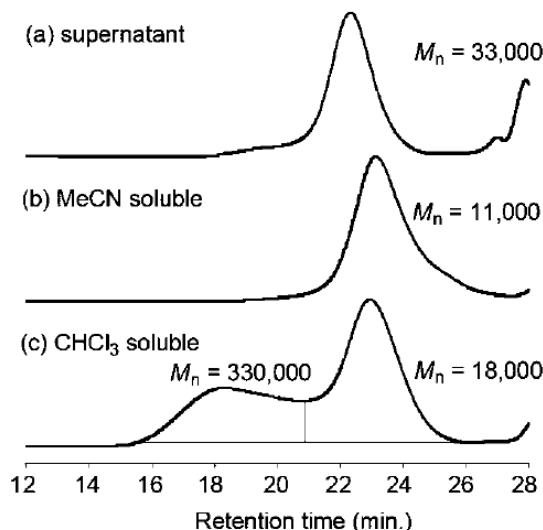


**Figure 8-7.** SEC traces of PMMA obtained with *it*-PMMA thin film on macroporous silica gels in MeOH/water (1:1 v/v): (a) The supernatant solution part of the template polymerization, (b) the acetonitrile-soluble part of the host *it*-PMMA, and (c) the acetonitrile-insoluble and CHCl$_3$-soluble part of the obtained PMMA with the host *it*-PMMA.

## 8. 4 CONCLUSIONS

LbL assemblies led to the successful formation of *it*-PMMA/*st*-PMAA stereocomplex films on QCM substrates and on silicagels to create the porous *it*-PMMA thin films as polymerization fields, although MAA polymerizability inside might depend on LbL assembly conditions. Without both azo-initiator and MAA monomer, blank polymerizations with the porous *it*-PMMA thin films showed that template polymerization fields, which created porous films, were stable in water at 70 °C for 3 h

and that increased weights on substrates after polymerization were ascribed to the polymer associated with the host *it*-PMMA. The postpolymerization of MAA in porous *it*-PMMA thin films was successfully achieved, implying that the polymer radical in the film possessed an adequate activity in a living polymerization manner. When MAA derivatives were polymerized, the smallersized monomer (AA) was polymerized in good C.E. yield, whereas the bigger size monomer (MAm) remained a low C.E. value. Those substituent effects proposed that very slight size changes affected the polymerizabilities inside porous *it*-PMMA films during polymerization, although the adsorption at monomer structures resulted in differences. When MMA was polymerized, an almost equivalent amount of PMMA was obtained as an acetonitrile-insoluble part with the host *it*-PMMA, implying that the stereocomplex was partially formed. It was also revealed that the strict monomer structure was necessary for the stereocontrol and molecular weight control, whereas the active radical was entrapped in the porous *it*-PMMA host film. The mechanism investigation of template polymerization in this study should supply useful information on future template polymerization systems.

## REFERENCES

1) R. Buter, Y. Y. Tan, G. Challa, *J. Polym. Sci., Part A: Polym. Chem.* **1972**, *10*, 1031.

2) R. Buter, Y. Y. Tan, G. Challa, *J. Polym. Sci., Part A: Polym. Chem.* **1973**, *11*, 1013.

3) J. H. G. M. Lohmeyer, Y. Y. Tan, G. Challa, *J. Macromol. Sci., Chem.* **1980**, *A14*, 945.

4) E. Schomaker, G. Challa, *Macromolecules* **1989**, *22*, 3337.

5) J. Kumaki, T. Kawauchi, K. Okoshi, H. Kusanagi, E. Yashima, *Angew. Chem., Int.*

*Ed.* **2007**, *46*, 5348.

6) T. Serizawa, K.-i. Hamada, M. Akashi, *Nature* **2004**, *429*, 52.

7) K.-i. Hamada, T. Serizawa, M. Akashi, *Macromolecules* **2005**, *38*, 6759.

8) G. Decher, J. D. Hong, *Makromol. Chem., Macromol. Symp.* **1991**, *46*, 321.

9) G. Decher, *Science* **1997**, *277*, 1232.

10) R. Advincula, E. Aust, W. Meyer, W. Knoll, *Langmuir* **1996**, *12*, 3536.

11) H. C. Yang, K. Aoki, H. G. Hong, D. D. Sackett, M. F. Arendt, S. L. Yau, C. M. Bell, T. E. Mallouk, *J. Am. Chem. Soc.* **1993**, *115*, 11855.

12) Y. Lvov, H. Haas, G. Decher, H. Moehwald, A. Mikhailov, B. Mtchedlishvily, E. Morgunova, B. Vainshtein, *Langmuir* **1994**, *10*, 4232.

13) F. Caruso, K. Niikura, D. N. Furlong, Y. Okahata, *Langmuir* **1997**, *13*, 3427.

14) Y. Lvov, K. Ariga, M. Onda, I. Ichinose, T. Kunitake, *Langmuir* **1997**, *13*, 6195.

15) J. Spevacek, B. Schneider, *Adv. Colloid Interface Sci.* **1987**, *27*, 81.

16) T. Serizawa, K.-i. Hamada, T. Kitayama, N. Fujimoto, K. Hatada, M. Akashi, *J. Am. Chem. Soc.* **2000**, *122*, 1891–1899.

17) K.-i. Hamada, T. Serizawa, T. Kitayama, N. Fujimoto, K. Hatada, M. Akashi, M. *Langmuir* **2001**, *17*, 5513.

18) T. Serizawa, K.-i. Hamada, T. Kitayama, K.-i. Katsukawa, K. Hatada, M. Akashi, *Langmuir* **2000**, *16*, 7112.

19) T. Serizawa, K.-i. Hamada, T. Kitayama, M. Akashi, *Angew. Chem., Int. Ed.* **2003**, *42*, 1118.

20) D. Kamei, H. Ajiro, C. Hongo, M. Akashi, *Chem. Lett.* **2008**, *37*, 332.

21) D. Kamei, H. Ajiro, C. Hongo, M. Akashi, *Langmuir* **2009**, *25*, 280.

22) H. Ajiro, D. Kamei, M. Akashi, *J. Polym. Sci., Part A: Polym. Chem.* **2008**, *46*,

5879.

23) K. Hatada, T. Kitayama, K. Ute, *Prog. Polym. Sci.* **1988**, *13*, 189.

24) T. Nakano, Y. Okamoto, *ACS Symp. Ser.* **1998**, *685*, 451.

25) S. Habaue, Y. Okamoto, *Chem. Rec.* **2001**, *1*, 46.

26) M. Kamigaito, K. Satoh, *Macromolecules* **2008**, *41*, 269.

27) B. Wu, R. W. Lenz, B. Hazer, *Macromolecules* **1999**, *32*, 6856.

28) W. Kaminsky, *Macromol. Chem. Phys.* **2008**, *209*, 459.

29) G. W. Coates, *Chem. Rev.* **2000**, *100*, 1223.

30) T. Matsugi, T. Fujita, *Chem. Soc. Rev.* **2008**, *37*, 1264.

31) T. Uemura, D. Hiramatsu, Y. Kubota, M. Takata, S. Kitagawa, *Angew. Chem., Int. Ed.* **2007**, *46*, 4987.

32) K. Tajima, T. Aida, *Chem. Commun.* **2000**, 2399.

33) T. Serizawa, M. Akashi, *Polym. J.* **2006**, *38*, 311.

34) K. Hatada, K. Ute, K. Tanaka, T. Kitayama, Y. Okamoto, Y. *Polym. J.* **1985**, *17*, 977.

35) T. Kitayama, S. He, Y. Hironaka, T. Iijima, K. Hatada, *Polym. J.* **1995**, *27*, 314.

36) H. Ajiro, D. Kamei, M. Akashi, *Polym. J.* **2009**, *41*, 90.

37) G. Sauerbrey, *Z. Phys.* **1959**, *155*, 206.

38) J. Biros, Z. Masa, J. Pouchly, *Eur. Polym. J.* **1974**, *10*, 629.

39) H. Macit, B. Hazer, *Eur. Polym. J.* **2007**, *43*, 3865.

40) F. Bosscher, D. Keekstra, G. Challa, *Polymer* **1981**, *22*, 124.

# Concluding Remarks

In this thesis, the molecular recognition and structural change of porous isotactic (*it*) poly(methyl methacrylate) (PMMA) thin films were investigated in order to understand the stereospecific template polymerization in the porous *it*-PMMA thin films.

First, the effects of the solvent on the motion of the polymer chains in the porous films were studied to obtain knowledge on nanospaces as a reaction field for template polymerization. The effect of acetonitrile solvation on porous *it*-PMMA films were analyzed at the nanolevel scale.

Second, morphological observations were used to confirm the stability (structural change) of the porous films. Surface analyses of the films were performed at the microlevel by scanning electron microscopy (SEM), atomic force microscopy (AFM), X-ray photoelectron spectroscopy (XPS), and static contact angles.

Third, the mechanisms responsible for template polymerization and the nanospaces of the porous *it*-PMMA thin films were investigated. The effects of the molecular structure on the porous films were analyzed by investigating the interactions (molecular recognition) between the template polymer *it*-PMMA and methacrylic acid (MAA), the oligomer, or syndiotactic (*st*) poly(methacrylic acid) (PMAA) in the porous thin films under hypothetical conditions as a model of template polymerization

Analyses of the dynamics of the polymer chains in porous thin films at the nano- and microlevel revealed that the stereoregular nanospaces, which were essential for the structural control of synthesized polymers during template polymerization, changed in the presence of acetonitrile. It was also revealed that template polymerization would

proceed via the Pick-up mechanism according to the adsorption tests of various methacrylate derivatives and the oligomers. The findings obtained from this thesis are summarized as follows.

In Chapter 1, the porous structure of *it*-PMMA films with stereoregular (*st*-PMAA) nanospaces was confirmed by X-ray diffraction (XRD). Furthermore, the polymer chains moved slightly at the interface, changing the packing distances. The porous *it*-PMMA films not only incorporated *st*-PMAA, but also slowly crystallized. Therefore, unlike the case of deoxyribonucleic acid (DNA) double-stranded helix formation from the same helices, competition between the formation of the double-stranded-helix of *it*-PMMA/*st*-PMAA and the double-stranded helix of *it*-PMMA/*it*-PMMA occurred when the porous films were immersed into an *st*-PMAA solution.

In Chapter 2, the structure of partially crystallized *it*-PMMA thin films and the mechanisms of *st*-PMAA incorporation into these films were nvestgated. The incorporation percentages of *st*-PMAA into the porous films decreased as the *it*-PMMA films crystallized, or with an increasing thickness of the porous *it*-PMMA films, probably due to the entanglement of the *it*-PMMA chains. The *st*-PMAA incorporation into the porous films gradually improved when the acetonitrile contents of the *st*-PMAA solution increased from 20 to 40 vol %. In contrast, *it*-PMMA crystallization as well as *st*-PMAA incorporation did not occur using only water, which is a nonsolvent for *it*-PMMA. Thus, it was revealed that the acetonitrile concentration in water is important for the dynamics of the *it*-PMMA chains in porous thin films.

In Chapter 3, it was demonstrated that *st*-PMAA incorporation in porous *it*-PMMA films depended on the stereoregularity, temperature, and solvent using quartz crystal microbalance (QCM) and infrared (IR) analyses. The first case of stereocomplex

formation using *st*-PMAA with lower tacticity (*rr* = 73%) in LbL films was reported. It was recognized that van der Waals interactions between *it*-PMMA and *st*-PMAA at the interface were important, because the lack of stereoregularity of *st*-PMAA decreased the incorporation percentage. The maximum *st*-PMAA incorporation increased from 25 to 40 ºC, but there were almost no differences between 40 and 55 ºC. This is likely because not only stereocomplex formation, but also *it*-PMMA crystallization, were promoted with increasing temperature. The studies on *st*-PMAA incorporation with various complexing solvents also revealed that the host *it*-PMMA in the porous films could only form the original stereocomplex with a 2/1 unit-molar stoichiometry (*st*-PMAA/*it*-PMMA) in acetonitrile/water or ethanol/water.

In Chapter 4, the morphological changes of porous thin films on a QCM substrate during *it*-PMMA crystallization were demonstrated, along with the subsequent *st*-PMAA incorporation. Dotted aggregates of crystallized *it*-PMMA appeared on the films on SEM and AFM images, although the films were not dissolved in a mixed solvent of acetonitrile/water. Gold substrate peaks were observed on the crystallized *it*-PMMA films using XPS. Therefore, this indicated that the absorbed *it*-PMMA spontaneously localized in the films to reform the surface profile. On the other hand, networks of crystallized *it*-PMMA and the stereocomplexes appeared on *st*-PMAA incorporated films.

In Chapter 5, the fusion of porous *it*-PMMA thin films prepared on silica nanoparticles was observed after gentle shaking in acetonitrile/water (4/6, v/v) and subsequent drying on a SEM stage, although dynamic light scattering showed only a few aggregates of silica particles in solution. These results suggest that leaving the solution at rest is important for film fusion on these particles, and that multiple spherical substrates

would promote the cross-linking of the *it*-PMMA chains on the particles.

In Chapter 6, the mechanism responsible for template polymerization was investigated using oligomers as an active intermediate model species. From the results of monomeric and oligomeric adsorption behavior, the template polymerization followed the Pick-up mechanism, in which the growing oligomer radical interacts with the template polymer, and monomers are freely supplied from the solution.

In Chapter 7, the syndiospecific template polymerization of MAA with *it*-PMMA films on silicagel was successfully achieved, although not all stereocomplex films were effective for template field creation deep inside the pores. The tacticity of the PMAA collected from solution was atactic, because a large amount of monomer polymerized as compared to the template thin films, which also decreased the yield in the template films. The template polymerization was repeated two times with almost the same yield. These reproducible results suggest that the template polymerization of MAA with *it*-PMMA on macroporous silicagels has practical applications for manufacturing using high-performance liquid chromatography systems.

In Chapter 8, the postpolymerization of MAA in porous *it*-PMMA thin films was successfully achieved, implying that the polymer radical in the films possessed adequate activity in a living polymerization manner. When MAA derivatives were polymerized, a smaller-sized monomer, acylic acid (AA), was polymerized wth good complex efficiency (C.E.) yield, whereas the bigger-sized monomer, methacrylamide, had a low C.E. value. Those substituent effects suggested that very slight size changes affected the polymerizabilities inside the porous *it*-PMMA films during polymerization. It was also revealed that a strict monomer structure was necessary for stereocontrol and molecular weight control, whereas the active radical was entrapped insde the porous *it*-PMMA

host film.

As a final conclusion of this thesis, first, the author hypothesized that macromolecules were dynamically moved and rearranged into the most stable conformation in the porous *it*-PMMA films by the effects of the solvent and temperature as well as complementary polymer-polymer interactions. Second, the author also demonstrated the importance of structural fitting between monomers and nanospaces in the porous films. The rearrangement and structural fitting of these complementary polymers would make it possible to synthesize stereoregular polymers by free-radical polymerization at the solid-liquid interface.

From the aforementioned findings in this thesis, I suggest a novel reaction field suitable for the template polymerization of vinyl polymers utilizing 1) a stereocomplex of polymethacrylates, and 2) nucleic acid bases.

# Future Perspective

## 1. Utilizing Stereocomplex of Polymethacrylates

In order to prevent the aforementioned crystallization of the template polymer and closing of the nanospaces, I suggest a novel reaction field for template polymerization, where the template polymers are immobilized by modification of their functional groups.

1) In the case of isotactic (*it*) poly(methyl methacrylate) (PMMA), the template polymers are fixed through termination by $CO_2$ bubbling to the *α*-end of the *it*-PMMA chains in anionic polymerization, which produces a carboxyl group, and the subsequent amidation with amino groups connected on the silicagel surfaces.[1] The distance between each *it*-PMMA brush should be controlled to prevent *it*-PMMA crystallization. For instance, the chain length of *it*-PMMA whose number-average molecular weight is 20000, is about 18 nm, since the pitch of the 10/1 *it*-PMMA helix is 0.92 nm. Therefore, it is necessary that the *it*-PMMA chains are fixed on the silicagel at least 36 nm away from one another.

Alternatively, a good solvent of *it*-PMMA such as chloroform could unravel the double-stranded helix of *it*-PMMA connected to the silicagel on the occurrence of *it*-PMMA crystallization, whereas porous *it*-PMMA films fabricated on the substrate will dissolve out with chloroform (Chapter 2). In other words, the reversible transformation between the single-stranded helix and the double-stranded helix forms of *it*-PMMA would become possible in this method.

2) The structure of the *it*-PMMA connected to the silicagel surface is considered to

be a single strand. Therefore, the polymerization of methyl methacrylate (MMA) onto the *it*-PMMA brushes in acetonitrile will reveal whether the double-stranded helix of crystallized *it*-PMMA or the stereocomplex of *it*-PMMA/syndiotactic (*st*) PMMA will form, since acetonitrile promotes both *it*-PMMA crystallization and stereocomplex formation (Chapter 1). Furthermore, the structural effects of the template *it*-PMMA will be confirmed by investigating its ability to form triple-stranded helical stereocomplex by the polymerization of MMA after the formation of the double-stranded helix of *it*-PMMA by crystallization of the *it*-PMMA brushes with normal linear *it*-PMMA.

3) In the case of *st*-poly(methacrylic acid) (PMAA), crosslinked assemblies may contain stereoregular nanospaces would be applicable for template polymerization. These assemblies are formed by a crosslinking reaction with the external carboxylic acid groups of helical *st*-PMAA in the *it*-PMMA/*st*-PMAA stereocomplex using 1,11-diamino-3-6-9-trioxaundecane and water soluble carbodiimide, and the subsequent *it*-PMMA removal under alkaline conditions.[2]

However, precise control of the thermal motion of guest polymer would be difficult on the polymer brushes or in the crosslinked assemblies. Thus, a precursor is formed between the template polymer and a PMMA macromer ($M_n$~2000) with a high tacticity (Chapter 6), which is synthesized by previously-reported methods,[3] in a strongly complexing solvent such as acetonitrile. This is based on the idea that deoxyribonucleic acid replication also needs a primer. Next, template polymerization would proceed by a reaction between the PMMA macromer and the supplied monomers on the *it*-PMMA brushes, or in the crosslinked *st*-PMAA assemblies with acetonitrile.

On the other hand, the *it*-PMMA films fabricated on a substrate could also open new doors for the template polymerization of methacrylates using the knowledge obtained

from this thesis.

4) The porous *it*-PMMA films prepared from the stereocomplex films of *it*-PMMA and *st*-PMAA with a lower stereoregularity (Chapter 3) would be useful for novel template polymerization in terms of technological applications.[4] This is because the syntheses of template polymers with high stereoregularities by conventional anionic polymerizations are very complex. Therefore, stereocomplex assemblies in which one component polymer is synthesized by radical polymerization are more desirable for repetitive synthesis, whereas polymers with the highest tacticity should be employed as the other component. However, the stereocomplex films of *it*-PMMA and *st*-PMAA with the lowest stereoregularity (*rr* = 62%) were not obtained under the same condition (Chapter 3). In order to increase the interaction points of the stereocomplex, *it*-PMMA with a lower molecular weight and *st*-PMAA (*rr* = 62%) with a higher molecular weight should be employed.

5) The removal of silica particles from the nanostructures prepared by the fusion of *it*-PMMA films (Chapter 5) will lead to a novel reaction field such as nanotubes[5] formed through one-dimensional fusion of hollow capsules.[6] If methacrylic acid (MAA) is included into the hollow capsules or nanotubes, then polymerization efficiency could be improved because the lost MAA polymerized in solution would be strongly suppressed. In addition, the template matrices and the assemblies after polymerization on the nanotubes will be more stable and easier to collect from solution than those on hollow capsules.

Controlling monomer sequences by template polymerization still remains challenging. The most simplified model of the sequence is a block copolymer composed of only two monomer units. I suggest a novel system to control the tacticities of the

block copolymer using radical polymerization in porous *it*-PMMA thin films.

6) The radical polymerization and postpolymerization of MAA and AA in the porous *it*-PMMA films yielded good complex efficiency (Chapter 8). Therefore, the tacticities and molecular weights of the block copolymer could be controlled by template polymerization of MAA, and the subsequent postpolymerization of AA in the porous *it*-PMMA films. Furthermore, the differences in surface morphologies like the smooth surface of porous *it*-PMMA films versus the dotted pattern of the crystallized *it*-PMMA films could be helpful in sorting out the copolymer from the homopolymer depending on the adsorption capabilities (Chapter 4).

7) In order to improve the yields of template polymerization in the porous thin films, I also suggest another new reaction field. Stereocomplex assemblies formed in a microchannel would have a larger surface area than those formed on a substrate of silicagel (Chapter 7). In addition, the process of the layer-by-layer assembly would become an easier system, because it is only flowing solutions or solvents alternately, and the amount of sample used will be less than a conventional LbL method.

## 2. Utilizing Nucleic Acid Bases

Designing novel monomer structures to control the tacticity of the obtained polymers by template polymerization is very difficult, because very few helical stereoregular polymers with vinyl polymer backbones have been reported in the designed synthetic polymer literatures. For example, poly(triphenylmethyl methacrylate), poly(*N*-triphenylmethylmethacrylamide), and their derivatives form helices by steric hindrance and in chiral solvents.[7,8] Almost all of the other reports are based on conjugated double bonds such as polyacetylene or polypeptide backbones. Therefore, a more rigid backbone should be designed in the case of the template polymerization of methacrylates bearing complementary nucleic acid bases connected by ethylene linkers.[9]
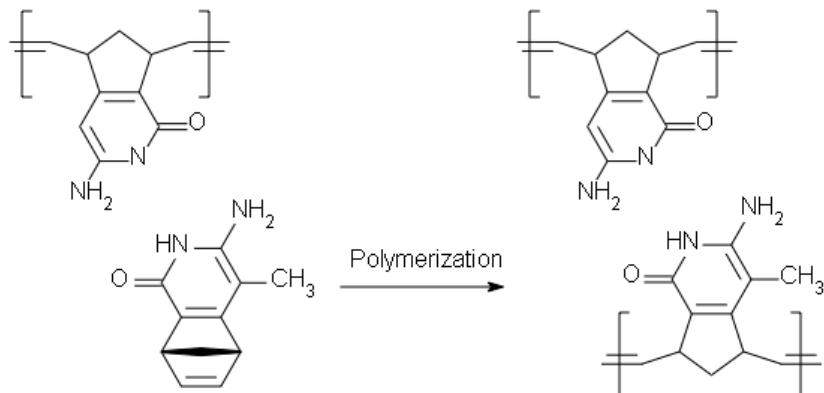


**Figure 6.** Schematic representation of the template polymerization of norbornene bearing nucleic acid bases and polynorbornene bearing the complementary nucleic acid base as a template polymer.

8) I suggest a polynorbornene backbone bearing a nucleic acid base as a template because the pentagonal ring of polynorbornene directly connected to the base is more rigid than the backbone of polymethacrylates. Thus, the polymerization of norbornene

170

bearing the complementary base could be achieved by template replication (Figure 6). Indeed, the ring-opening metathesis polymerization of a bisnorbornene derivative with a ferrocene linker yielded a double-stranded ladder polymer.[10] Polynorbornene as the template bearing pendant norbornene units also yielded the corresponding double-stranded ladder polymer by a ring-opening metathesis polymerization.[11]

## References

1) P. K. Jal, S. Patel, B. K. Misha, *Talanta* **2004**, *62*, 1005.

2) H. Ajiro, M. Maegawa, M. Akashi, *J. Polym. Sci., Part A: Polym. Chem.* **2012**, *50*, 1469.

3) K. Hatada, T. Shinozaki, K. Ute, T. Kitayama, *Polym. Bull.* **1988**, *19*, 231.

4) M. Maegawa, H. Ajiro, D. Kamei, M. Akashi, *Polym. J.* in press.

5) K. Kondo, T. Kida, Y. Ogawa, Y. Arikawa, M. Akashi, *J. Am. Chem. Soc.* **2012**, *132*, 8236.

6) T. Kida, M. Mouri, M. Akashi, *Angew. Chem., Int. Ed.* **2006**, *45*, 7534.

7) T. Nakano, Y. Okamoto, *Chem. Rev.* **2001**, *101*, 4013.

8) N. Hoshikawa, Y. Hotta, Y. Okamoto, *J. Am. Chem. Soc.* **2003**, *125*, 12380.

9) M. Akashi, H. Takada, Y. Inaki, K. Takemoto, *J. Polym. Sci., Polym Chem. Ed.* **1979**, *17,* 747.

10) H.-C. Yang, S.-Y. Lin, H.-C. Yang, C.-L. Lin, L. Tsai, S.-L. Hang, I. W.-P. Chen, C.-h. Chen, B.-Y. Jin, T.-Y. Luh, *Angew. Chem., Int. Ed.* **2006**, *45*, 726.

11) N.-T. Lin, S.-Y. Lin, S.-L. Lee, C.-h. Chen, C.-H. Hsu, L. P. Hwang, Z.-Y. Xie, C.-H. Chen, S.-L. Hang, T.-Y. Luh, *Angew. Chem., Int. Ed.* **2007**, *46*, 4481.

# List of Publications

## Chapter 1

<u>Daisuke Kamei</u>, Hiroharu Ajiro, Chizuru Hongo, Mitsuru Akashi

"Dynamics of Polymer Chains in Porous Thin Films Prepared by Layer-by-layer Assembly of Isotactic Poly(methyl methacrylate) and Syndiotactic Poly(methacrylic acid)"

*Chem. Lett.* **2008**, *37*, 332—333.

## Chapter 2

<u>Daisuke Kamei</u>, Hiroharu Ajiro, Chizuru Hongo, Mitsuru Akashi

"Solvent Effects on Isotactic Poly(methyl methacrylate) Crystallization and Syndiotactic Poly(methacrylic acid) Incorporation in Porous Thin Films Prepared by Stepwise Stereocomplex Assembly"

*Langmuir* **2009**, *25*, 280—285.

## Chapter 3

<u>Daisuke Kamei</u>, Hiroharu Ajiro, Mitsuru Akashi

"Specific Recognition of Syndiotactic Poly(methacrylic acid) in Porous Isotactic Poly(methyl methacrylate) Thin Films Based on the Effects of Stereoregularity, Temperature, and Solvent"

*J. Polym. Sci., Part A: Polym. Chem.* **2010**, *48*, 3051—3657.

## Chapter 4

<u>Daisuke Kamei</u>, Hiroharu Ajiro, Mitsuru Akashi

"Morphological Changes of Isotactic Poly(methyl methacrylate) Thin Films via Self-organization and Stereocomplex Formation"

*Polym. J.* **2010**, *42*, 131—137.

## Chapter 5

Daisuke Kamei, Hiroharu Ajiro, Mitsuru Akashi

"Fusion of Porous Isotactic Poly(methyl methacrylate) Thin Films Fabricated on Silica Nanoparticles with Stepwise Stereocomplex Assembly"

*J. Nanosci. Nanotechnol.* **2011**, *11*, 2545—2548.


## Chapter 6

Hiroharu Ajiro, Daisuke Kamei, Mitsuru Akashi

"Methacrylic Acid and Methyl Methacrylate Oligomers Adsorbed to Porous Isotactic Poly(methyl methacrylate) Ultrathin Filims and Mechanistic Studies of Living Template Polymerization"

*J. Polym. Sci., Part A: Polym. Chem.* **2008**, *46*, 5879—5886.


## Chapter 7

Hiroharu Ajiro, Daisuke Kamei, Mitsuru Akashi

"Macroporous Silicagel Substrate for Stereoregular Template Polymerization of Methacrylic Acid Using Stereocomplex Assembled Thin Films"

*Polym. J.* **2009**, *41*, 90—93.


## Chapter 8

Hiroharu Ajiro, Daisuke Kamei, Mitsuru Akashi

"Mechanistic Studies on Template Polymerization in Porous Isotactic Poly(methyl methacrylate) Thin Films by Radical Polymerization and Post-polymerization of Methacrylate Derivatives"

*Macromolecules* **2009**, *42*, 3019—3025.

# Other Publications

Hiroharu Ajiro, Chizuru Hongo, Masumi Maegawa, <u>Daisuke Kamei</u>, Sono Sasaki, Hiroaki Ogawa, Hiroyasu Masunaga, Yukie Takemoto, Kazuyuki Horie, Mitsuru Akashi

"Structural Nanospace Feature and Substrate Contribution to Maintaining Stable Porosity of Polymer Chain in Layer-by-Layer Assembled Isotactic Poly(methyl methacrylate) Films"

*Macromolecules* **2012**, *45*, 7660—7663.


Masumi Maegawa, Hiroharu Ajiro, <u>Daisuke Kamei</u>, Mitsuru Akashi

"A Study on Template Effect Using Irregular Porous Isotactic Poly(methyl methacrylate) Films Constructed with Syndiotactic Rich Poly(methacrylic acid) and Isotactic Poly(methyl methacrylate)"

*Polym. J.* **2013**, *45*, 898—903.

# Acknowledgements